27053

Report HSRI-71-129

TIRE TRACTION GRADING PROCEDURES AS DERIVED FROM THE MANEUVERING CHARACTERISTICS OF A TIRE-VEHICLE SYSTEM

VOLUME I

P. Fancher
L. Segel
C. MacAdam
H. Pacejka

Final Report
Contract No.: 1-35715

June 13, 1972

Prepared for:

Tire Systems Section
Office of Vehicle Systems Research
National Bureau of Standards
Washington, D.C.

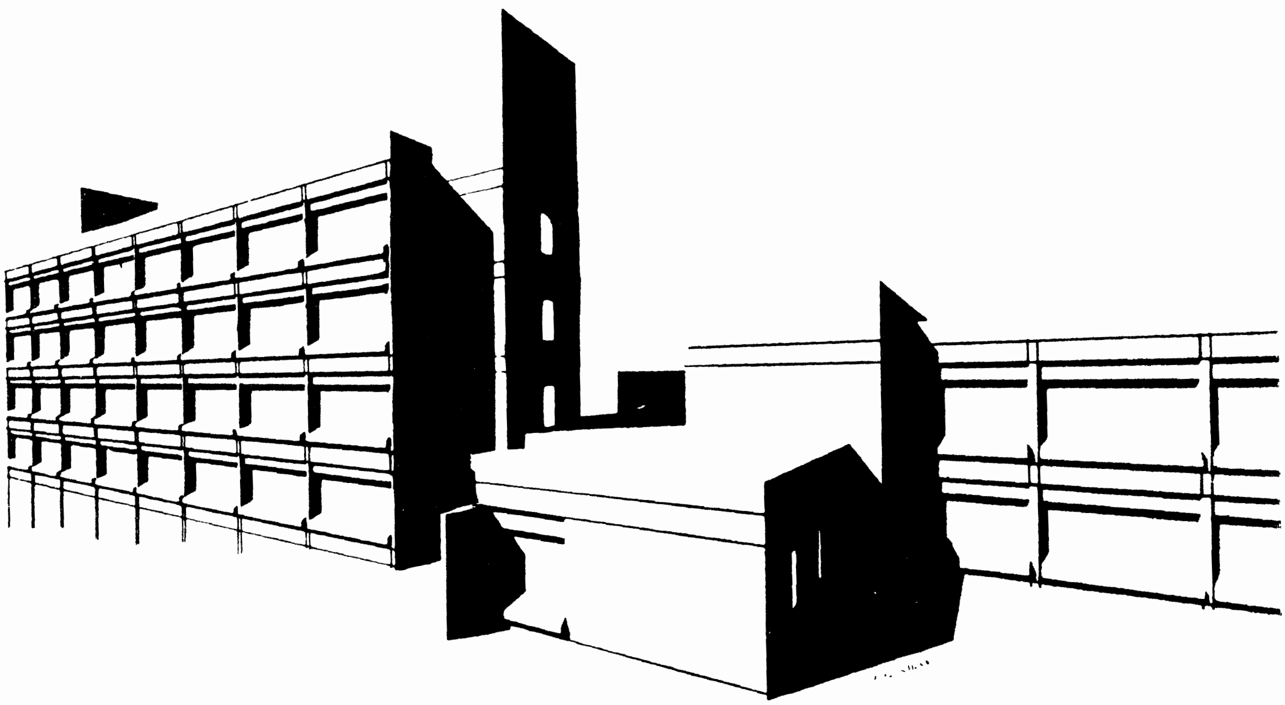

HIGHWAY SAFETY RESEARCH INSTITUTE
THE UNIVERSITY OF MICHIGAN ANN ARBOR

Report HSRI-71-129

TIRE TRACTION GRADING PROCEDURES AS DERIVED FROM THE MANEUVERING CHARACTERISTICS OF A TIRE-VEHICLE SYSTEM

P. Fancher
L. Segel
C. MacAdam
H. Pacejka

Highway Safety Research Institute
Institute of Science and Technology
The University of Michigan
Ann Arbor, Michigan 48105

June 13, 1972

Final Report
Contract No.: 1-35715

Prepared for:
Tire Systems Section
Office of Vehicle Systems Research
National Bureau of Standards
Washington, D.C.

This report was prepared in fulfillment of the National Bureau of Standards Contract No. 1-35715 (funded by the National Highway Traffic Safety Administration through the NBS, Contract FH-11-6090). The opinions, findings, and conclusions expressed in this publication are those of the authors and not necessarily those of the National Bureau of Standards nor the National Highway Traffic Safety Administration.

ACKNOWLEDGEMENTS

The authors wish to acknowledge the contributions made to this program by Mr. A. H. Neill, Jr., of NHTSA. We thank Mr. Neill and his colleagues, Messrs. Boyd and Barton, for their cooperation in supplying us with vehicle test data and tires.

Special thanks are also due to Mr. R. Wild of HSRI for collecting an extensive set of tire data.

TABLE OF CONTENTS

LIST OF TABLES

LIST OF TABLES (Continued)

LIST OF FIGURES

LIST OF FIGURES (Continued)

1. INTRODUCTION

This report presents the results obtained and the recommendations derived from a research and application study entitled, "Tire Traction Grading Procedure as Derived from Emergency Maneuvering Characteristics of a Tire-Vehicle System." The study was completed by the Highway Safety Research Institute (HSRI) of The University of Michigan for the Safety Systems Laboratory (SSL) of the National Highway Traffic Safety Administration (NHTSA). Originally, the work was funded by the National Bureau of Standards (NBS) through the Office of Vehicle Systems Research (OVS). During this contract period the Office of Vehicle Systems Research was transferred to NHTSA and it was renamed the "Safety Systems Laboratory."

The overall purpose of this study is to aid SSL in formulating recommendations for a tire traction quality grading procedure.

The results reported herein include (1) the measurement of tire longitudinal and/or lateral shear-force, (2) the representation of tire shear forces in terms of characterizing functions and tire parameters, and (3) the simulation and analysis of tire-vehicle system performance on wet surfaces in (a) diagonal-braking, locked-wheel stopping distance tests and (b) J-turn maneuvers at, or near, a limiting velocity. Tire shear force measurements were performed both with HSRI's Mobile Tire Tester and Flat Bed Machine [1]*. During the course of this study the model that was previously developed to describe the shear force mechanics of a pneumatic tire [2] was extended and refined. This refinement has included significant changes in both the form of

*Numbers in square brackets are used to indicate references.

the model (i.e., the characterizing functions) and the traction parameters--their definition and measurement.

In order to establish a means of grading the traction characteristics of tires related to extreme vehicle maneuvers, OVS-NBS personnel have made many driver-controlled tire-vehicle system tests using different sets of tires on specially prepared wet surfaces at the Texas Transportation Institute (TTI). These driver-vehicle tests were used to rank tires in two ways: (1) by comparing the length of skidding distance obtained in locked-wheel diagonal-braking tests and (2) by comparing the limit velocity at which a 288-foot radius turn can be maintained without "breakaway." Consequently, the simulation and analysis effort conducted in this study constitutes an attempt to apply tire mechanics knowledge, as it exists today, to explain the results that were obtained by OVS-NBS in their testing program.

The body of this report is devoted to summarizing the results obtained in this study. The report concludes with a presentation of recommendations concerning tire-traction quality grading procedures both with respect to the near and the far term. Detailed results, derivations and discussions are presented in several appendices. A comprehensive set of tire data is given in one appendix and the results of processing this data to obtain tire parameters are presented in a second appendix.

Included in a second volume are descriptions of (a) an extension of the tire model, which is intended to treat the combined longitudinal and lateral force cases more accurately than heretofore, and (b) a mathematical method for curve-fitting tire shear force data.

2. RESULTS

Five specific tasks were performed in this study: (1) test a group of tires (previously used in the OVS driver-vehicle tests) with the aid of HSRI's tire-test equipment, (2) compare traction findings produced by tire testing with the findings produced by tire-vehicle system tests, (3) revise and improve the tire model developed previously [2] under OVS auspices, (4) study tire-vehicle system test procedures and results with the aid of vehicle dynamic simulation and analysis, and (5) formulate recommendations for an interim tire traction quality grading procedure. The results obtained in tasks (1) through (4) are summarized below with the recommendations being presented in Section 3.

2.1. TIRE DATA

Table 1 lists the ten tire configurations that were common to this study and the OVS driver-vehicle test program. Note that the test sample consists of three carcass constructions, each with three levels of tread wear, plus an SAE-type reference tire. These tires were tested with the mobile tire tester on the same surfaces used by NBS at TTI to perform the tire-vehicle tests. Attempts were made to keep the watering conditions in the two different test exercises as close as possible.

For each of these 10 tires, carpet plots of (a) longitudinal force versus longitudinal slip and vertical load and (b) lateral force versus slip angle and vertical load were produced from data gathered on three surfaces: wet concrete, wet asphalt, and wet jennite. By superimposing curves of longitudinal force and lateral force versus velocity on these plots, comprehensive graphical descriptions of (a) lateral force as a function of slip angle, load, velocity and surface and (b) longitudinal force as a function of longitudinal slip, load, velocity and surface were produced. These plots, as produced for all ten tires, are presented in Appendix 1.

TABLE 1. TIRES TESTED

TIRE	TYPE	SIZE	TREAD DEPTH IN THOUSANDS OF AN INCH
A-1	Bias	8.25/14	75 to 100
A5-1	Bias	8.25/14	140 to 165
A-5	Bias	8.25/14	360
RB-5	Radial	205R-14	115
RB-1	Radial	205R-14	200
H-5	Radial	205R-14	320
D-2	Belted-Bias	G78-14	75 to 100
WA-5	Belted-Bias	G78-14	205
WA-9	Belted-Bias	G78-14	370
S-2-47	Bias-SAE	7.75/14	New

In addition to making the above measurements, namely, lateral force with zero longitudinal slip and braking force with zero lateral slip, combined lateral and longitudinal shear force data were also gathered. Specifically, longitudinal slip was varied from zero to unity with the slip angle fixed at 8° for all tires operated on all three surfaces. (These data were reduced to peak resultant shear force by graphical means.) Finally, a complete traction field, consisting of lateral and longitudinal shear force measurements at 3 speeds, 3 loads, 7 slip angles, with longitudinal slip, s, varied from zero to unity, were obtained with the new radial tire (H-5) for the purpose of developing a detailed mathematical representation of tire shear force characteristics. Experimental findings resulting from testing tires at combined lateral and longitudinal slip will also be found in Appendix 1.

For purposes of evaluating traction quality, the shear force data gathered for the 10 tires has been analyzed in terms of (1) maximum lateral force, (2) locked-wheel braking force, (3) maximum braking force and, (4) maximum resultant force at 8° slip angle with longitudinal slip variable. These findings are summarized in Tables 2 through 5.

For these particular tires the radial tires produced larger shear forces (on the average) than the belted bias tires and the belted bias tires produced larger forces than the cross bias tires. It is interesting to note that in some cases the fully-worn radial tire's performance exceeded the performance of the half-worn radial tire. Similarly, the fully-worn belted bias tire's performance exceeded the half-worn belted bias tire performance in some cases.

2.2. COMPARISON OF TIRE RANKINGS AS DERIVED FROM TIRE TESTS AND TIRE-VEHICLE SYSTEM TESTS

The traction measurements summarized in Tables 2 through 5 have been analyzed to rank the 10 tested tires according to

TABLE 2. MAXIMUM LATERAL FORCE

Fy_{max}

LOAD/SPEED	A-1	A5-1	A-5	RB-5	RB-1	H-5	D-2	WA-5	WA-9	S-2-47	SURFACE
600 lbs/30 mph	300	420	470*	475	465	480	440	450	485*	415	Concrete
1000/30	500*	650*	640*	715	760*	780*	630	670*	680*	665	Concrete
1400/30	775*	860*	870*	930*	1000*	975*	965	880*	915*	925*	Concrete
1000/10	670*	695*	740*	760*	820*	845*	755	710	735*	665	Concrete
1000/50	-	485	620	630	-	720	350	580*	615*	620	Concrete
600 lbs/30 mph	355	360	440	445	400	480	400	375	420	320	Asphalt
1000/30	500	490	680	660	635	780	620	605*	710*	555	Asphalt
1400/30	700	805	940*	900*	935*	970*	870	865	910*	730*	Asphalt
1000/10	575	510	740*	635	710*	820*	660	660*	725	580*	Asphalt
1000/50	-	450	590	630	-	750	570	615	635*	510	Asphalt
600 lbs/30 mph	190	250	345	330	310	370	290	275	345	285	Jennite
1000/30	285*	380	390	470	480	650	420	375	460	500	Jennite
1400/30	420*	535	430	650	660	690	590	535	580	590	Jennite
1000/10	590	560	555	650	640	710	655	600	640	685	Jennite
1000/50	-	280	320	440	-	585	315	310	385	420	Jennite

*Denotes Fy @ 16° slip is the maximum

TABLE 3. BRAKING FORCE - Fx

100% Slip - Fully Locked
(0° Steer Angle)

LOAD/SPEED	A-1	AS-1	A-5	RB-5	RB-1	H-5	D-2	WA-5	WA-9	S-2-47	SURFACE
600 lbs/30 mph	190	265	319	315	325	340	250	325	375	315	Concrete
1000/30	300	430	470	485	525	540	420	500	575	530	Concrete
1400/30	480	575	625	680	720	700	610	610	700	685	Concrete
1000/10	560	575	575	605	640	645	575	585	625	550	Concrete
1000/50	110	275	230	285	-	320	90	220	435	400	Concrete
600 lbs/30 mph	180	200	220	240	210	280	200	240	275	200	Asphalt
1000/30	280	325	375	400	350	430	375	355	415	320	Asphalt
1400/30	390	375	510	575	480	580	475	495	540	430	Asphalt
1000/10	345	430	475	475	450	550	490	415	475	375	Asphalt
1000/50	310	325	355	350	-	410	350	335	430	355	Asphalt
600 lbs/30 mph	70	120	110	115	100	120	75	110	160	100	Jennite
1000/30	115	150	135	220	225	220	175	200	225	170	Jennite
1400/30	210	160	175	325	200	260	230	220	290	190	Jennite
1000/10	240	250	220	270	280	270	305	250	280	240	Jennite
1000/50	45	70	105	125	-	170	85	130	150	130	Jennite

TABLE 4. MAXIMUM BRAKING FORCE

Fx_{max}
(0° Steer Angle)

LOAD/SPEED	A-1	A5-1	A-5	RB-5	RB-1	H-5	D-2	WA-5	WA-9	S-2-47	SURFACE
600 lbs/30 mph	280	395	430	465	450	470	335	445	480	410	Concrete
1000/30	465	655	680	675	725	700	570	650	760	690	Concrete
1400/30	695	875	885	1000	1010	960	880	925	950	990	Concrete
1000/10	640	680	660	735	735	770	755	705	735	635	Concrete
1000/50	240	460	590	560		650	330	480	675	625	Concrete
600 lbs/30 mph	280	330	350	350	325	415	325	325	400	280	Asphalt
1000/30	430	490	650	655	560	690	600	550	640	480	Asphalt
1400/30	620	545	825	940	765	860	700	740	800	630	Asphalt
1000/10	450	560	650	635	600	700	710	560	600	455	Asphalt
1000/50	410	500	515	565		735	490	480	560	410	Asphalt
600 lbs/30 mph	145	200	300	310	240	375	210	225	380	250	Jennite
1000/30	215	340	385	460	425	530	370	365	455	365	Jennite
1400/30	330	400	515	750	545	700	510	495	650	495	Jennite
1000/10	550	510	515	540	540	670	655	530	555	520	Jennite
1000/50	145	175	325	300		490	210	250	375	220	Jennite

TABLE 5. MAXIMUM TOTAL FORCE - $\overline{F}$(MAX), LBS. AT 8° SLIP ANGLE

LOAD/SPEED	TIRE: A-1	A5-1	A-5	RB-5	RB-1	H-5	D-2	WA-5	WA-9	S-2-47	SURFACE
1000#/30 mph, 8°	491	679	743	686	723	790	610	684	759	717	Concrete
1000#/30 mph, 8°	502	549	710	584	518	805	552	565	700	501	Asphalt
1000#/30 mph, 8°	281	322	518	360	370	600	375	361	539	433	Jennite

their lateral force, longitudinal force, and combined lateral and longitudinal force output. These rankings were developed for 3 speeds (10, 30, and 50 mph), 3 loads (600, 1000, and 1400 lbs), and 3 surfaces (concrete, jennite, and asphalt) except for the maximum resultant force data which were obtained at only one combination of speed and load. The resulting rankings are given in Appendix 2.

It is both tedious and difficult to compare rankings of tires as obtained from direct traction measurements and tire-vehicle system performance tests. Accordingly, rank-difference correlations [3] have been computed in selected cases where meaningful comparisons are thought to exist. For example, the velocity at "breakaway" in a J-turn is related to the lateral acceleration at breakaway and, since the lateral acceleration of the vehicle is clearly related to the lateral force produced by the tires, it is meaningful to compare rankings of tires based on maximum velocity achieved before breakaway (in vehicle tests) with rankings based on measurements of peak lateral force. The individual rankings of tires according to their peak lateral force output were combined to yield the "average" rankings tabulated in Table 6. Rank-difference correlations with the overall ranking* obtained in the J-turn maneuver are:

(1) .948 based on the average ranking obtained in tire tests conducted at 10, 30, and 50 mph at 1000 lbs. on all 3 test surfaces.

(2) .964 based on the average ranking obtained in tire tests conducted at 50 mph at 1000 lbs. on all 3 test surfaces.

*The NBS J-turn rankings were supplied by the Bureau of Standards.

TABLE 6. RANKINGS OF 10 TIRES BY LATERAL FORCE

	A	B	C	D	E
Highest	H-5	H-5	H-5	H-5	H-5
	RB-5	RB-5	RB-5	RB-1	RB-5
	WA-9	RB-1	RB-1	RB-5	RB-1
	RB-1	WA-9	WA-9	WA-9	WA-9
	A-5	S-2-47 } Tie	S-2-47	A-5	A-5
	S-2-47	A-5 } Tie	A-5	D-2	D-2
	WA-5	D-2	WA-5	S-2-47	S-2-47
	A5-1	WA-5	D-2	WA-5	WA-5
	D-2	A5-1	A5-1	A5-1	A5-1
Lowest	A-1	A-1	A-1	A-1	A-1

A) NBS combined J-curve breakaway-speed rankings, averaged for 3 surfaces.

B) MTT peak lateral force data average ranking for 10, 30, and 50 mph at 1000 lbs on all three surfaces.

C) MTT peak lateral force data average ranking for 50 mph at 1000 lbs on all three surfaces.

D) MTT peak lateral force data average ranking for 30 mph at 600, 1000, and 1400 lbs on all three surfaces.

E) MTT peak lateral force data average ranking for 10, 30, and 50 mph; 600, 1000, and 1400 lbs on all three surfaces.

(3) .891 based on the average ranking obtained in tire tests conducted at 30 mph at 600, 1000, and 1400 lbs. on all three test surfaces.

(4) .915 based on the overall speed-load ranking for peak lateral force (Column E of Table 6).

The above cited correlations indicate that good correspondence exists between vehicle tests and measurements made with the mobile tire tester. During a J-turn test, each tire operates at a different load (due to load transfer) and thus it appears reasonable to average across loads. Since, for the most part, the J-turn tests were conducted at velocities between 40 and 50 mph, it is reasonable to anticipate that a comparison based on tire data collected at 50 mph should yield a higher rank-difference correlation as was actually obtained. In general, the results seem to indicate that a J-turn test and measurements of peak lateral force will give nearly the same traction ranking for a set of tires with some slight reordering due to different load and speed conditions.

In the locked-wheel stopping distance tests, load is transferred from the rear to the front tires and the speed of the vehicle decreases from the initial velocity to zero. Accordingly, it seems appropriate to compare the ranking of the ten test tires obtained at a 100 percent slip condition averaged over all speeds and loads with rankings based on the NBS skidding distance overall average (see Table 7). On so doing, a rank-difference correlation of .879 was obtained. Clearly, better correlation is obtained in the J-turn than in the locked-wheel stopping distance test. Since peak longitudinal force measurements are obtained with the MTT, it is of interest to compare rankings based on peak longitudinal force with rankings based on skidding distance and also with rankings based on 100% slip measurements.

TABLE 7. SKIDDING DISTANCE VERSUS PEAK LONGITUDINAL FORCE AND LOCKED-WHEEL BRAKING FORCE

	A	B	C
Highest	WA-9	H-5	WA-9
	H-5	WA-9	H-5
	RB-1	RB-5	RB-5
	A-5	RB-1	RB-1
	RB-5	A-5	WA-5
	WA-5	D-2	A-5
	A5-1	WA-5	S-2-47
	S-2-47	S-2-47	D-2
	A-1	A5-1	A5-1
Lowest	D-2	A-1	A-1

A) NBS skidding distance average ranking for 3 surfaces.

B) MTT data average ranking of peak longitudinal force for 10, 30, and 50 mph, at 600, 1000, and 1400 lbs, on all 3 surfaces.

C) MTT data average ranking of longitudinal force for 100% slip for 10, 30, and 50 mph, at 600, 1000, and 1400 lbs, on all 3 surfaces.

A correlation of .818 is obtained on comparing peak longitudinal force versus skidding distance; a correlation of .927 exists between peak longitudinal force measurements and the 100% slip measurements (see Table 7). In general, the rankings based on skidding distance measurement compare reasonably well with the rankings based on tire test data. Note that the vehicle test does not exercise the tire over its full range of braking performance, namely, from peak braking to the locked-wheel condition.

Comparisons of peak resultant force ranking with the tire rankings based on free-rolling side force, 100% slip braking force, and peak braking force yield correlations of .864, .802, and .923, respectively (see Table 8). Thus it appears that peak resultant force cannot be used interchangeably with free-rolling side force or 100% slip longitudinal force rankings (or vice versa).

The correlations which have been obtained in this study are high. This is not surprising from the viewpoint of vehicle mechanics, that is, tire forces determine vehicle motion and thus the tire forces which are most important in a particular vehicle maneuver correlate closely with the vehicle motion. However, one might expect lower correlations due to the experimental difficulty in conducting skidding distance tests. It is believed that the number of tire test conditions which were combined into the tire rankings was sufficiently large to establish uniform results. Thus, high correlations were obtained.

2.3. TIRE REPRESENTATION AND TIRE PARAMETERS

2.3.1. TIRE REPRESENTATION. In a previous study [2] a tire shear force model which was designed to be valid for representing both lateral and longitudinal force components when the tire is operated at various combinations of load, speed, slip angle, and longitudinal slip was developed. This model is described by the following equations:

TABLE 8. PEAK RESULTANT FORCE VERSUS PEAK LATERAL AND LONGITUDINAL FORCE COMPONENTS

	A	B	C	D
Highest	H-5	H-5	WA-9	H-5
	WA-9	RB-1	H-5	WA-9
	A-5	RB-5 } Tie	RB-1 } Tie	RB-5
	RB-1 } Tie	WA-9 }	RB-5 }	RB-1
	RB-5 }	S-2-47	WA-5	A-5
	WA-5 } Tie	A-5	S-2-47	D-2
	S-2-47 }	D-2 } Tie	D-2	S-2-47
	D-2	WA-5 }	A-5	WA-5
	A5-1	A5-1	A5-1	A5-1
Lowest	A-1	A-1	A-1	A-1

A) MTT data peak resultant force at 8° slip angle, 30 mph, 1000 lbs load, averaged for 3 surfaces.

B) MTT data peak lateral force at 30 mph, 1000 lbs load, averaged for 3 surfaces.

C) MTT data 100% slip braking force at 30 mph, 1000 lbs load, averaged for 3 surfaces.

D) MTT data peak braking force at 30 mph, 1000 lbs load, averaged for 3 surfaces.

$$F_x = -\left(\frac{C_s\, s}{1-s}\right) f(\lambda) \tag{1}$$

$$F_y = -\left(\frac{C_\alpha \tan\alpha}{1-s}\right) f(\lambda) \tag{2}$$

with

$$f(\lambda) = \begin{cases} (2-\lambda)\,\lambda, & \text{for } \lambda < 1 \\ 1 & \text{, for } \lambda \geqq 1 \end{cases}$$

where

$$\lambda = \left(\frac{\mu\, F_z(1-s)}{2}\right)[(C_s s)^2 + (C_\alpha \tan\alpha)^2]^{-1/2} \tag{3}$$

$$V_s = U_w(s^2 + \tan\alpha^2)^{1/2} \tag{4}$$

$$\mu = \mu_o(1 - A_s V_s) \tag{5}$$

and where

F_x is the longitudinal force

F_y is the lateral force

V_s is the sliding velocity

Fz is the vertical load

U_w is the velocity of travel of the wheel

α is the slip angle

s is the longitudinal slip

C_s is the longitudinal stiffness of the tire

C_α is the cornering stiffness of the tire

μ_o is the zero speed value of friction coefficient, μ

A_s is the decrease in friction coefficient with sliding velocity, V_s.

In Section 1 of volume II the assumptions which led to this compact simple tire model are re-examined and the model is extended in order to ensure that the resultant tire force in the sliding region of the contact patch opposes the direction of sliding. A "transition" region between the adhesion region and the sliding region of the contact patch is defined. These changes in the model have large influences in cases where the tire is required to operate at large lateral and longitudinal slip simultaneously. In cases where the tire is required to produce primarily longitudinal or lateral force, but not both, such as diagonal braking or J-turn maneuvers, the extended model has little advantage over the original model.

Difficulties in justifying the assumptions required to develop a simple tire shear force model have caused many researchers to look for mathematical methods for representing tires in vehicle dynamics studies. One such method, called the "similarity method," has been found to have considerable utility for describing tire lateral force characteristics [4]. In Section 2 of Volume II this mathematical procedure for fitting tire data is extended to the complete tire traction field. Also, an example in which this method is applied to the H-5 tire is given in Section 2 of Volume II.

Because of their size and complexity, neither the extended model nor the similarity method representation were used in this study to analyze the locked-wheel diagonal-braking and J-turn maneuvers. Instead, the friction expression (5) in the original model was made a linear function of both sliding speed and load. Further, the values of the parameters used in the model were selected to provide a least mean square error fit to the tire test data over the range of tire operating conditions of most importance in the vehicle maneuvers involved. Thus, separate friction parameters were obtained for the J-turn and the diagonal-braking stop.

2.3.2. TIRE PARAMETERS.

2.3.2.1. Longitudinal Force Friction Parameters. Obviously, locked-wheel skidding distance results depend only on the 100% slip value of longitudinal force. The elastic properties of the tire which are represented by the longitudinal stiffness parameter C_s are unimportant in determining the longitudinal force at 100% slip.

The tire-road interface characteristics are functions of speed and load. For the purposes of this study the form of friction law used was:

$$\mu_x = \mu_{ox} - A_x V_s - B_x F_z \tag{6}$$

where V_s is the sliding velocity of the tire and F_z is the vertical load on the tire. The parameters μ_{ox}, A_x, and B_x, which minimize the squared error between the friction law (6) and locked-wheel tire data at the following 5 combinations of load and speed: 1000 lbs/10 mph, 1000 lbs/30 mph, 1000 lbs/50 mph, 600 lbs/30 mph, and 1400 lbs/30 mph, have been determined for each of the 10 tires on three different surfaces in wet condition and they are given in Appendix 3. Also, a comparison between the friction law (6) and tire data at each of the 5 combinations of speed and load is given in Appendix 3. (Each data point is the average of at least 6 repetitions with the mobile tire tester.)

The average RMS error between μ_x and the test data is approximately 0.02 to 0.03 for this range of operating conditions on these surfaces. In general, the magnitude of the error is fairly uniformly spread over all 5 operating conditions and it is not concentrated at any one condition. (Partially, this is a result of the process of minimizing the squared error.)

The following properties of the tire longitudinal friction law parameters have been obtained by examination of Table 15 in Appendix 3:

(1) μ_{ox} is much greater on concrete than on asphalt or jennite for all 10 tires.

(2) Usually, A_x is greater on concrete than on asphalt (or jennite). Thus, the values of μ_x for asphalt are only about 25% less than the values for concrete even though μ_{ox} is much greater for concrete than for asphalt. The values for μ_x on jennite are approximately 50% of those for asphalt.

(3) A_x is always positive.

(4) The median value of A_x for wet concrete is approximately .0055. At 44 ft/sec (30 mph), this produces a reduction in μ_x from the zero speed value of about 0.24. On both asphalt and jennite the median value of A_x is approximately 0.002.

(5) The magnitude of B_x seldom exceeds 10^{-4}. Thus, for 1000 pounds load, the change in μ_x from zero load is usually less than 0.1 due to load.

(6) In a few cases, B_x is negative, indicating an increase in μ_x with an increase in load.

2.3.2.2. Lateral Force Parameters. The maximum side force generated by a pneumatic tire operating at any slip angle less than or equal to 16° is dependent upon the elastic properties of the tire and the tire-road interface friction law.

For the case of a purely sideslipping tire, the general tire model (Eqns. (1) - (5)) can be reduced to the following form:

at "large" slip angles, that is, for $|\tan \alpha| > \mu F_z/2C_\alpha$

$$F_y = -\mu F_z \left(1 - \frac{\mu F_z}{4C_\alpha |\tan \alpha|} \right) \mathrm{sgn}(\alpha) \tag{7}$$

where μ is the tire-road interface lateral friction law,

F_z is the vertical load on the tire,

C_α is the tire cornering stiffness,

and α is the tire slip angle.

In this study, the lateral friction μ is represented by the following function:

$$\mu_y = \mu_{oy} - A_y V_s - B_y F_z \tag{8}$$

where V_s is the sliding velocity of the tire. (For a purely sideslipping tire, $V_s = U_w \tan \alpha$.)

The value of cornering stiffness parameter, C_α, depends upon the elastic properties of the tire and it can be determined from the slope of the lateral force versus slip angle curve at low slip angles. Previous experience measuring lateral tire force on dry and moderately wetted* surfaces indicated that C_α could be best determined from flat bed test results. Consequently, C_α was determined from flat bed tests of each of the 10 test tires at the 3 loads used in the mobile tire tester work. However, an examination of the mobile tire tester data, given in Appendix 1, indicates that the rate of change of lateral force with slip angle (at low slip angles) varies with both speed and load for some

---

*The internal watering system on the mobile tire tester produces a nominal water depth of 0.02 inches.

tires when tested on the wet surfaces used in this study. The values of C_α, as determined from the mobile tire tester data, are given in Table 17 of Appendix 3 for 3 vertical loads at 30 mph and in Table 18 of Appendix 3 for 3 speeds at 1000 pounds vertical load. In general, the values of C_α, determined from the mobile tire tester data, are less than the corresponding values of C_α determined from the flat bed machine data. A significant reduction of C_α with increasing speed was measured for the following tire-surface combinations:

Tire	Description	Surface
A-1	fully worn cross bias	jennite
A-1	fully worn cross bias	concrete
A-5-1	half-worn cross bias	jennite
A-5-1	half-worn cross bias	concrete
D-2	fully worn belted bias	jennite
D-2	fully worn belted bias	concrete

The A-5 tire had exceptionally low values of C_α for all combinations of load and speed except 600 pounds at 30 mph. These results for C_α indicate that the cornering stiffness, defined as the slope of the lateral force versus slip angle curve at low slip angle, is a function of speed and load for wet surfaces and that it represents tire-road interface properties as well as tire elastic properties.

The process of obtaining the lateral force parameters for a tire consisted of: first, obtaining C_α from the mobile tire tester data, second, computing μ from (7) using test data obtained at a slip angle of 16 degrees, and third, computing μ_{oy}, A_y, and B_y to minimize the error between μ and μ_y as defined by (8). The values calculated for μ_{oy}, A_y, and B_y are listed in Table 19, Appendix 3 for each of the 10 tires tested on the three wet surfaces.

The values for μ_y as presented in Table 19, Appendix 3 are much higher than the values of μ_x, presented in Table 15, Appendix 3. This same finding was obtained in a previous study [5] where it was observed that there is a need to differentiate between a lateral and a longitudinal friction factor.

The results given in Table 19, Appendix 3, shows that the zero-speed/zero-load value of friction, μ_{oy}, ranges from 0.628 to 1.09 on wet concrete, from 0.444 to 1.04 on wet asphalt, and from 0.479 to 1.05 on wet jennite. These values of μ_{oy} can be very deceiving since B_y can be positive or negative which means that μ_y can decrease or increase with increasing vertical load. In one case, namely, the S-2-47 tire tested on asphalt, the data show a slight increase in μ_y with speed (A_y negative). In general, μ_y is much less sensitive to speed (A_y smaller) on the asphalt surface than on the concrete or jennite surfaces. (The asphalt surface has a much greater macrotexture than the concrete or jennite surfaces.)

For purposes of simulating performance in a J-turn maneuver, it appeared advisable to select combinations of load, speed, and slip angle (for extracting μ_{oy}, A_y, and B_y) that lie within the range of conditions at which a tire operates in a J-turn maneuver. Accordingly, a least squares fit of μ_y to the lateral friction was generated for the following five test conditions:

LOAD, POUNDS	SPEED, MPH	SLIP ANGLE DEGREES
1400	30	8
1400	30	16
1000	50	8
1000	50	16
1000	30	8

The results are given in Table 20, Appendix 3. On using these values of μ_{oy}, A_y, and B_y, 80% of the side forces computed with Equation (7) were within 30 pounds of the measured side forces over a range of conditions of importance to the J-turn maneuver.

2.3.2.3. Summary of Tire Parameter Results. Tables 15, 20, 17 and 18 in Appendix 3 give the tire parameters (μ_{ox}, A_x, B_x, μ_y, A_y, B_y, and C_α) needed for simulating tire shear force characteristics in locked-wheel braking and J-turn maneuvers. The assumed linear friction laws give an average RMS error of about 0.02 to 0.03 in either μ_y or μ_x over the range of speeds, loads, and surfaces used in the tire test program. It is likely that a nonlinear friction law would be more representative of the observed phenomena. However, greater knowledge concerning the events taking place at the tire-road interface is needed in order to develop the appropriate form for a friction law.

2.4. ANALYSIS AND SIMULATION OF TIRE-VEHICLE SYSTEM PERFORMANCE

2.4.1. ANALYSIS AND SIMULATION OF LOCKED-WHEEL DIAGONAL-BRAKING. Consideration of the locked-wheel diagonal-braking maneuver leads to the conclusion that a very simple model can be used to compute skidding distance. The following differential equation applies:

$$m\ddot{x} = -(\mu_{xF}F_{zF} + \mu_{xR}F_{zR}) \tag{9}$$

where

m is the mass of the vehicle

x is the skidding distance

μ_{xF} is the friction expression for the braked front tire

μ_{xR} is the friction expression for the braked rear tire

F_{zF} is the load on the braked front tire

F_{zR} is the load on the braked rear tire.

In Appendix 4 it is shown that (9) can be reduced to the following form:

$$\ddot{x} = \mu_x \frac{g}{2} \tag{10}$$

where

$$\mu_x = \mu_{ox} - A_x \dot{x} - B_x \frac{W}{4}$$

where

$$V_s = \dot{x} \text{ for a locked wheel and } W = mg.$$

The solution to (10), yielding the stopping distance, x, is

$$x(t_f) = -\frac{1}{A}(\dot{x}(o) + Bt_f) \tag{11}$$

where t_f is the stopping time,

$$t_f = \frac{1}{A} \ln \left[\frac{1}{(\frac{A}{B})\dot{x}(o) + 1} \right] \tag{12}$$

and $\dot{x}(o)$ is the initial velocity with

$$A = \frac{g}{2} A_x$$

$$B = -\frac{g}{2}\left(\mu_{ox} - \frac{B_x W}{4}\right)$$

For example:

For the SAE reference tire, S-2-47, on wet concrete, Table 15, Appendix 3 gives $\mu_{ox} = .656$, $A_x = 0.00255$, and $B_x = 0.0000446$. For $\dot{x}(o) = 44$ ft/sec (30 mph), Equations (11) and (12) predict a skidding distance, $x(t_f)$ of 114 feet.

Values of skidding distance computed from (11) for all 10 tires on all three surfaces are presented in Table 9 for initial velocities of 30 and 50 mph. Also, the results of the vehicle tests [6] are given in Table 9. For 30 mph on wet concrete, a simple model of the tire-vehicle system does extraordinarily well at predicting skidding distance. Fairly good results are obtained on the other two surfaces at 30 mph. At 50 mph there are numerous cases where the computed skidding distances are slightly longer than the measured distances. The reasons for these differences will be explained in a following discussion on the sensitivity of skidding distance to test conditions (especially to tire/road interface parameters).

The values of the partial derivatives of skidding distance, x, with respect to the tire parameters (μ_{ox}, A_x, and B_x), the vehicle weight, W, and the initial velocity, V_o, are given in Table 21, Appendix 4. These values can be used to evaluate the influence of tire parameters, load, and initial velocity changes on skidding distance. In general, the values of these partial derivatives (sometimes called sensitivity coefficients) indicate that skidding distance is a very sensitive function of initial velocity and the friction parameters, μ_{ox} and A_x. Accordingly, very precise control of initial velocity, water depth, and surface friction properties are needed to minimize the amount of scatter obtained in skidding distance tests and likewise very precise control of velocity, water depth, and surface friction properties are needed to obtain repeatable results using tire test devices. Also, tire test results at a number of velocities are needed to predict skidding distance since skidding distance is highly dependent upon the rate of change of friction with velocity, i.e., A_x. Specific examples will be given later.

The hybrid computer was used to examine the wheel lockup process in more detail because in the vehicle tests the initial velocity was recorded at brake application but skidding distance

TABLE 9. SKIDDING DISTANCE COMPARISON
Entries are Skidding Distance in Feet

	ASPHALT				JENNITE		CONCRETE			
	30 mph		50 mph		30 mph		30 mph		50 mph	
	Vehicle Test	Computed	Vehicle Test	Computed	Vehicle Test	Computed	Vehicle Test	Computed	Vehicle Test	Computed
TIRE										
A-1	150	197	459	570	287	321	128	138	439	694
A5-1	147	176	420	549	291	354	115	123	378	447
A-5	129	144	370	447	269	372	115	119	356	449
RB-5	144	136	406	420	270	236	111	111	346	398
RB-1	143	152	405	522	270	279	106	105	340	341
H-5	135	127	379	395	265	263	109	105	326	372
D-2	154	145	439	459	300	258	126	119	394	558
WA-5	150	159	396	478	266	295	126	118	382	457
WA-9	120	142	360	411	233	253	114	107	362	340
S-2-47	150	179	413	509	276	326	120	114	355	354

was measured from the point where the wheels locked up. The time from brake application to wheel lockup was reported to be approximately 0.25 seconds [6]. In the simulation, the rate of brake pressure increase was controlled to produce lockup of both the front and rear wheel in 0.25 seconds. The velocity of the vehicle at wheel lockup was determined, assuming stops with two different tires (a high- and low-friction tire). Assuming an initial velocity of 44 ft/sec (30 mph), the following results were obtained:

Tire		Velocity at Lock ft/sec	ΔV, ft/sec
	Wet Concrete Surface		
A-1		42.55	1.45
RB-1		42.23	1.77
	Wet Asphalt Surface		
A-1		43.36	0.64
H-5		42.78	1.22
	Wet Jennite Surface		
A-5		43.67	0.33
RB-5		43.38	0.62

Assuming an initial velocity of 73.3 ft/sec (50 mph), the following results were obtained:

Tire		Velocity at Lock ft/sec	ΔV, ft/sec
	Wet Concrete Surface		
A-1		71.35	1.98
RB-5		70.75	2.58

At 44 ft/sec, the sensitivity (partial derivative) of x with respect to initial velocity is 8.17 ft/$_{ft/sec}$ for the A-1 tire on wet concrete, and 5.28 ft/$_{ft/sec}$ for the RB-1 tire (see Table 21). The net change in skidding distance for the A-1 tire is $(\frac{\partial x}{\partial V})$ (ΔV) or (8.17) (1.45) = 12 feet. For the RB-1 tire the net change in skidding distance is about 9.3 feet. For the asphalt and jennite surfaces, ΔV is smaller but the sensitivity $(\frac{\partial x}{\partial V})$ is larger than for concrete so that the change in skidding distance due to 0.25 second lockup time is about 7 feet. Thus, if lockup time is 0.25 seconds (which seems short), a 10-foot change in skidding distance is a reasonable estimate of the influence of lockup time on measured skidding distance at 30 mph. This effect is magnified for longer lockup times.

At 50 mph (73.3 ft/sec), the skidding distance sensitivities to initial velocity are greatly increased. For the A-1 tire on wet concrete, $(\frac{\partial x}{\partial V})$ = 41.7 ft/$_{ft/sec}$ and for the RB-1 tire, $(\frac{\partial x}{\partial V})$ = 11.3 ft/$_{ft/sec}$. These values mean skidding distance changes of 83 feet and 29 feet, respectively, due to 0.25 seconds of lock-up time.

Figure 1 shows a typical set of time histories produced in a simulation of a diagonal-braking, locked-wheel-stop from 50 mph on wet concrete. The longitudinal deceleration trace shows a high peak value at the beginning of the stop due to the high ratio of peak to slide longitudinal force near 50 mph. As the car slows down, the longitudinal deceleration gradually increases because the friction increases with decreasing velocity. Thus, in the first part of the stop before wheel lockup, there is a relatively large loss in velocity due to the high peak braking force and at the end of the stop the vehicle slows down more rapidly due to the change of friction with velocity.

It is of interest to compare test findings with results predicted by the hybrid simulation. The simulation of the complete tire-vehicle system as mechanized on a hybrid computer cannot

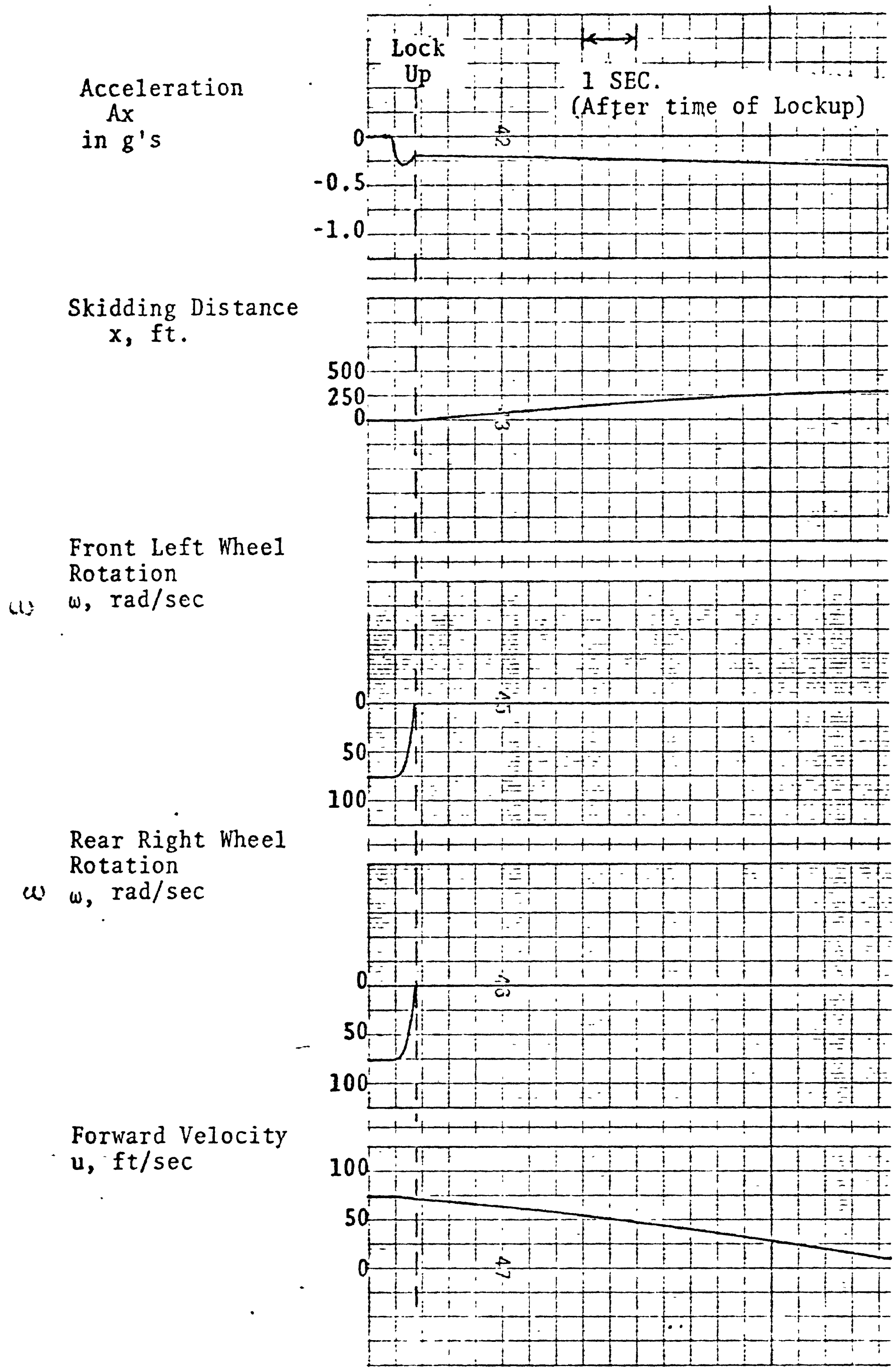

FIGURE 1. TYPICAL SIMULATION RESULT, DIAGONAL BRAKING LOCKED WHEEL STOP, RB-1 TIRE ON WET CONCRETE.

operate at zero or low velocities. Thus, to compute skidding distance the computation was stopped at 10 ft/sec and total skidding distance was obtained by estimating the additional skidding distance required to bring the vehicle to zero velocity (about 5 or 6 feet on wet concrete). The results obtained for a high-friction tire and a low-friction tire on wet concrete are:

Speed	Tire	Distance From Lockup To 10 ft/sec Velocity (ft)	Computed Total Skidding Distance (ft)	Measured Skidding Distance (ft)
30	A-1	117	123	128
30	RB-1	88	93	106
50	A-1	539	545	439
50	RB-1	290	295	346

These differences between computed and measured skidding distances are not surprising in light of the sensitivity of skidding distance to friction parameters and test conditions. Note that the total differential for Δx is expressed by:

$$\Delta x = \frac{\partial x}{\partial \mu_{ox}} \Delta\mu_{ox} + \frac{\partial x}{\partial A_x} \Delta A_x + \frac{\partial x}{\partial B_x} \Delta B_x + \frac{\partial x}{\partial W} \Delta W + \frac{\partial x}{\partial V_o} \Delta V_o$$

For example, on substituting the sensitivity values for the A-1 tire at 50 mph on wet concrete (see Table 21), we obtain

$$\Delta x = -3520\ \Delta\mu_{ox} + 217{,}000\ \Delta A_x + 4{,}410{,}000\ \Delta B_x - 0.0288\ \Delta W + 41.7\ \Delta V_o$$

Ten percent variations in μ_{ox}, A_x, and B_x (i.e., $\Delta\mu_{ox} \doteq .06$, $\Delta A_x \doteq .0008$, and $\Delta B_x \doteq .000004$) will lead to changes of approximately 200 feet, 170 feet, and 17 feet in x, respectively. A 1000 pound change in load yields a 28.8-foot change in skidding distance and a 2 ft/sec change in initial velocity yields an 83.4-foot change in skidding distance. Since the vehicle tests and tire tests were done at different times, the depth of water on the surface could have changed by a significant amount from one day to another day several months later.

The sensitivities for skidding distance are reduced at 30 mph. The total differential for the A-1 tire on wet concrete at 30 mph is:

$$\Delta x = -329\ \Delta\mu_{ox} + 10{,}700\ \Delta A_x + 412{,}000\ \Delta B_x - .00269\ \Delta W + 8.17\ \Delta V_o$$

For the same variations as before (i.e., $\Delta\mu_{ox} = .06$, $\Delta A_x = .0008$, $\Delta B_x = .000004$, $\Delta W = 1000$ lbs., and $\Delta V_o = 2$ ft/sec), the corresponding changes in Δx are approximately 20 feet, 8 feet, 2 feet, 2.7 feet, and 16.3 feet, respectively.

In summary, skidding distance is a difficult quantity to measure reliably and consistently because very careful controls on initial velocity and road surface conditions are required. The sensitivity of skidding distance to these test conditions increases as speed increases. Since the locked wheel tire longitudinal shear force increases significantly as velocity decreases, it is necessary to test a tire at several speeds to predict skidding distance with reasonable accuracy. One might be better advised to work with deceleration rather than skidding distance.

2.4.2. ANALYSIS AND SIMULATION OF J-TURN MANEUVERS. An analysis of the J-turn is complicated since it involves solving highly non-linear differential equations. An exact solution is best obtained by computer simulation. However, a simple closed form analysis is valuable for understanding the maneuver, for predicting approximate results, and for evaluating the influence of variations in the test conditions.

In the development presented in Appendix 5, it is assumed that the lateral acceleration for a limit velocity steady turn can be equated to the maximum lateral acceleration the tire forces can produce. The resulting equation is:

$$\frac{V_L^{\,2}}{R} = g\left(\mu_y - \frac{\mu_y^{\,2}\, W}{16\, C_\alpha \tan \alpha_p}\right) \tag{13}$$

where

V_L is the limit velocity

R is the path radius of curvature

μ_y is the lateral friction expression

W is the weight of the vehicle

C_α is the cornering stiffness of the tires

and α_p is the slip angle for maximum tire force.

Examination of the tire data indicates that 8° is a rough approximation to α_p for these tires on these surfaces. The lateral friction coefficient is expressed as

$$\mu_y = \mu_{oy} - A_y V_L \tan \alpha_p - \frac{B_y W}{4} \tag{14}$$

Equation (13), in combination with Equation (14), has been solved for all 10 tires on each of the 3 surfaces to obtain V_L. These results are given in Table 22, Appendix 5. Further, Equations (13) and (14) have been differentiated to obtain the rate of change of

V_L with μ_{oy}, A_y, B_y, C_α and W. The values of these sensitivity coefficients are presented in Table 22, Appendix 5.

The limit velocity predicted by the simple analysis with the aid of tire test data is compared in Table 10 with the test results obtained by NBS. It is seen that the calculated limit velocity is about 10% higher than the measured limit velocity. There is some reordering in the relative ranking of the tires, but the rank correlations between measured and computed results (0.824 for wet concrete, 0.852 for wet asphalt, and 0.782 for wet jennite) are fairly high.

The values of the sensitivity coefficients indicate that the J-turn limit velocity, V_L, is fairly insensitive to A_y, B_y, and C_α and that it is sensitive to μ_{oy} and W. Typically, a 5% change in μ_{oy} produces close to a 2 ft/sec change in V_L. This maneuver does not appear to be as sensitive to test conditions as the skidding distance test.

It is interesting to note that V_L varies approximately as the square root of the tire lateral force, F_y. Thus, for the same percentage resolution in F_y as in V_L a better ranking of tires can be obtained by using F_y rather than by using V_L.

A more exact analysis of the J-turn was made with the aid of a hybrid computer simulation [6] of the SSL '68 Belair Chevrolet. The simulation, developed in an earlier study performed for NBS [2], was revised to compute tire force characteristics on the digital computer. This change permitted a more complex representation of the side force characteristics of the tires. The values of C_α given in Tables 17 and 18 were used in these calculations. The friction μ_y was treated as a function of speed and load as given by (8), with μ_{oy}, A_y, and B_y as tabulated in Table 19, Appendix 3.

TABLE 10. J-TURN LIMIT VELOCITY COMPARISON

Surface	Tire	Measured Velocity (MPH)	Measured Velocity (ft/sec)	Rank	Idealized Calculation (ft/sec)	Rank
Concrete	A-1	38.7	56.8	10	71.1	10
"	A5-1	41.0	60.1	9	73.8	8.5
"	A-5	45.0	66.0	6	73.8	8.5
"	RB-5	48.3	70.9	1	75.6	3
"	RB-1	47.0	69.0	4	79.5	1
"	H-5	48.0	70.4	2	79.2	2
"	D-2	41.3	60.5	8	74.9	5.5
"	WA-5	43.0	63.0	7	74.4	7
"	WA-9	47.5	69.6	3	75.1	4
"	S-2-47	46.0	67.5	5	74.9	5.5
Asphalt	A-1	39.0	57.1	10	65.0	10
"	A5-1	42.0	61.6	8.5	71.3	7.5
"	A-5	45.3	66.4	5	75.8	2.5
"	RB-5	47.7	70.0	3	73.5	5
"	RB-1	47.0	69.0	4	74.9	4
"	H-5	48.0	70.4	2	77.4	1
"	D-2	42.0	61.6	8.5	71.3	7.5
"	WA-5	43.5	63.7	7	73.0	6
"	WA-9	48.5	71.1	1	75.8	2.5
"	S-2-47	45.0	66.0	6	67.4	9
Jennite	A-1	34.1	50.0	10	59.4	9
"	A5-1	37.5	55.0	6.5	60.2	8
"	A-5	37.5	55.0	6.5	56.7	10
"	RB-5	40.5	59.4	3	62.2	5
"	RB-1	41.0	60.1	2	64.8	2
"	H-5	41.5	60.8	1	69.2	1
"	D-2	36.3	53.2	9	60.5	7
"	WA-5	37.5	55.0	6.5	61.7	6
"	WA-9	39.7	58.2	4	62.3	4
"	S-2-47	37.5	55.0	6.5	63.8	3

In simulating the J-turn manevuer as conducted by NBS, two questions arise: (1) What is the proper steering wheel input? and (2) How is "breakaway" determined analytically? In the vehicle tests, the driver finds the proper steering input to execute the 288-foot radius turn marked on the skid pad. Apparently, he is able to do this after considerable practice. Clearly, to simulate this maneuver, a steering time history has to be specified. An examination of uncalibrated recordings of steering wheel angle showed that the form and duration of the driver's steering input is a waveform that can be approximated by a filtered ramp-fronted step function. By increasing the final amplitude of this waveform, vehicle turns of decreasing radius of curvature can be generated and an input signal producing roughly a 288-foot radius turn can be found. However, a different input is required for different vehicle speeds and different tire-surface combinations. See Appendix 6 for a detailed presentation and discussion of the J-turn simulation.

Two types of "breakaway" response were found. An example of a breakaway which is characterized by a divergent yaw rate response is shown in Figure 2 for the A-1 tire on wet concrete. This tire had the lowest J-turn limit velocity in the idealized calculation (Table 10). In contrast for the RB-1 tire, which had the highest calculated limit velocity on wet concrete (Table 10), the yaw rate signal developed an oscillatory behavior as shown in Figure 3. Note that the lateral acceleration signal shows a "dip" and then increases again. (This is the criteria used by NBS to identify breakaway.) The vehicle develops a very large sideslip angle (lateral velocity, v, large) during the first part of the turn. The oscillation in the yaw rate signal is large. Presumably this result would be upsetting to the driver and he would try to steer to eliminate the resulting oscillations in lateral velocity and yaw rate. This type of response was not anticipated and its occurrence makes "breakaway" more difficult

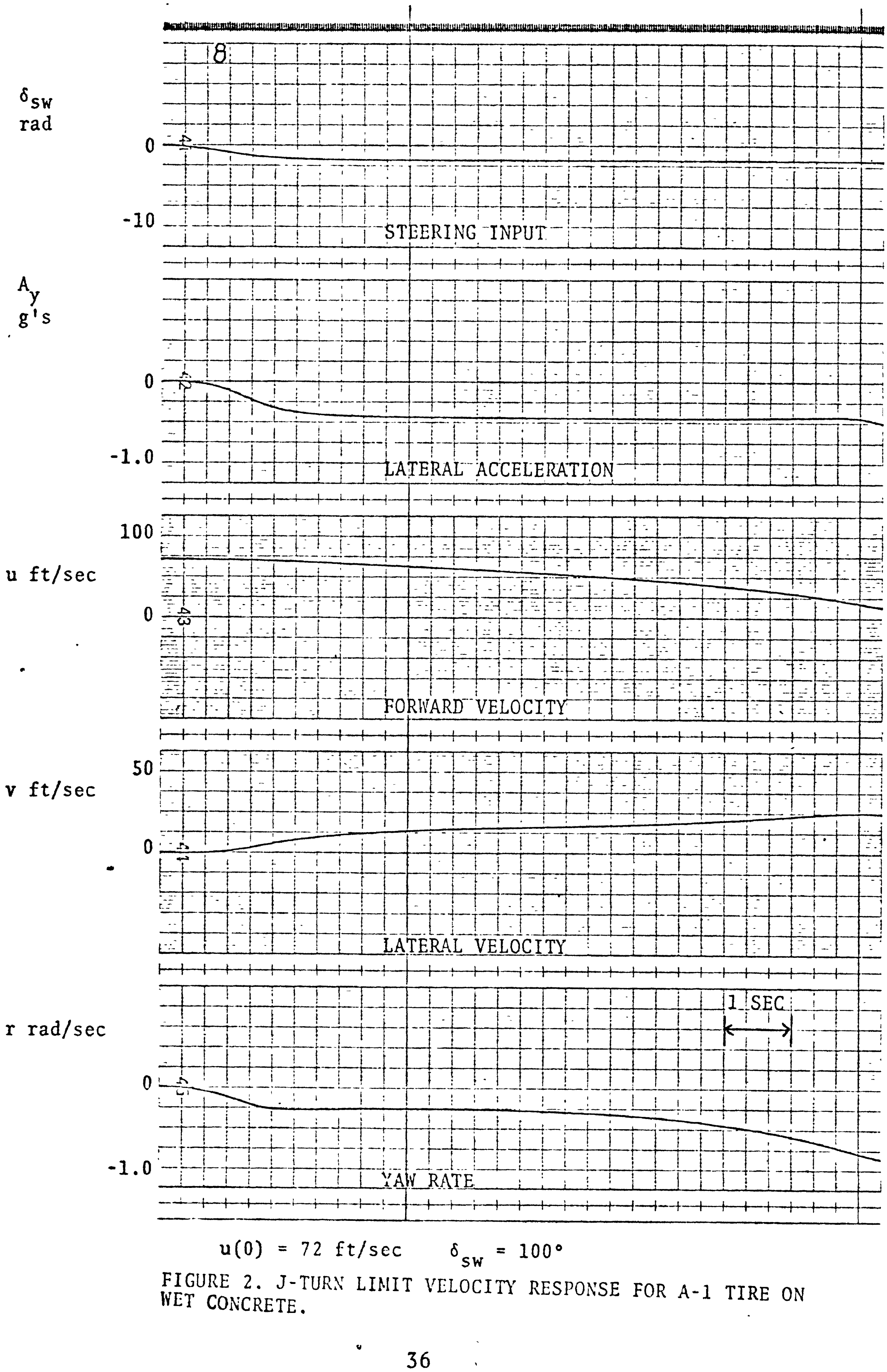

$u(0) = 72$ ft/sec $\quad \delta_{sw} = 100°$

FIGURE 2. J-TURN LIMIT VELOCITY RESPONSE FOR A-1 TIRE ON WET CONCRETE.

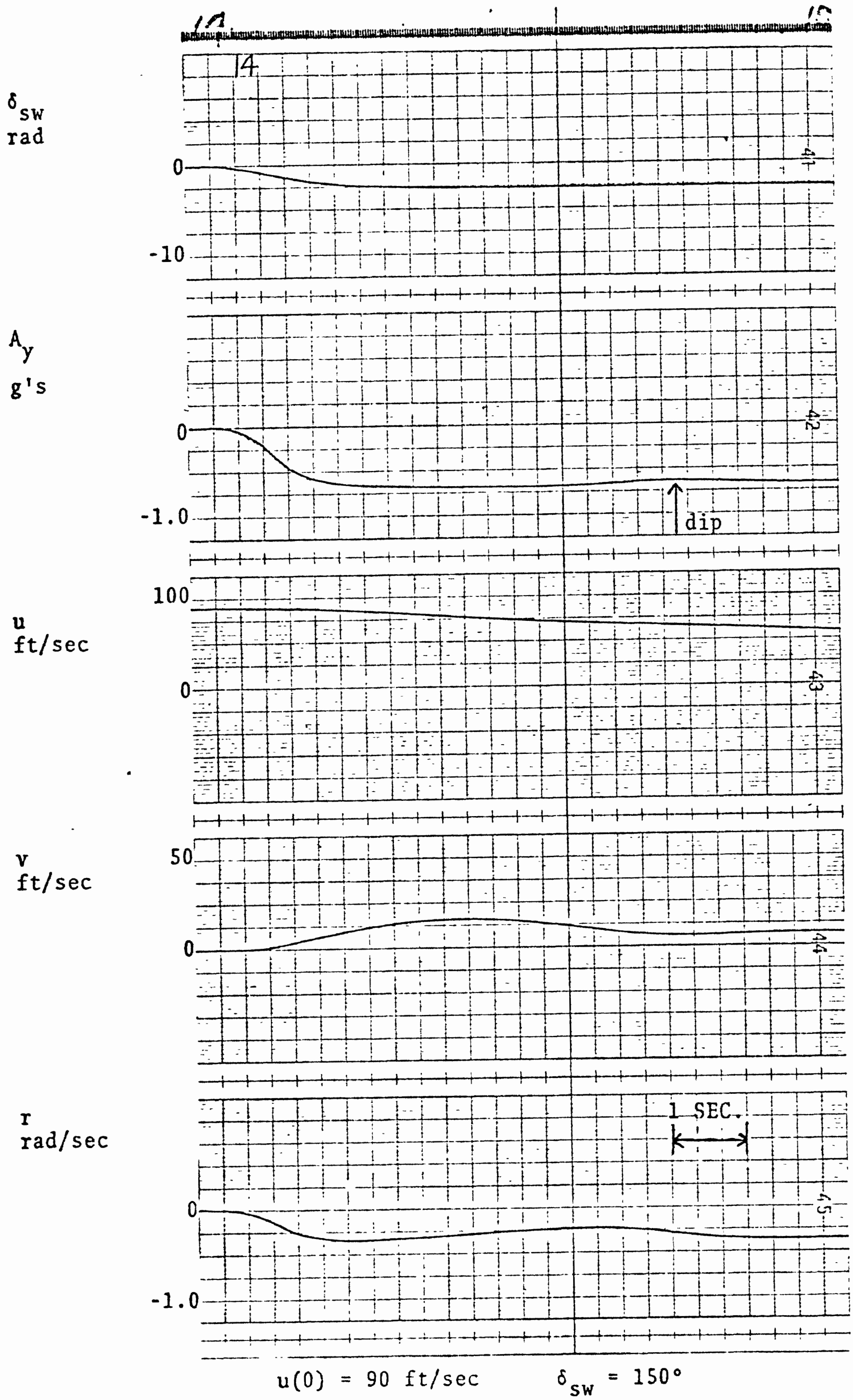

FIGURE 3. J-TURN RESPONSE FOR RB-1 TIRE ON WET CONCRETE.

to determine than in cases in which the yaw rate simply diverges. Even though the response of the vehicle is very oscillatory, the trajectory is reasonably smooth and the vehicle, in all likelihood, would not go out of control if the driver did not try to steer after the steady steering angle was established.

In the J-turn maneuver, the steering input required and the criterion for observing breakaway are not clearly understood. An open-loop steering command or sequence of commands adjusted to speed, and possibly to radius of curvature, would serve to make the test more objective. A criterion based on quantitative measures of yaw rate and/or lateral acceleration (or some other measurable quantity) is needed to establish breakaway in an objective manner.

Given the lack of one-to-one correspondence between simulation runs and tire-vehicle system tests, the simulation was not used to see if changes in the vehicle parameters (i.e., a different vehicle) would produce a different rank ordering of the tires. However, computer runs were made to illustrate how differences in certain vehicle parameters and test conditions influence the results for the A-1 and RB-1 tires. (See Appendix 6.) The results obtained are as follows:

(1) When the vehicle center of gravity is moved rearward by 5% of the wheel base, the yaw rate response for the A-1 tire on wet concrete changes from a divergent character to an oscillatory response. This result is interesting in that it appears that the oscillatory yaw rate response is a bounded non-linear oscillation. The linearized version of the vehicle is unstable for small perturbations about the steady turn operating conditions but due to the non-linear tire characteristics a bounded yaw rate oscillation is maintained.

(2) When the vehicle center of gravity is moved forward by 5% of the wheelbase, the yaw rate response for either the A-1 or the RB-1 tire does not change appreciably.

(3) When the total roll stiffness of the vehicle is held constant but the front and rear roll stiffnesses are made equal, the vehicle develops a much larger side-slip angle than before, but the nature of the yaw rate response is unchanged.

(4) When the total roll damping of the vehicle is doubled, the change in vehicle response is negligible for either the A-1 or the RB-1 tire.

(5) When the J-turn is done at constant throttle rather than at closed throttle, the path curvature does not increase as rapidly at the end of the turn as it does for the closed throttle condition. Thus, by maintaining the throttle it is easier to stay near a constant radius path. Closing the throttle has the advantages that throttle position need not be controlled by the driver and that the interaction between tire longitudinal and lateral force cannot influence the test result.

(6) The nature of the yaw rate response for the A-1 tire changes from surface to surface. The yaw rate response is oscillatory on the asphalt surface and it is divergent on the concrete and jennite surfaces.

The nature of the yaw response for the RB-1 tire is oscillatory on the concrete and jennite surfaces and divergent on the asphalt surface.

Apparently, for a given tire, the type of yaw rate response depends upon the surface. On one surface an oscillatory response may be obtained while on another a divergent response may occur. An examination of the friction parameters for the A-1 tire and for the RB-1 tire on three surfaces indicates that the different types of yaw rate response are due to the parameter B_y. For a large value of B_y a divergent yaw rate response was obtained while for a small value of B_y an oscillatory yaw rate response was obtained. Thus on each test surface tire lateral shear force measurements at several vertical loads are required to obtain the data necessary to predict vehicle response during a J-turn maneuver.

In conclusion, there are many combinations of tire parameters, input waveforms, vehicle parameters, and surface conditions which have not been studied. Clearly, the number of possibilities which can be considered is enormous. Hopefully, the cases treated herein will help explain the results that have been obtained in both J-turn and skidding distance tests.

3. RECOMMENDATIONS

3.1. ELEMENTS OF AN INTERIM TIRE TRACTION GRADING PROCEDURE

Even though further work is recommended in Section 3.2, it is of considerable interest to address the question: what would constitute a reasonable interim method of rating tire traction quality? A complete specification of an interim method of rating tire traction quality will not be attempted here, but, based on the results of this study, a partial list of the elements of a preliminary method for rating tire traction quality will be presented.

First, tire tests should be made on at least 2 surfaces corresponding to the asphalt and concrete skid pads used in this program, because the rate of change of longitudinal friction with speed, that is, A_x, is smaller on the asphalt pad (with course macro-texture) than on the concrete or jennite pads and because it is difficult to obtain results without a relatively large amount of scatter on the jennite surface.

Second, tires should be tested for rating both longitudinal and lateral friction characteristics in order to demonstrate how they will perform in rapid stopping and turning maneuvers.

The results of this study show that peak lateral tire shear force correlates well with limit velocity in a J-turn maneuver. The results show that changes in the vertical load on the tires can change the nature of the limit J-turn response. Thus, a measure of the peak lateral force at all slip angles at rated load and the change of peak lateral force with vertical load, that is, B_y, could serve to rate the lateral friction capability of a tire. Also, since the limit velocity changes with the radius of the curve attempted, it is worthwhile to measure the rate of change of lateral friction with velocity, that is, A_y.

In this study, vehicle skidding distance was shown to be highly dependent upon the rate of change of locked-wheel longitudinal friction with sliding velocity. Thus, longitudinal friction should be measured at 3 or more speeds in order to obtain values of μ_{ox} and A_x which can be used to predict skidding distance. It has been pointed out that skidding distance does not test the peak longitudinal force capability of a tire on a wet surface and that skidding distance is a difficult quantity to measure. The peak longitudinal friction of a tire and its rate of change with velocity are important measures of tire performance which are directly related to the maximum stopping capability of a vehicle. Thus a curve of longitudinal force versus longitudinal slip at rated load should be measured to allow the ratio of peak to slide longitudinal force to be used in determining μ_{ox} and A_x for a given tire.

Clearly, these specific recommendations are based on the premise that tires should be tested and rated to ensure that vehicle performance with these tires can be assessed. In conclusion, a method of rating tire traction which is related to rapid straight-line stopping and to making a limit-velocity turn could be developed in a short time and it could be readily performed with modern tire testing equipment (e.g., the mobile tire tester).

3.2. FUTURE WORK

The specific recommendations presented here were derived to a large extent from the following general recommendations:

(1) Tire tests should be used to rate tires, thereby removing the possibility that the results are influenced by the particular driver-tire-vehicle system used.

(2) Those tire characteristics which can be shown to correlate with vehicle performance in limit maneuvers that are related to accident avoidance situations should be used to rate tire traction quality.

(3) The tire test results should be reduced to numerical descriptors which can be used not only to rank tires but predict differences in tire-vehicle system performance in limit maneuvers.

(4) The number of descriptors and the tire tests needed to obtain these descriptors should be minimized in order to obtain an economically practical method of rating tire traction quality.

(5) The tire descriptors should reflect different surface characteristics and they should apply to as many road surfaces as possible.

At this time, given the current state of tire shear force measurement technology, modeling of tire shear force generation, and vehicle dynamics knowledge concerning limit maneuvers, it is not possible to define a rational method for identifying, quantifying and rating the limit-traction performance of tires in a manner which completely satisfies these general recommendations. In order to fill in some of the gaps in the understanding of tire traction quality that currently exist it is recommended that:

(1) A survey should be made to provide a quantified data base of the range of tire shear force performance existing in the current tire population.

(2) A study of the influence of different road surfaces on the wet shear force performance of pneumatic tires should be made to develop a numeric or a set of numerics for quantifying road surface characteristics.

(3) A research program should be conducted to extend the existing state of knowledge of the influence of tire characteristics on the limit performance response of a motor vehicle in the following open-loop maneuvers:

(a) straight-line braking
(b) step steer
(c) braking in a turn
(d) lane change
(e) drastic brake-steer

Once the tire characteristics which are most important in steering, braking, and combined steering and braking maneuvers have been identified, then they can be quantified, average, and/or combined to produce a set of tire traction quality descriptors. Clearly, this process is of prime interest in selecting an efficient tire traction quality grading system which relates to the limit maneuvering performance of motor vehicles.

Data on the characteristics of the current tire population and an enhanced understanding of the mechanisms of tire-shear force generation may lead to ways of relating longitudinal and lateral friction and thereby reducing the number of tire tests required. Research on the influence of tire characteristics in other accident avoidance maneuvers may lead to indications of the need to measure other tire characteristics, particularly combined longitudinal and lateral shear force. Further study of the influence of surface characteristics could lead to another approach to the problem of specifying the surface or surfaces for rating tire traction quality.

Admittedly, the recommended interim method will be of limited scope until further knowledge of tire shear force generation and of the influence of tires on accident avoidance maneuvers can be obtained. Then, hopefully, the number of tire tests can be reduced while the scope of applicability of the results is increased.

APPENDIX 1

TIRE DATA PLOTS

This appendix contains the tire force data obtained on the 10 tires listed in Table 1. Each graph is labelled in a self-explanatory manner. Due to the wide variety of possible interests, the data are presented for the reader's perusal without interpretation.

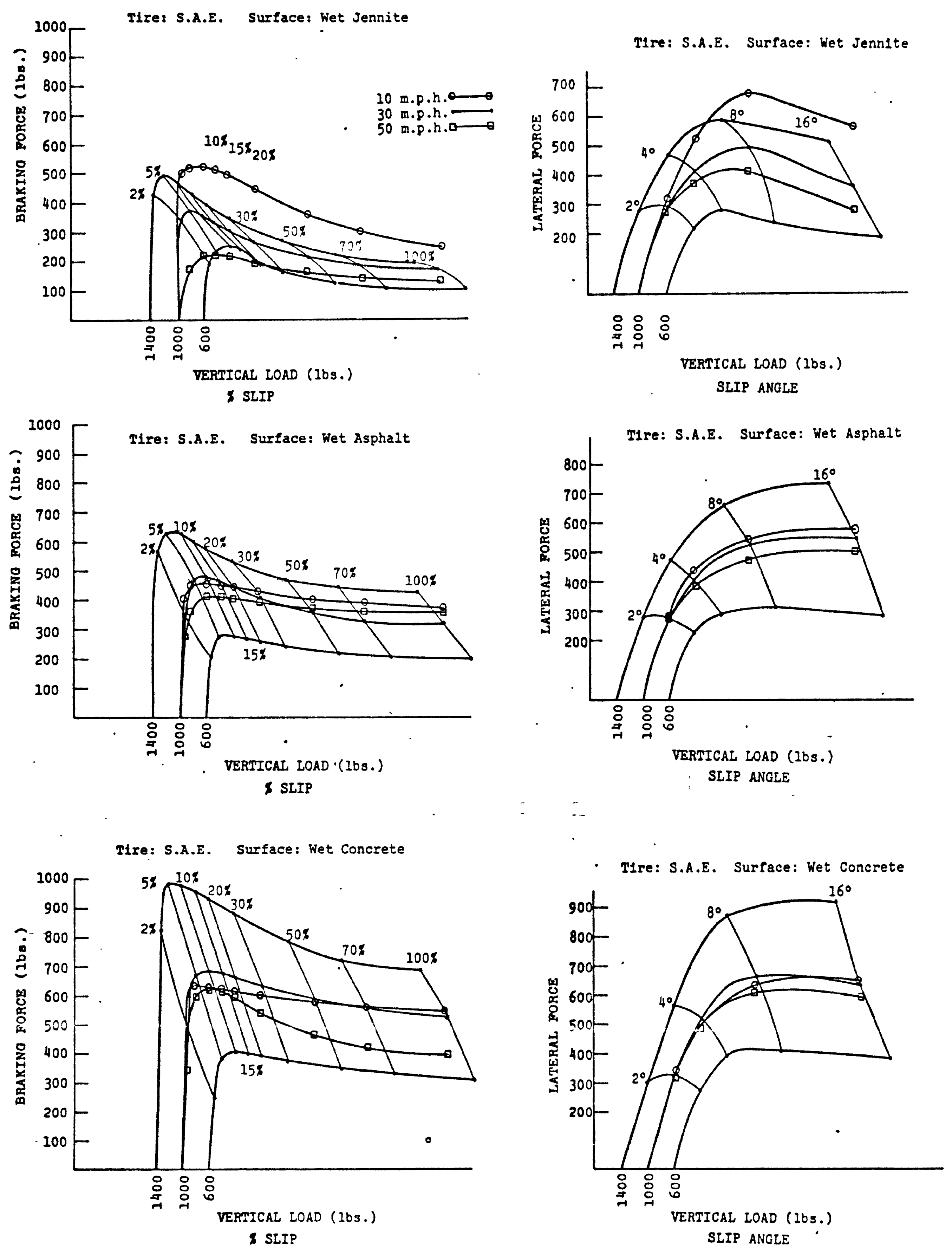

Figure 4. Longitudinal and Lateral Force
S-2-47 Tire (S.A.E. Reference Tire)

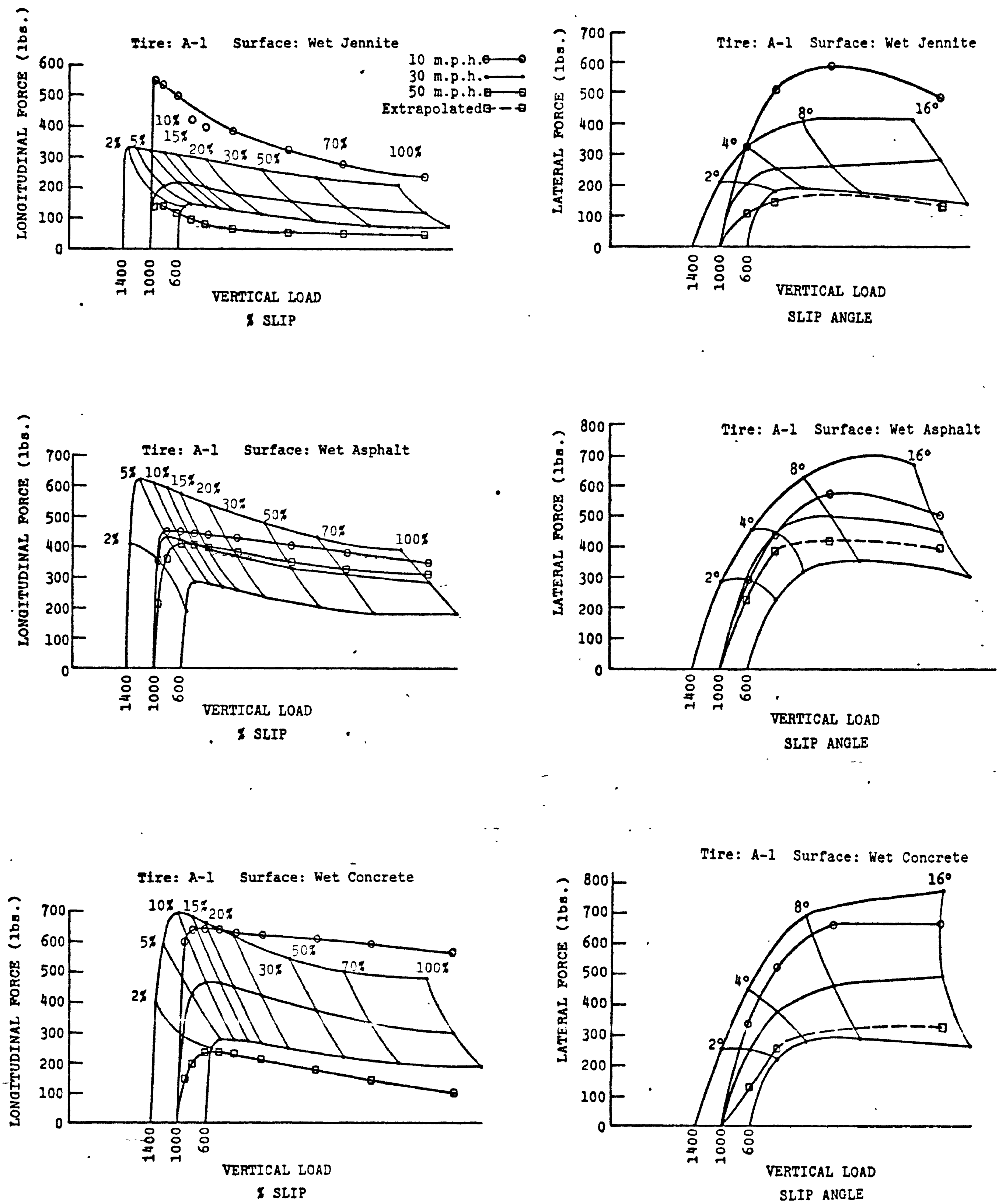

Figure 5. Longitudinal and Lateral Force
A-1 Tire

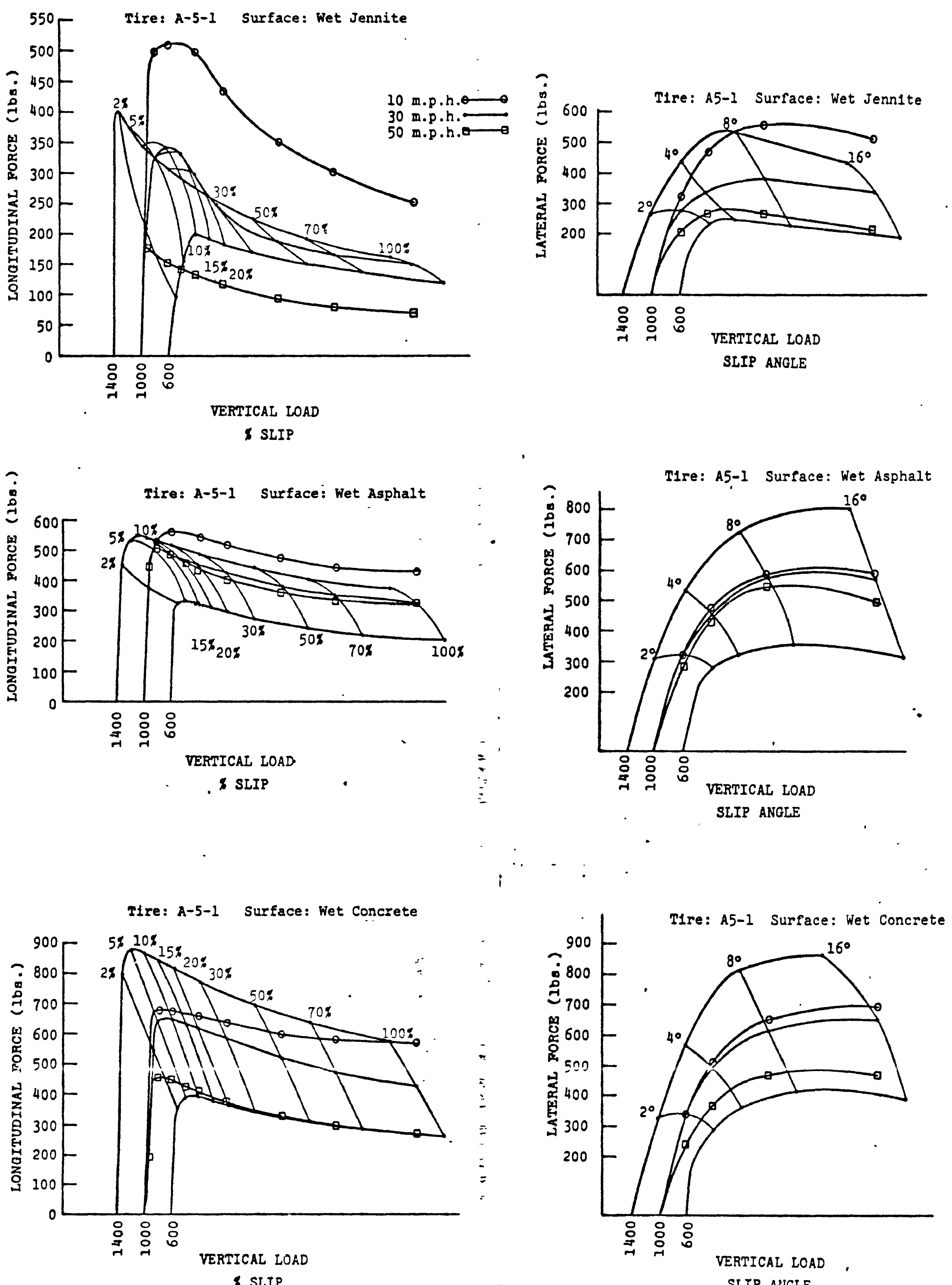

Figure 6. Longitudinal and Lateral Force
A-5-1 Tire

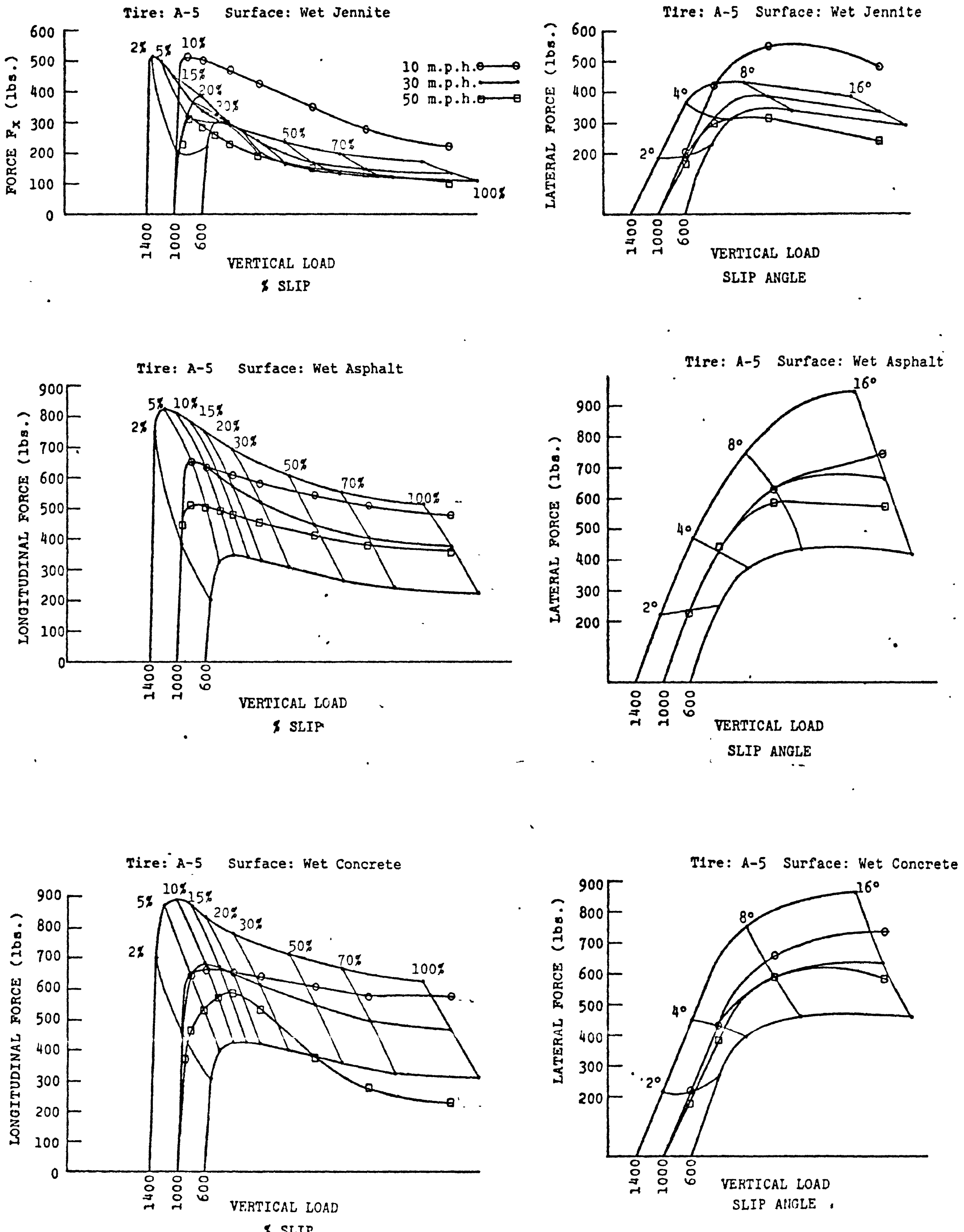

Figure 7. Longitudinal and Lateral Force
A-5 Tire

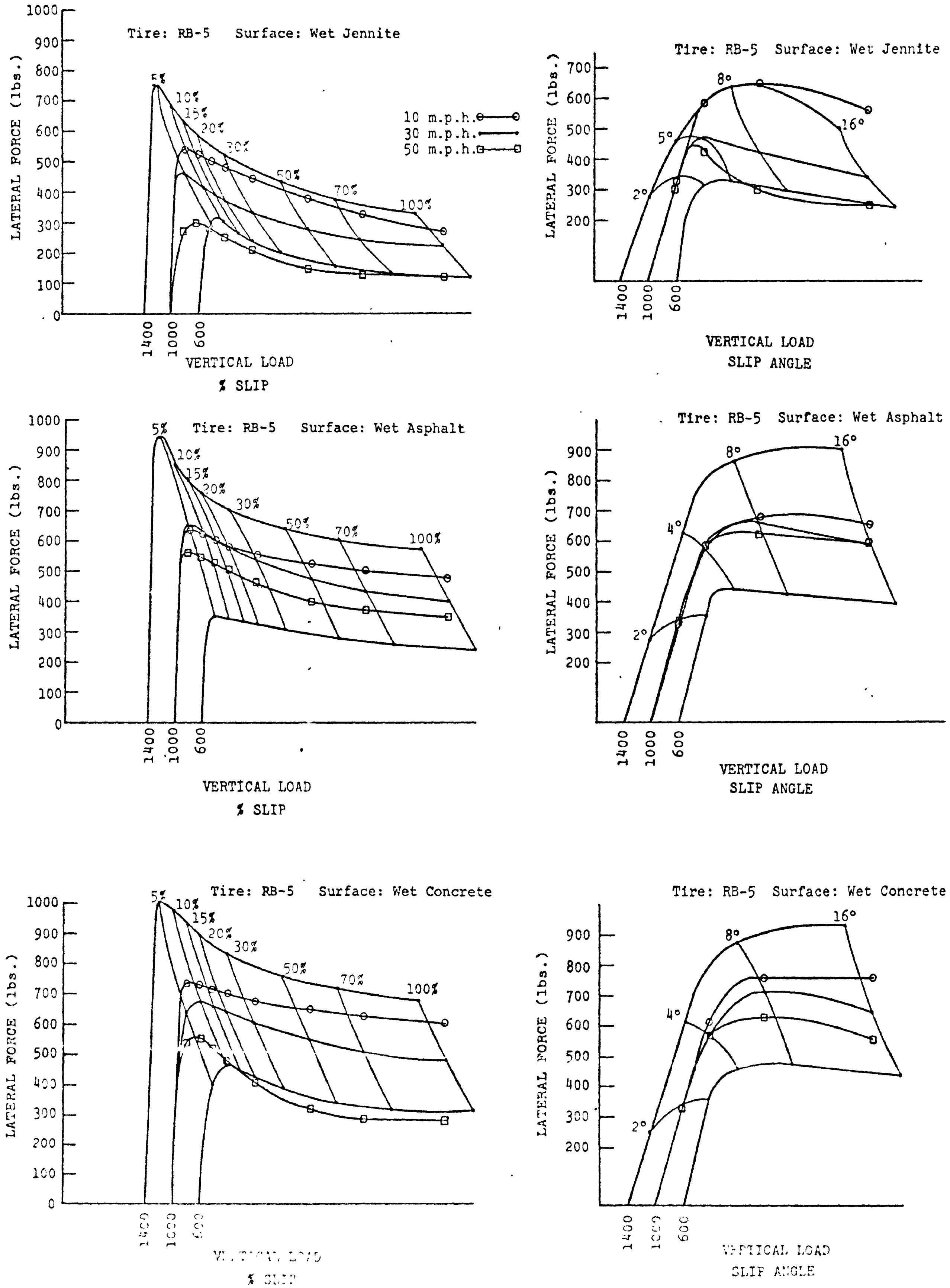

Figure 8. Longitudinal and Lateral Force
RB-5 Tire

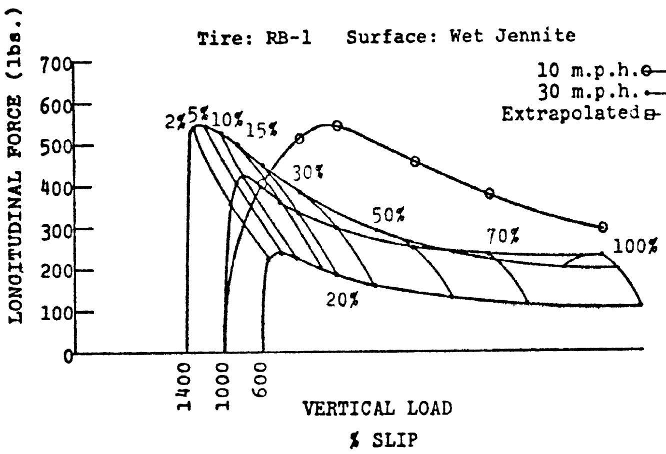

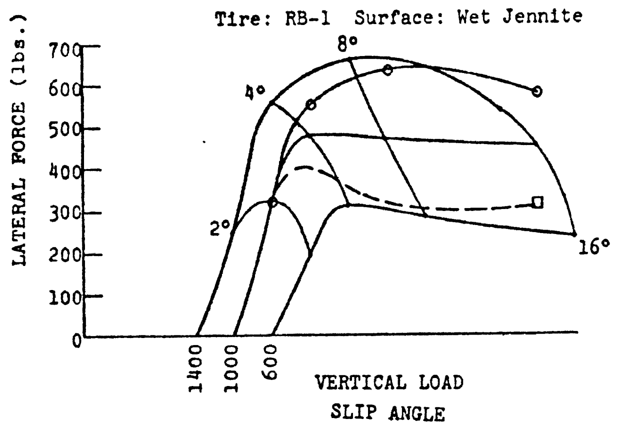

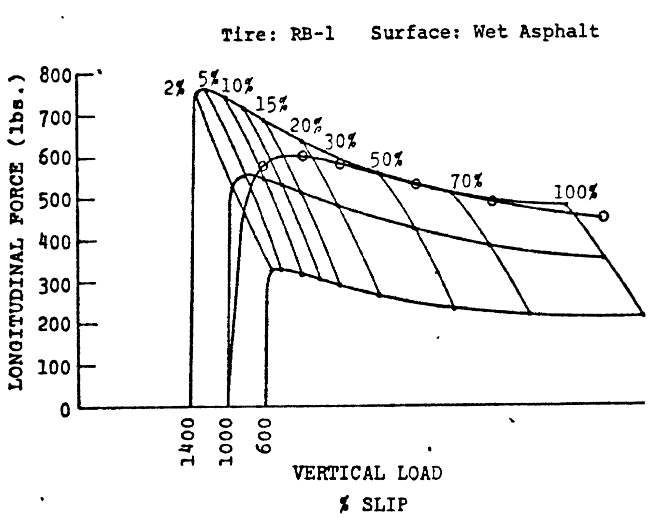

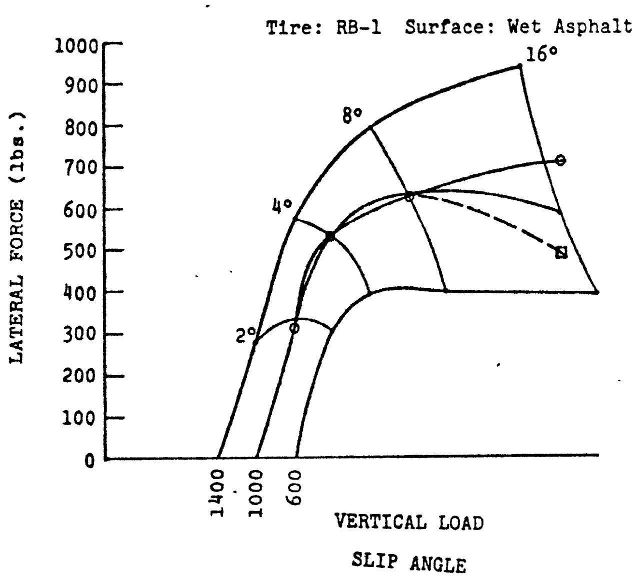

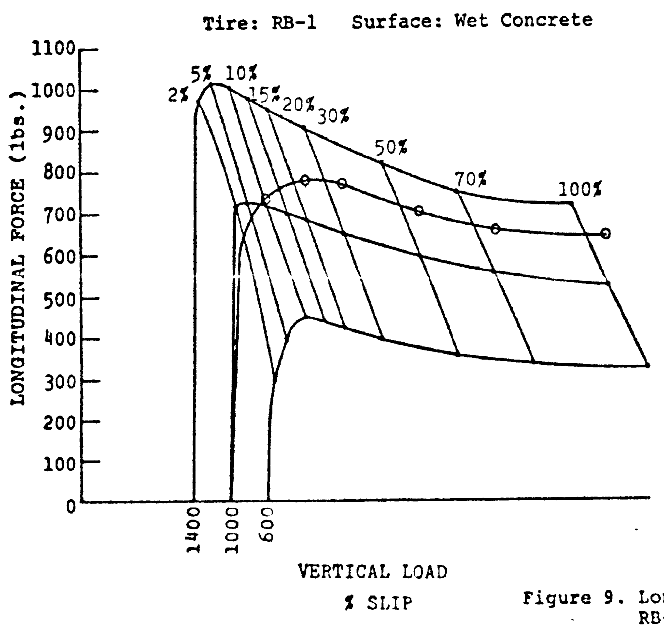

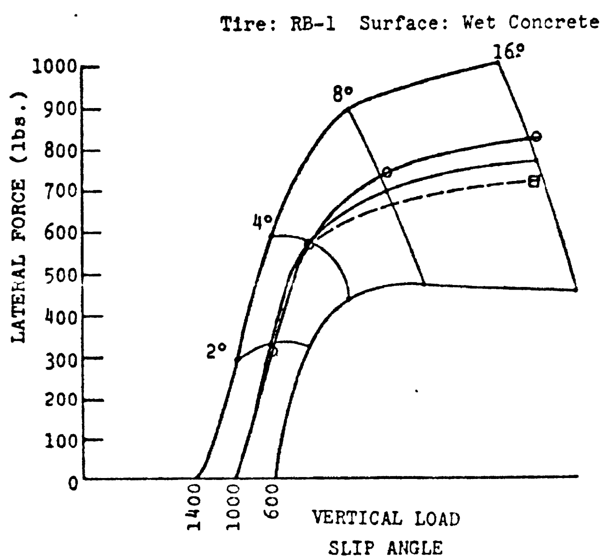

Figure 9. Longitudinal and Lateral Force
RB-1 Tire

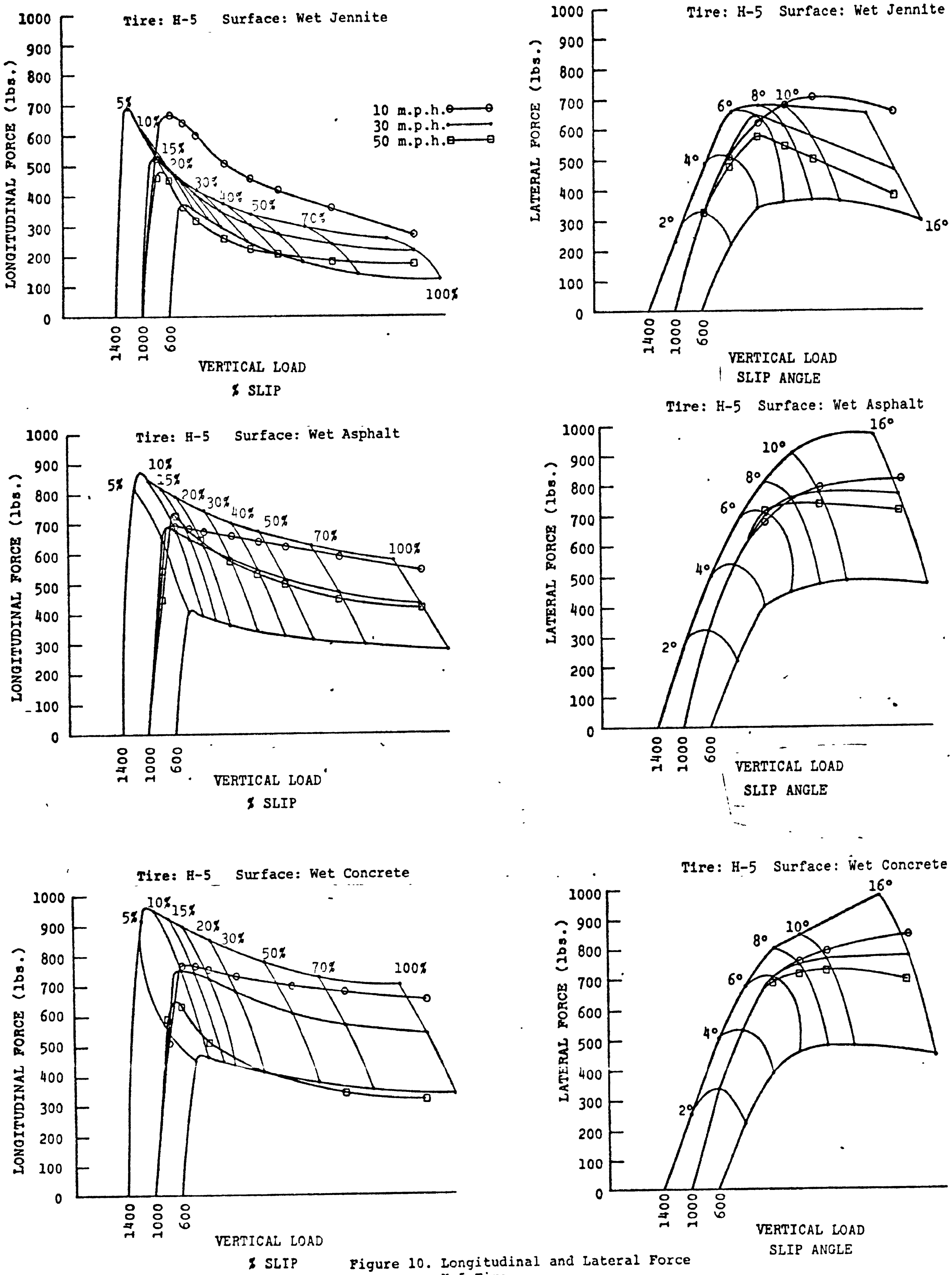

Figure 10. Longitudinal and Lateral Force H-5 Tire

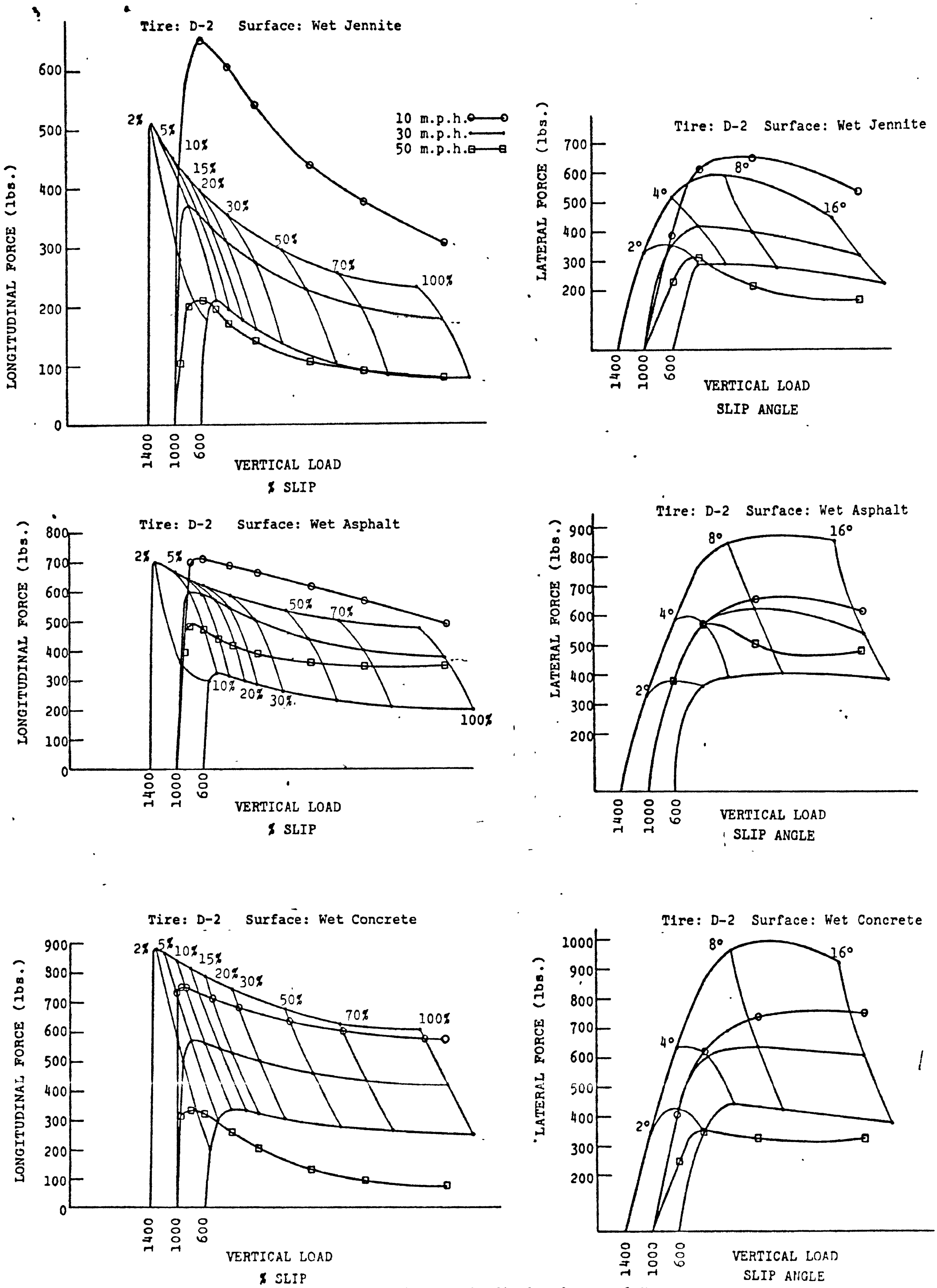

Figure 11. Longitudinal and Lateral Force
D-2 Tire

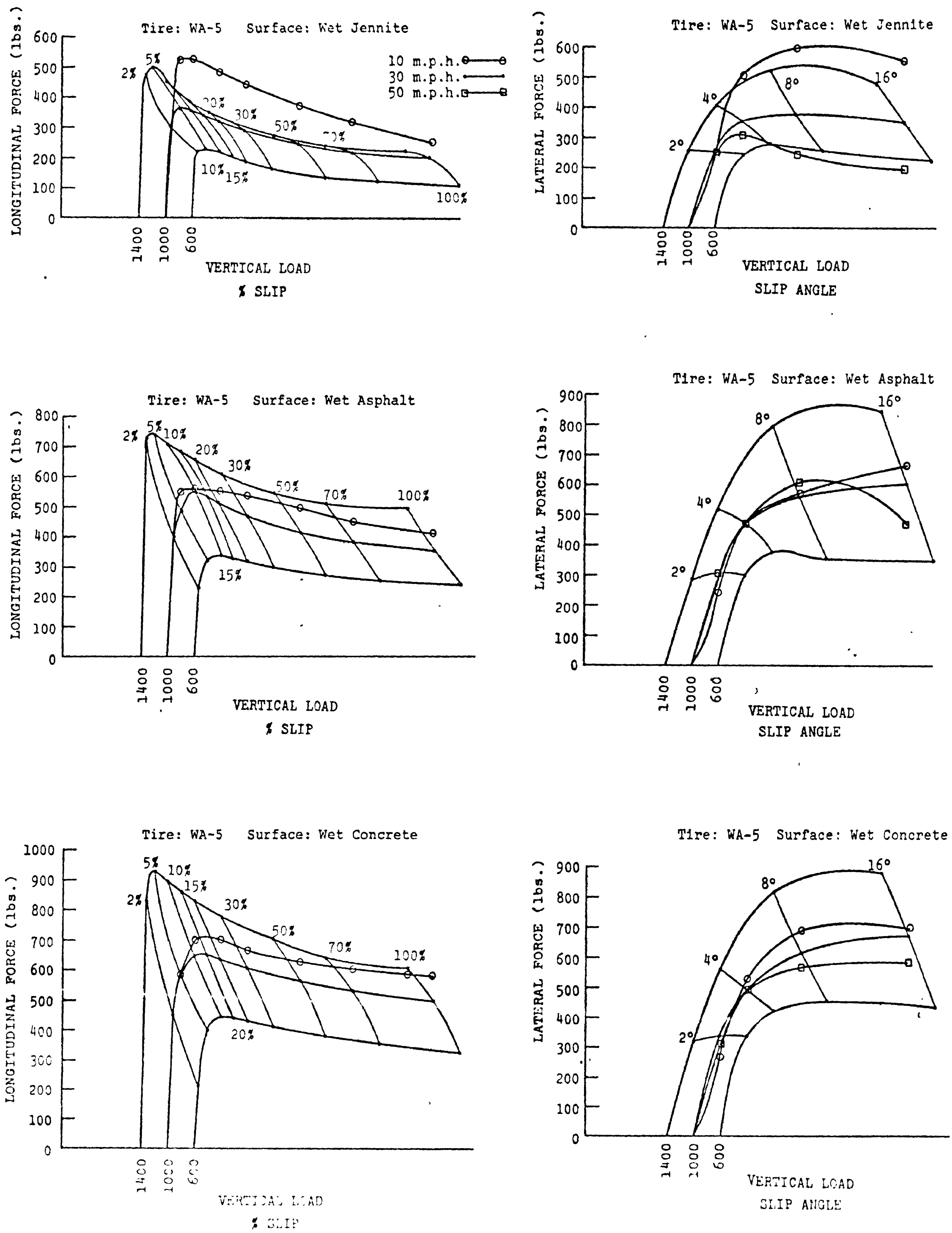

Figure 12. Longitudinal and Lateral Force
WA-5 Tire

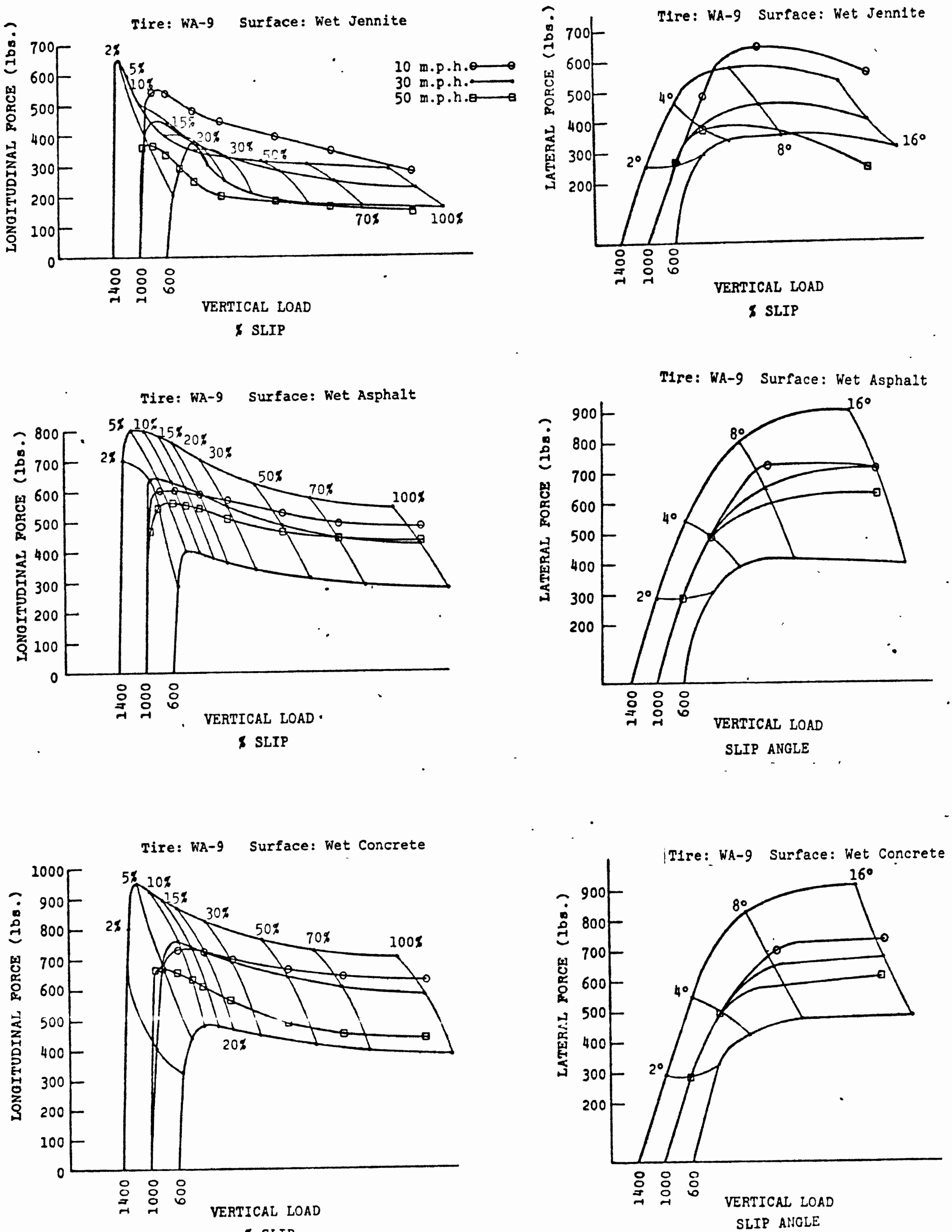

Figure 13. Longitudinal and Lateral Force
WA-9 Tire

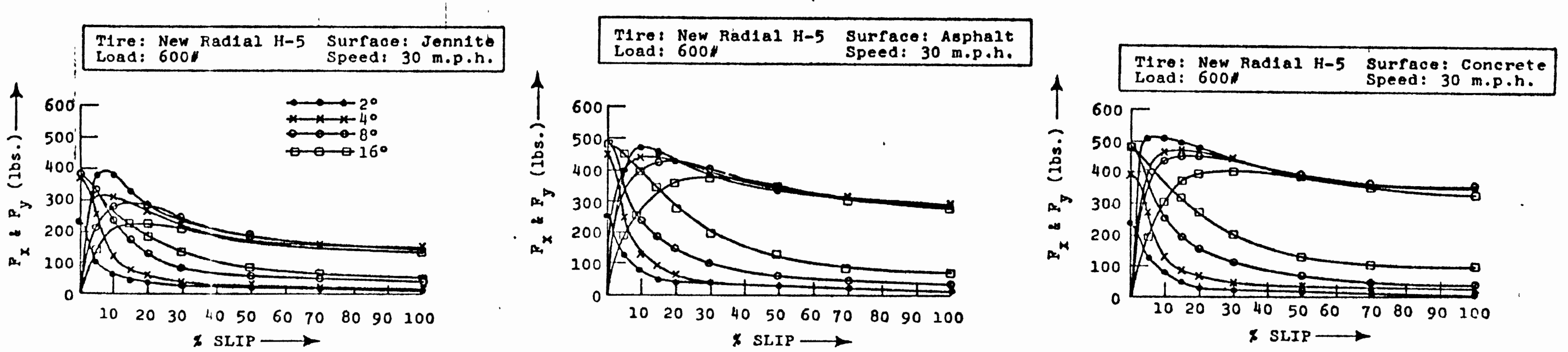

Figure 14a. Wet Traction Field - H-5 Tire

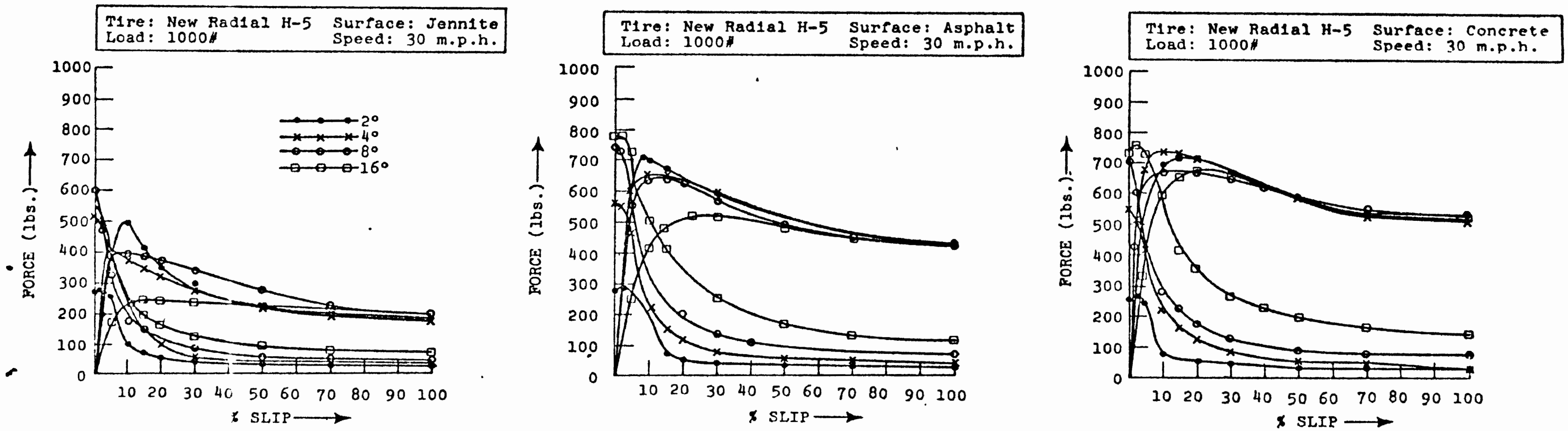

Figure 14b. Wet Traction Field - H-5 Tire

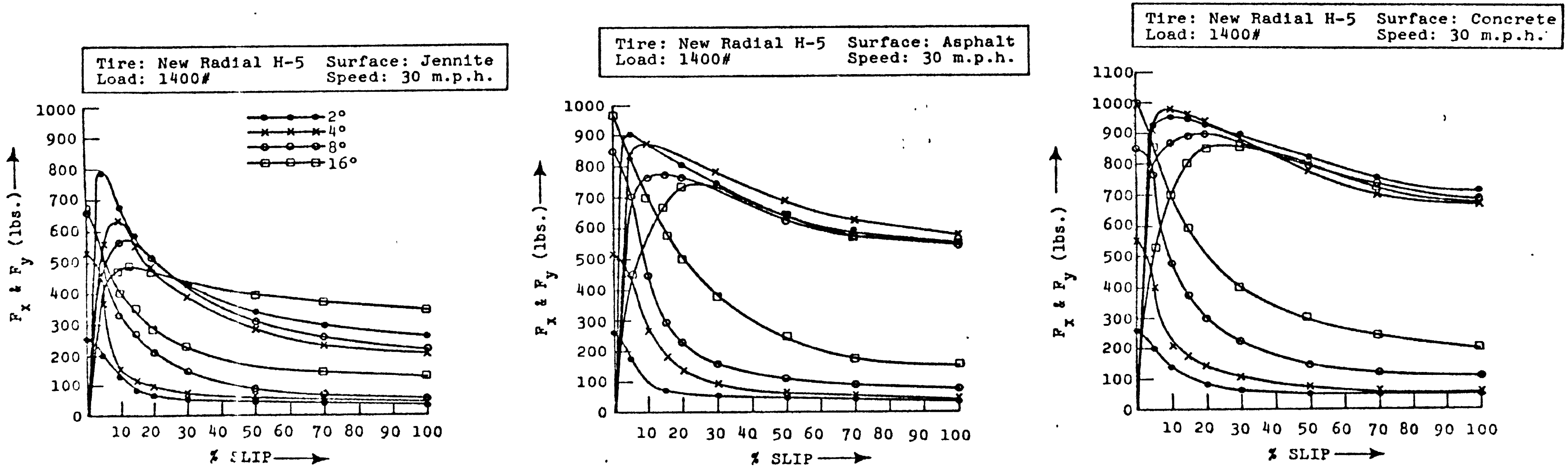

Figure 14c. Wet Traction Field - H-5 Tire

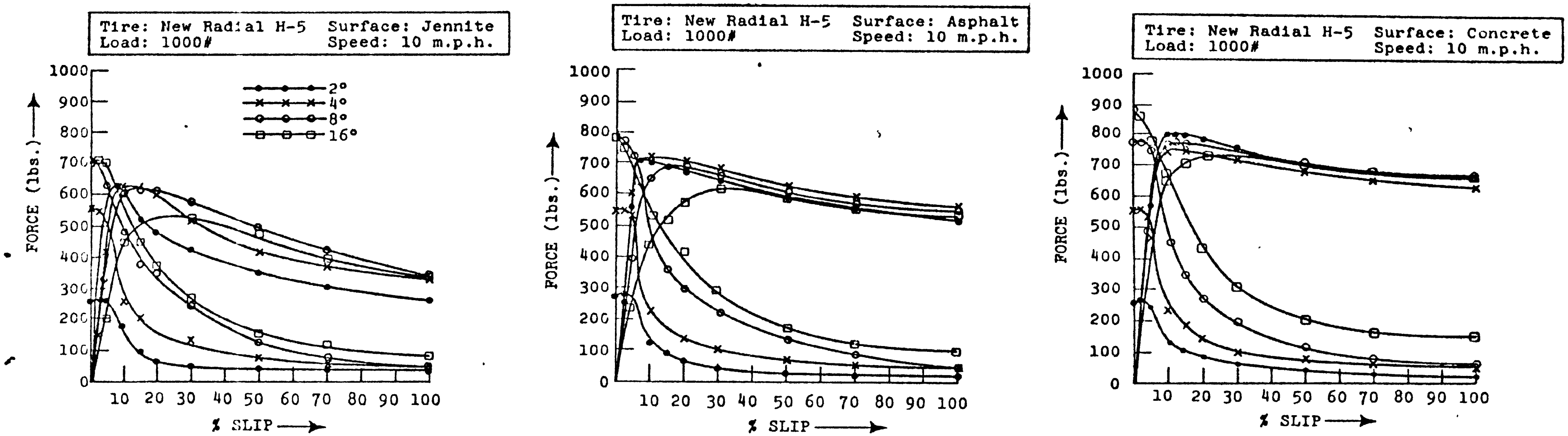

Figure 14d. Wet Traction Field - H-5 Tire

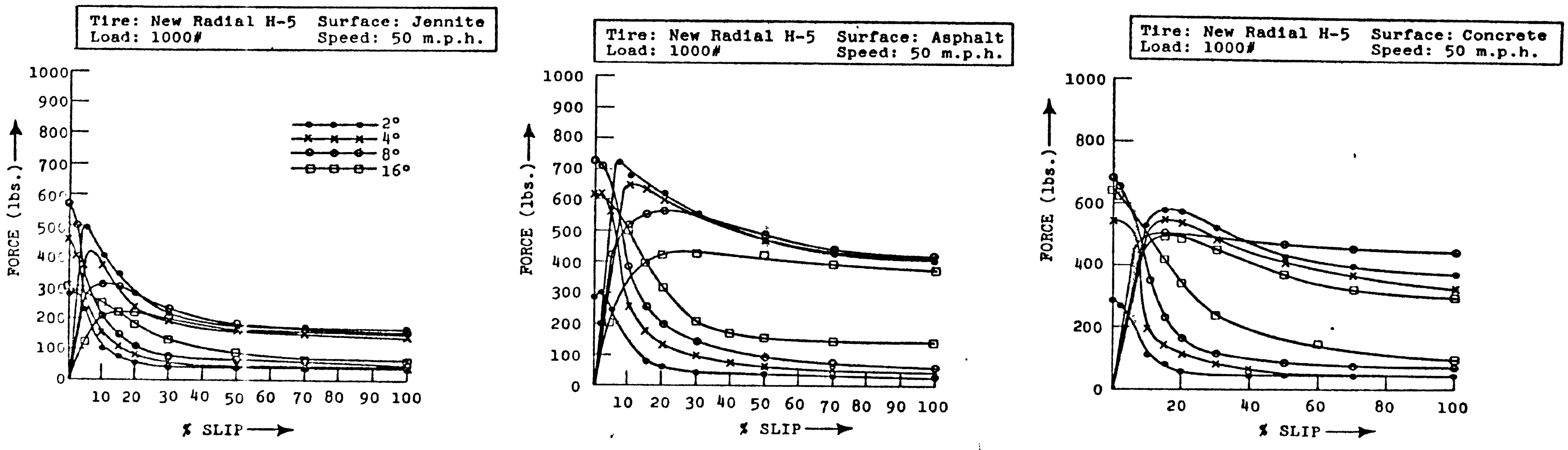

Figure 14e. Wet Traction Field - H-5 Tire

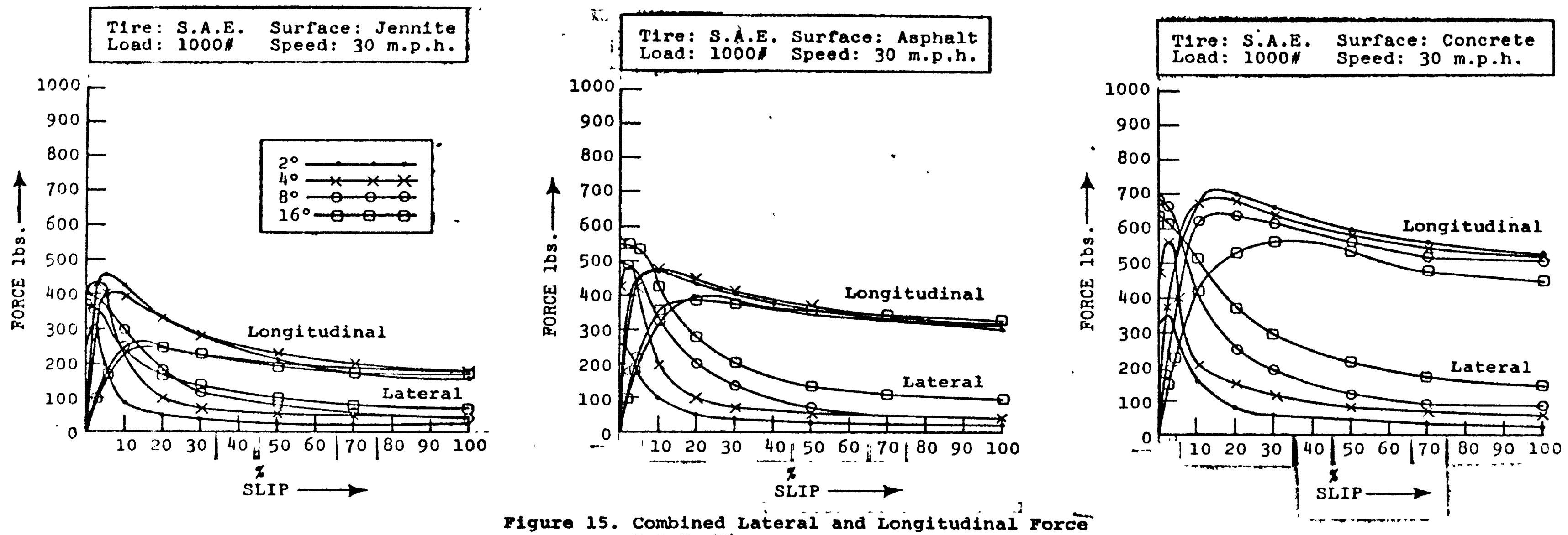

Figure 15. Combined Lateral and Longitudinal Force S.A.E. Tire

APPENDIX 2

TIRE RANKINGS

The relative ranking according to the magnitude of longitudinal and/or lateral shear force of the 10 tires listed in Table 1 are presented in this appendix for 5 combinations of speed and load on 3 test surfaces. Also, the average ranking and the overall ranking are given for each tire.

TABLE 11

RANKING OF 10 TIRES BY LATERAL FORCES*

LOAD/SPEED	TIRE: A-1	A5-1	A-5	RB-5	RB-1	H-5	D-2	WA-5	WA-9	S-2-47	SURFACE
600 lbs/30 mph	10	8	4	3	5	2	7	6	1	9	Concrete
1000/30	10	7	8	3	2	1	9	5	4	6	Concrete
1400/30	10	9	8	4	1	2	3	7	6	5	Concrete
1000/10	9	8	5	3	2	1	4	7	6	10	Concrete
1000/50	10	8	4.5	2	3	1	9	7	6	4.5	Concrete
Avg.	9.80	8.0	5.9	3.0	2.6	1.4	6.4	6.4	4.6	6.9	
Rank:	10	9	5	3	2	1	6.5	6.5	4	8	Concrete
600 lbs/30 mph	9	8	3	2	5.5	1	5.5	7	4	10	Asphalt
1000/30	9	10	3	4	5	1	6	7	2	8	Asphalt
1400/30	10	8	2	5	3	1	6	7	4	9	Asphalt
1000/10	9	10	2	7	4	1	5.5	5.5	3	8	Asphalt
1000/50	9	10	6	3	4	1	7	5	2	8	Asphalt
Avg.	9.2	9.2	3.2	4.2	4.3	1	6.0	6.3	3.0	8.6	
Rank:	9.5	9.5	3	4	5	1	6	7	2	8	Asphalt
600 lbs/30 mph	10	9	2.5	4	5	1	6	8	2.5	7	Jennite
1000/30	10	8	7	4	3	1	6	9	5	2	Jennite
1400/30	10	7.5	9	3	2	1	4.5	7.5	6	4.5	Jennite
1000/10	8	9	10	4	5.5	1	3	7	5.5	2	Jennite
1000/50	10	9	6	2	4	1	7	8	5	3	Jennite
Avg.	9.6	8.5	6.9	3.40	3.9	1.00	5.3	7.9	4.8	3.70	
Rank:	10	9	7	2	4	1	6	8	5	3	Jennite
Sum of 3 Averages:	28.6	25.7	16.0	10.6	10.8	3.4	17.7	20.6	12.4	19.2	
Overall Rank:	10	9	5	2	3	1	6	8	4	7	
	A-1	A5-1	A-5	RB-5	RB-1	H-5	D-2	WA-5	WA-9	S-2-47	

*Tires were ranked from 1 to 10 for every condition with 1 being the highest/best, and 10 being the lowest. In the case of a tie, the average of the two ranks was given.

TABLE 12

RANKING OF 10 TIRES BY BRAKING FORCE* AT 100% SLIP

LOAD/SPEED		TIRE: A-1	A5-1	A-5	RB-5	RB-1	H-5	D-2	WA-5	WA-9	S-2-47	SURFACE
600 lbs/30 mph		10	8	6	6	3.5	2	9	3.5	1	6	Concrete
1000/30		10	8	7	6	4	2	9	5	1	3	Concrete
1400/30		10	9	6	5	1	2.5	7.5	7.5	2.5	4	Concrete
1000/10		9	7	7	4	2	1	7	5	3	10	Concrete
1000/50		9	6	7	5	3	4	10	8	1	2	Concrete
	Avg.	9.6	7.6	6.6	5.2	2.7	2.3	8.5	5.8	1.7	5.0	
	Rank:	10	8	7	5	3	2	9	6	1	4	Concrete
600 lbs/30 mph		10	8	5	3.5	6	1	8	3.5	2	8	Asphalt
1000/30		10	8	4.5	3	7	1	4.5	6	2	9	Asphalt
1400/30		9	10	4	2	6	1	7	5	3	8	Asphalt
1000/10		10	7	4	4	6	1	2	8	4	9	Asphalt
1000/50		10	9	3.5	6	6	2	6	8	1	3.5	Asphalt
	Avg.	9.8	8.4	4.2	3.7	6.2	1.2	5.5	6.1	2.4	7.5	
	Rank:	10	9	4	3	7	1	5	6	2	8	Asphalt
600 lbs/30 mph		10	2.5	5.5	4	7.5	2.5	9	5.5	1	7.5	Jennite
1000/30		10	8	9	3.5	1.5	3.5	6	5	1.5	7	Jennite
1400/30		6	10	9	1	7	3	4	5	2	8	Jennite
1000/10		8.5	6.5	10	4.5	2.5	4.5	1	6.5	2.5	8.5	Jennite
1000/50		10	9	7	6	5	1	8	3.5	2	3.5	Jennite
	Avg.	8.9	7.2	8.1	3.8	4.7	2.9	5.6	5.1	1.8	6.9	
	Rank:	10	8	9	3	4	2	6	5	1	7	Jennite
Sum of 3 Averages:		28.3	23.2	18.9	12.7	13.6	6.4	19.6	17.0	5.9	19.4	
Overall Rank:		10	9	6	3	4	2	8	5	1	7	
		A-1	A5-1	A-5	RB-5	RB-1	H-5	D-2	WA-5	WA-9	S-2-47	

*Tires were ranked from 1 to 10 for every condition with 1 being the highest/best and 10 being the lowest. In the case of a tie, the average of the two ranks was given.

TABLE 13

RANKING* OF 10 TIRES BY BRAKING FORCE AT POINT OF MAXIMUM BRAKING FORCE

LOAD/SPEED		A-1	A5-1	A-5	RB-5	RB-1	H-5	D-2	WA-5	WA-9	S-2-47	SURFACE
		TIRE:										
600 lbs/30 mph		10	8	6	3	4	2	9	5	1	7	Concrete
1000/30		10	7	5	6	2	3	9	8	1	4	Concrete
1400/30		10	9	7	2	1	4	8	6	5	3	Concrete
1000/10		9	7	8	4	4	1	2	6	4	10	Concrete
1000/50		10	8	5	6	3	2	9	7	1	4	Concrete
	Avg.	9.8	7.8	6.2	4.2	2.8	2.4	7.4	6.4	2.4	5.6	
	Rank:	10	9	6	4	3	1.5	8	7	1.5	5	Concrete
600 lbs/30 mph		9.5	5	3.5	3.5	7	1	7	7	2	9.5	Asphalt
1000/30		10	8	3	2	6	1	5	7	4	9	Asphalt
1400/30		9	10	3	1	5	2	7	6	4	8	Asphalt
1000/10		10	7.5	3	4	5.5	2	1	7.5	5.5	9	Asphalt
1000/50		9.5	5	4	2	6	1	7	8	3	9.5	Asphalt
	Avg.	9.6	7.1	3.3	2.5	5.9	1.4	5.4	7.1	3.7	9.0	
	Rank:	10	7.5	3	2	6	1	5	7.5	4	9	Asphalt
600 lbs/30 mph		10	9	4	3	6	2	8	7	1	5	Jennite
1000/30		10	9	5	2	4	1	6	7.5	3	7.5	Jennite
1400/30		10	9	5	1	4	2	6	7.5	3	7.5	Jennite
1000/10		4	10	9	5.5	5.5	1	2	7	3	8	Jennite
1000/50		10	9	3	4	5	1	8	6	2	7	Jennite
	Avg.	8.8	9.2	5.2	3.1	4.9	1.4	6.0	7.0	2.4	7.0	
	Rank:	9	10	5	3	4	1	6	7.5	2	7.5	Jennite
Sum of 3 Averages:		28.2	24.1	14.7	9.8	13.6	5.2	18.8	20.5	8.9	21.6	
Overall Rank:		10	9	5	3	4	1	6	7	2	8	
		A-1	A5-1	A-5	RB-5	RB-1	H-5	D-2	WA-5	WA-9	S-2-47	

*Tires were ranked from 1 to 10 for every condition with 1 being the highest/best and 10 being the lowest. In the case of a tie, the average of the two ranks was given. A(-) indicates a point where no data was available.

TABLE 14

RANKING OF 10 TIRES BY MAXIMUM TOTAL FORCE

$$\vec{F}_{(MAX)} = (\vec{F}_{(x)} + \vec{F}_y)_{MAX}$$

Load = 1000#
Speed = 30 mph
Steer Angle = 8°

	CONCRETE	ASPHALT	JENNITE	OVERALL	
Highest	H-5	H-5	H-5	H-5	
	WA-9	A-5	WA-9	WA-9	
	A-5	WA-9	A-5	A-5	
	RB-1	RB-5	S-2-47	RB-1	Tie
	S-2-47	WA-5	D-2	RB-5	
	RB-5	D-2	RB-1	WA-5	Tie
	WA-5	A5-1	WA-5	S-2-47	
	A5-1	RB-1	RB-5	D-2	
	D-2	A-1	A5-1	A5-1	
Lowest	A-1	S-2-47	A-1	A-1	

APPENDIX 3

TIRE PARAMETERS

In Table 15, the influence of the longitudinal friction parameters μ_{ox}, A_x, and B_x can be seen by looking at the entries under the headings U1 through U5. The labels U1 through U5 stand for the value of the friction law μ_x (Equation (6) of the text) at the 5 tire operating conditions, 1000 lbs/10 mph, 1000 lbs/30 mph, 1000 lbs/50 mph, 600 lbs/30 mph, and 1400 lbs/30 mph, respectively. For example, for the WA-5 tire on wet concrete the value of μ_{ox} is 0.862 but U2, the value of μ_x at 30 mph and 1000 pounds vertical load, is only 0.456 due to the values of A_x and B_x.

A comparison of the tire data with the linear friction law (Equation (6)) is given for each tire entry in the table. The quantity labeled "RMS" is the root mean square error between the friction law (6) and the 5 data points. (Each data point is the average of at least 6 repetitions with the mobile tire tester.) The 5 data points for each tire are entered in Table A following the label "U(I)=".

The same format as used for Table 15 is used for Table 19 which contains lateral friction parameters. Reading of the other tables is self-explanatory. The meaning of these tables is discussed in the body of the report.

TABLE 15. LONGITUDINAL FRICTION PARAMETERS FOR WET CONCRETE.

TIRE	UOX	AX	BX	U1 1000 lb/ 10 mph	U2 1000 lb/ 30 mph	U3 1000 lb/ 50 mph	U4 600 lb/ 30 mph	U5 1400 lb/ 30 mph
A-1	0.630E 00	0.767E-02	-0.327E-04	0.550E 00	0.325E 00	0.101E 00	0.312E 00	0.338E 00
	RMS =	0.131E-01	U(I) =	0.560E 00	0.300E 00	0.110E 00	0.316E 00	0.342E 00
A5-1	0.690E 00	0.511E-02	0.386E-04	0.576E 00	0.426E 00	0.276E 00	0.441E 00	0.410E 00
	RMS =	0.187E-02	U(I) =	0.575E 00	0.430E 00	0.275E 00	0.441E 00	0.410E 00
A-5	0.806E 00	0.588E-02	0.982E-04	0.621E 00	0.449E 00	0.276E 00	0.488E 00	0.409E 00
	RMS =	0.386E-01	U(I) =	0.575E 00	0.470E 00	0.230E 00	0.525E 00	0.446E 00
RB-5	0.766E 00	0.545E-02	0.491E-04	0.637E 00	0.477E 00	0.317E 00	0.496E 00	0.457E 00
	RMS =	0.273E-01	U(I) =	0.605E 00	0.485E 00	0.285E 00	0.525E 00	0.485E 00
RB-1	0.732E 00	0.392E-02	0.342E-04	0.641E 00	0.526E 00	0.411E 00	0.539E 00	0.512E 00
	RMS =	0.148E-02	U(I) =	0.640E 00	0.525E 00	0.410E 00	0.541E 00	0.514E 00
H-5	0.841E 00	0.554E-02	0.833E-04	0.676E 00	0.514E 00	0.351E 00	0.547E 00	0.480E 00
	RMS =	0.261E-01	U(I) =	0.645E 00	0.540E 00	0.320E 00	0.566E 00	0.500E 00
D-2	0.727E 00	0.826E-02	-0.238E-04	0.630E 00	0.387E 00	0.145E 00	0.377E 00	0.396E 00
	RMS =	0.450E-01	U(I) =	0.575E 00	0.420E 00	0.900E-01	0.416E 00	0.435E 00
WA-5	0.862E 00	0.622E-02	0.132E-03	0.639E 00	0.456E 00	0.274E 00	0.509E 00	0.403E 00
	RMS =	0.443E-01	U(I) =	0.585E 00	0.500E 00	0.220E 00	0.541E 00	0.435E 00
WA-9	0.850E 00	0.323E-02	0.156E-03	0.647E 00	0.551E 00	0.457E 00	0.614E 00	0.489E 00
	RMS =	0.185E-01	U(I) =	0.625E 00	0.575E 00	0.435E 00	0.625E 00	0.500E 00
S-2-47	0.656E 00	0.255E-02	0.446E-04	0.573E 00	0.498E 00	0.423E 00	0.516E 00	0.480E 00
	RMS =	0.212E-01	U(I) =	0.550E 00	0.530E 00	0.400E 00	0.525E 00	0.489E 00

TABLE 15. LONGITUDINAL FRICTION PARAMETERS FOR WET ASPHALT.

TIRE	UOX	AX	BX	U1 1000 lb/ 10 mph	U2 1000 lb/ 30 mph	U3 1000 lb/ 50 mph	U4 600 lb/ 30 mph	U5 1400 lb/ 30 mph
A-1	0.355E 00	0.596E-03	0.267E-04	0.320E 00	0.302E 00	0.285E 00	0.313E 00	0.291E 00
	RMS =	0.205E-01	U(I) =	0.345E 00	0.280E 00	0.310E 00	0.300E 00	0.278E 00
A5-1	0.496E 00	0.178E-02	0.818E-04	0.388E 00	0.336E 00	0.283E 00	0.368E 00	0.303E 00
	RMS =	0.348E-01	U(I) =	0.430E 00	0.325E 00	0.325E 00	0.333E 00	0.267E 00
A-5	0.480E 00	0.204E-02	0.297E-05	0.447E 00	0.387E 00	0.327E 00	0.388E 00	0.385E 00
	RMS =	0.229E-01	U(I) =	0.475E 00	0.375E 00	0.355E 00	0.366E 00	0.364E 00
RB-5	0.487E 00	0.213E-02	-0.133E-04	0.469E 00	0.407E 00	0.344E 00	0.401E 00	0.412E 00
	RMS =	0.477E-02	U(I) =	0.475E 00	0.400E 00	0.350E 00	0.400E 00	0.410E 00
RB-1	0.507E 00	0.340E-02	0.892E-05	0.448E 00	0.348E 00	0.248E 00	0.352E 00	0.344E 00
	RMS =	0.172E-02	U(I) =	0.450E 00	0.350E 00	0.250E 00	0.350E 00	0.342E 00
H-5	0.624E 00	0.238E-02	0.654E-04	0.524E 00	0.454E 00	0.384E 00	0.480E 00	0.427E 00
	RMS =	0.213E-01	U(I) =	0.550E 00	0.430E 00	0.410E 00	0.466E 00	0.414E 00
D-2	0.475E 00	0.238E-02	-0.744E-05	0.447E 00	0.377E 00	0.307E 00	0.374E 00	0.380E 00
	RMS =	0.374E-01	U(I) =	0.490E 00	0.375E 00	0.350E 00	0.333E 00	0.339E 00
WA-5	0.489E 00	0.136E-02	0.580E-04	0.411E 00	0.371E 00	0.331E 00	0.394E 00	0.348E 00
	RMS =	0.839E-02	U(I) =	0.415E 00	0.355E 00	0.335E 00	0.400E 00	0.353E 00
WA-9	0.557E 00	0.767E-03	0.907E-04	0.455E 00	0.432E 00	0.410E 00	0.469E 00	0.396E 00
	RMS =	0.162E-01	U(I) =	0.475E 00	0.415E 00	0.430E 00	0.458E 00	0.385E 00
S-2-47	0.385E 00	0.340E-03	0.327E-04	0.348E 00	0.338E 00	0.328E 00	0.351E 00	0.324E 00
	RMS =	0.219E-01	U(I) =	0.375E 00	0.320E 00	0.355E 00	0.333E 00	0.307E 00

TABLE 15. LONGITUDINAL FRICTION PARAMETERS FOR WET JENNITE.

TIRE	UOX	AX	BX	U1 1000 lb/ 10 mph	U2 1000 lb/ 30 mph	U3 1000 lb/ 50 mph	U4 600 lb/ 30 mph	U5 1400 lb/ 30 mph
A-1	0.237E 00	0.332E-02	-0.416E-04	0.230E 00	0.133E 00	0.359E-01	0.116E 00	0.149E 00
	RMS =	0.100E-01	U(I) =	0.240E 00	0.115E 00	0.450E-01	0.116E 00	0.150E 00
A5-1	0.399E 00	0.306E-02	0.107E-03	0.246E 00	0.156E 00	0.669E-01	0.199E 00	0.113E 00
	RMS =	0.363E-02	U(I) =	0.250E 00	0.150E 00	0.700E-01	0.200E 00	0.114E 00
A-5	0.312E 00	0.196E-02	0.729E-04	0.211E 00	0.153E 00	0.962E-01	0.182E 00	0.124E 00
	RMS =	0.100E-01	U(I) =	0.220E 00	0.135E 00	0.105E 00	0.183E 00	0.125E 00
RB-5	0.265E 00	0.247E-02	-0.505E-04	0.280E 00	0.207E 00	0.135E 00	0.187E 00	0.227E 00
	RMS =	0.890E-02	U(I) =	0.270E 00	0.220E 00	0.125E 00	0.191E 00	0.232E 00
RB-1	0.309E 00	0.187E-02	0.297E-04	0.251E 00	0.196E 00	0.141E 00	0.208E 00	0.184E 00
	RMS =	0.343E-01	U(I) =	0.280E 00	0.225E 00	0.170E 00	0.166E 00	0.142E 00
H-5	0.302E 00	0.170E-02	0.178E-04	0.259E 00	0.209E 00	0.159E 00	0.216E 00	0.201E 00
	RMS =	0.132E-01	U(I) =	0.270E 00	0.220E 00	0.170E 00	0.200E 00	0.185E 00
D-2	0.286E 00	0.375E-02	-0.491E-04	0.280E 00	0.170E 00	0.609E-01	0.151E 00	0.190E 00
	RMS =	0.225E-01	U(I) =	0.305E 00	0.175E 00	0.850E-01	0.125E 00	0.164E 00
WA-5	0.306E 00	0.204E-02	0.327E-04	0.244E 00	0.184E 00	0.124E 00	0.197E 00	0.170E 00
	RMS =	0.118E-01	U(I) =	0.250E 00	0.200E 00	0.130E 00	0.183E 00	0.157E 00
WA-9	0.397E 00	0.221E-02	0.744E-04	0.290E 00	0.225E 00	0.160E 00	0.255E 00	0.195E 00
	RMS =	0.982E-02	U(I) =	0.280E 00	0.225E 00	0.150E 00	0.266E 00	0.207E 00
S-2-47	0.289E 00	0.187E-02	0.386E-04	0.223E 00	0.168E 00	0.113E 00	0.183E 00	0.152E 00
	RMS =	0.151E-01	U(I) =	0.240E 00	0.170E 00	0.130E 00	0.166E 00	0.135E 00

// END 09 DEC 71 12.286 HRS

TABLE 16. CORNERING STIFFNESS FROM FLAT BED MACHINE
C_α LBS/RAD, FLAT BED

Tire	Load/100	C_α
A-1	6	11,335
	10	12,233
	14	11,259
A-5-1	6	10,939
	10	12,118
	14	11,182
A-5	6	8,422
	10	10,285
	14	10,027
RB-5	6	11,431
	10	11,602
	14	10,227
RB-1	6	10,351
	10	12,548
	14	11,307
H-5	6	8,680
	10	11,430
	14	10,704
D-2	6	11,316
	10	12,519
	14	11,168
WA-5	6	11,058
	10	12,548
	14	11,287
WA-9	6	8,995
	10	11,001
	14	10,356
S-2-47	6	11,588
	10	13,034
	14	12,046

TABLE 17. VARIATION OF C_α WITH LOAD AND SURFACE

Tire	Surface	600/30	1000/30	1400/30
A-1	Jennite	6,100	6,000	5,200
	Asphalt	6,500	8,300	8,000
	Concrete	6,600	7,500	7,500
A-5-1	Jennite	6,600	7,700	7,700
	Asphalt	8,200	9,200	8,900
	Concrete	8,200	9,700	9,500
A-5	Jennite	6,900	5,400	5,200
	Asphalt	7,200	6,600	6,300
	Concrete	7,500	6,600	6,300
RB-5	Jennite	9,000	9,200	7,600
	Asphalt	10,300	9,700	7,600
	Concrete	10,000	9,200	7,300
RB-1	Jennite	5,700	8,900	7,200
	Asphalt	8,700	9,500	7,900
	Concrete	9,200	9,500	7,900
H-5	Jennite	6,300	9,200	6,300
	Asphalt	6,300	9,200	7,200
	Concrete	6,300	9,700	7,200
D-2	Jennite	8,300	10,000	9,600
	Asphalt	10,300	10,900	9,500
	Concrete	9,600	12,000	10,000
WA-5	Jennite	7,000	7,200	7,500
	Asphalt	8,600	8,600	8,000
	Concrete	9,700	9,700	9,200
WA-9	Jennite	8,300	7,500	7,500
	Asphalt	8,900	8,000	8,300
	Concrete	9,300	8,000	8,300
S-2-47	Jennite	6,300	8,600	8,200
	Asphalt	6,600	8,000	8,000
	Concrete	8,000	9,700	8,600

TABLE 18. VARIATION OF C_α WITH SPEED AND SURFACE

Tire	Surface	1000/10	1000/30	1000/50
A-1	Jennite	9,500	6,000	3,200
	Asphalt	8,300	8,300	6,600
	Concrete	9,700	7,500	4,000
A-5-1	Jennite	9,200	7,700	5,700
	Asphalt	9,200	9,200	8,000
	Concrete	9,700	9,700	6,900
A-5	Jennite	5,700	5,400	4,900
	Asphalt	6,600	6,600	6,600
	Concrete	6,600	6,600	5,200
RB-5	Jennite	9,500	9,200	8,600
	Asphalt	9,200	9,700	9,700
	Concrete	9,700	9,200	9,200
RB-1	Jennite	8,900	8,900	8,900
	Asphalt	9,500	9,500	9,500
	Concrete	8,900	9,500	9,500
H-5	Jennite	9,200	9,200	8,600
	Asphalt	9,200	9,200	9,200
	Concrete	9,800	9,700	9,700
D-2	Jennite	10,900	10,000	6,900
	Asphalt	10,900	10,900	10,900
	Concrete	12,000	12,000	7,200
WA-5	Jennite	7,200	7,200	7,200
	Asphalt	6,900	8,600	8,600
	Concrete	7,500	9,700	8,600
WA-9	Jennite	7,500	7,500	7,500
	Asphalt	8,000	8,000	8,000
	Concrete	8,000	8,000	8,000
S-2-47	Jennite	9,200	8,600	8,000
	Asphalt	8,300	8,000	7,500
	Concrete	9,700	9,700	9,700

TABLE 19. LATERAL FRICTION PARAMETERS FOR WET CONCRETE (16° SLIP ANGLE DATA)

TIRE	UOY	AY	BY	U1 1000 lb/ 10 mph	U2 1000 lb/ 30 mph	U3 1000 lb/ 50 mph	U4 600 lb/ 30 mph	U5 1400 lb/ 30 mph
A-1	0.576E 00	0.202E-01	-0.228E-03	0.720E 00	0.549E 00	0.379E 00	0.458E 00	0.641E 00
	RMS =	0.887E-02	U(I) =	0.712E 00	0.542E 00	0.371E 00	0.468E 00	0.651E 00
A5-1	0.835E 00	0.139E-01	-0.742E-05	0.784E 00	0.667E 00	0.549E 00	0.664E 00	0.670E 00
	RMS =	0.331E-01	U(I) =	0.744E 00	0.704E 00	0.509E 00	0.685E 00	0.691E 00
A-5	0.100E 01	0.105E-01	0.102E-03	0.855E 00	0.766E 00	0.677E 00	0.807E 00	0.725E 00
	RMS =	0.279E-01	U(I) =	0.850E 00	0.719E 00	0.672E 00	0.836E 00	0.754E 00
RB-5	0.892E 00	0.136E-01	-0.490E-06	0.836E 00	0.721E 00	0.606E 00	0.721E 00	0.721E 00
	RMS =	0.286E-01	U(I) =	0.820E 00	0.684E 00	0.591E 00	0.754E 00	0.755E 00
RB-1	0.903E 00	0.879E-02	-0.302E-04	0.897E 00	0.823E 00	0.749E 00	0.811E 00	0.835E 00
	RMS =	0.381E-02	U(I) =	0.900E 00	0.825E 00	0.752E 00	0.806E 00	0.830E 00
H-5	0.106E 01	0.167E-01	0.187E-04	0.977E 00	0.837E 00	0.696E 00	0.844E 00	0.829E 00
	RMS =	0.241E-01	U(I) =	0.968E 00	0.800E 00	0.687E 00	0.871E 00	0.856E 00
D-2	0.887E 00	0.269E-01	-0.832E-04	0.857E 00	0.630E 00	0.403E 00	0.596E 00	0.663E 00
	RMS =	0.544E-01	U(I) =	0.794E 00	0.638E 00	0.340E 00	0.655E 00	0.722E 00
WA-5	0.904E 00	0.829E-02	0.765E-04	0.792E 00	0.723E 00	0.653E 00	0.753E 00	0.692E 00
	RMS =	0.210E-01	U(I) =	0.767E 00	0.735E 00	0.627E 00	0.772E 00	0.711E 00
WA-9	0.100E 01	0.853E-02	0.134E-03	0.836E 00	0.764E 00	0.692E 00	0.818E 00	0.710E 00
	RMS =	0.297E-01	U(I) =	0.809E 00	0.745E 00	0.665E 00	0.854E 00	0.746E 00
S-2-47	0.670E 00	0.314E-02	-0.620E-04	0.719E 00	0.693E 00	0.666E 00	0.668E 00	0.717E 00
	RMS =	0.213E-01	U(I) =	0.697E 00	0.687E 00	0.644E 00	0.693E 00	0.742E 00

TABLE 19. LATERAL FRICTION PARAMETERS FOR WET ASPHALT (16° SLIP ANGLE DATA)

TIRE	UDY	AY	BY	U1 1000 lb/ 10 mph	U2 1000 lb/ 30 mph	U3 1000 lb/ 50 mph	U4 600 lb/ 30 mph	U5 1400 lb/ 30 mph
A-1	0.574E 00	0.695E-02	-0.478E-05	0.549E 00	0.491E 00	0.432E 00	0.489E 00	0.493E 00
	RMS =	0.266E-01	U(I) =	0.529E 00	0.466E 00	0.412E 00	0.521E 00	0.525E 00
A5-1	0.566E 00	0.560E-02	-0.100E-03	0.642E 00	0.595E 00	0.548E 00	0.555E 00	0.635E 00
	RMS =	0.296E-01	U(I) =	0.625E 00	0.654E 00	0.530E 00	0.543E 00	0.624E 00
A-5	0.824E 00	0.122E-01	-0.755E-04	0.848E 00	0.745E 00	0.641E 00	0.715E 00	0.775E 00
	RMS =	0.175E-01	U(I) =	0.831E 00	0.737E 00	0.624E 00	0.736E 00	0.796E 00
RB-5	0.658E 00	0.394E-02	-0.630E-04	0.705E 00	0.672E 00	0.638E 00	0.646E 00	0.697E 00
	RMS =	0.301E-01	U(I) =	0.701E 00	0.619E 00	0.635E 00	0.676E 00	0.727E 00
RB-1	0.775E 00	0.164E-01	-0.949E-04	0.800E 00	0.662E 00	0.524E 00	0.624E 00	0.700E 00
	RMS =	0.463E-01	U(I) =	0.763E 00	0.623E 00	0.486E 00	0.681E 00	0.757E 00
H-5	0.103E 01	0.110E-01	0.991E-04	0.892E 00	0.799E 00	0.706E 00	0.839E 00	0.759E 00
	RMS =	0.413E-01	U(I) =	0.842E 00	0.836E 00	0.655E 00	0.871E 00	0.792E 00
D-2	0.691E 00	0.844E-02	-0.185E-04	0.674E 00	0.603E 00	0.532E 00	0.596E 00	0.611E 00
	RMS =	0.437E-01	U(I) =	0.641E 00	0.562E 00	0.499E 00	0.649E 00	0.664E 00
WA-5	0.719E 00	0.142E-01	-0.870E-04	0.747E 00	0.627E 00	0.508E 00	0.592E 00	0.662E 00
	RMS =	0.149E-01	U(I) =	0.729E 00	0.645E 00	0.490E 00	0.602E 00	0.671E 00
WA-9	0.784E 00	0.630E-02	-0.308E-04	0.789E 00	0.736E 00	0.683E 00	0.723E 00	0.748E 00
	RMS =	0.246E-01	U(I) =	0.790E 00	0.780E 00	0.683E 00	0.700E 00	0.725E 00
S-2-47	0.442E 00	-0.149E-02	-0.834E-04	0.532E 00	0.544E 00	0.557E 00	0.511E 00	0.578E 00
	RMS =	0.210E-01	U(I) =	0.515E 00	0.585E 00	0.541E 00	0.507E 00	0.573E 00

TABLE 19. LATERAL FRICTION PARAMETERS FOR WET JENNITE (16° SLIP ANGLE DATA)

TIRE	UOY	AY	BY	U1 1000 lb/ 10 mph	U2 1000 lb/ 30 mph	U3 1000 lb/ 50 mph	U4 600 lb/ 30 mph	U5 1400 lb/ 30 mph
A-1	0.479E 00	0.220E-01	-0.986E-04	0.485E 00	0.299E 00	0.114E 00	0.260E 00	0.339E 00
	RMS =	0.260E-01	U(I) =	0.515E 00	0.295E 00	0.144E 00	0.232E 00	0.311E 00
A5-1	0.589E 00	0.189E-01	-0.133E-05	0.510E 00	0.351E 00	0.191E 00	0.350E 00	0.351E 00
	RMS =	0.261E-01	U(I) =	0.540E 00	0.351E 00	0.221E 00	0.321E 00	0.322E 00
A-5	0.840E 00	0.157E-01	0.259E-03	0.514E 00	0.381E 00	0.248E 00	0.485E 00	0.277E 00
	RMS =	0.169E-01	U(I) =	0.516E 00	0.349E 00	0.250E 00	0.499E 00	0.291E 00
RB-5	0.693E 00	0.195E-01	0.427E-04	0.568E 00	0.404E 00	0.240E 00	0.421E 00	0.387E 00
	RMS =	0.288E-01	U(I) =	0.598E 00	0.356E 00	0.269E 00	0.415E 00	0.381E 00
RB-1	0.608E 00	0.142E-01	-0.270E-04	0.575E 00	0.454E 00	0.334E 00	0.444E 00	0.465E 00
	RMS =	0.446E-01	U(I) =	0.618E 00	0.475E 00	0.378E 00	0.390E 00	0.411E 00
H-5	0.106E 01	0.262E-01	0.164E-03	0.786E 00	0.565E 00	0.345E 00	0.631E 00	0.500E 00
	RMS =	0.305E-01	U(I) =	0.750E 00	0.580E 00	0.308E 00	0.661E 00	0.529E 00
D-2	0.677E 00	0.224E-01	0.439E-04	0.539E 00	0.350E 00	0.161E 00	0.367E 00	0.332E 00
	RMS =	0.161E-01	U(I) =	0.555E 00	0.322E 00	0.177E 00	0.365E 00	0.330E 00
WA-5	0.699E 00	0.232E-01	0.319E-04	0.570E 00	0.375E 00	0.180E 00	0.387E 00	0.362E 00
	RMS =	0.147E-01	U(I) =	0.588E 00	0.359E 00	0.197E 00	0.377E 00	0.352E 00
WA-9	0.853E 00	0.200E-01	0.163E-03	0.605E 00	0.436E 00	0.267E 00	0.501E 00	0.370E 00
	RMS =	0.224E-01	U(I) =	0.588E 00	0.414E 00	0.250E 00	0.529E 00	0.398E 00
S-2-47	0.575E 00	0.182E-01	-0.610E-04	0.559E 00	0.406E 00	0.252E 00	0.381E 00	0.430E 00
	RMS =	0.388E-01	U(I) =	0.607E 00	0.383E 00	0.300E 00	0.346E 00	0.395E 00

// END 08 DEC 71 16.600 HRS

TABLE 20. J-TURN LATERAL TIRE PARAMETERS

Tire	μ_{oy}	A_y	B_y	RMS Error
		(WET CONCRETE)		
A-1	0.328	$.108 \times 10^{-1}$	$-.280 \times 10^{-3}$	$.129 \times 10^{-1}$
A5-1	0.539	$.109 \times 10^{-1}$	$-.182 \times 10^{-3}$	$.779 \times 10^{-2}$
A-5	0.833	$.625 \times 10^{-2}$	$+.191 \times 10^{-4}$	$.257 \times 10^{-2}$
RB-5	0.815	$.174 \times 10^{-1}$	$-.126 \times 10^{-3}$	$.557 \times 10^{-2}$
RB-1	0.810	$.615 \times 10^{-2}$	$-.665 \times 10^{-4}$	$.405 \times 10^{-2}$
H-5	1.052	$.113 \times 10^{-1}$	$+.992 \times 10^{-4}$	$.278 \times 10^{-1}$
D-2	0.058	$.205 \times 10^{-1}$	$-.663 \times 10^{-3}$	$.421 \times 10^{-2}$
WA-5	0.628	$.523 \times 10^{-2}$	$-.937 \times 10^{-4}$	$.249 \times 10^{-3}$
WA-9	0.859	$.806 \times 10^{-2}$	$+.224 \times 10^{-4}$	$.414 \times 10^{-2}$
S-2-47	0.712	$.907 \times 10^{-2}$	$-.105 \times 10^{-3}$	$.294 \times 10^{-2}$
		(WET ASPHALT)		
A-1	0.592	$.910 \times 10^{-2}$	$-.189 \times 10^{-4}$	$.980 \times 10^{-2}$
A5-1	0.692	$.715 \times 10^{-2}$	$-.746 \times 10^{-6}$	$.963 \times 10^{-2}$
A-5	0.773	$.957 \times 10^{-2}$	$-.696 \times 10^{-4}$	$.208 \times 10^{-1}$
RB-5	0.715	$.102 \times 10^{-1}$	$-.120 \times 10^{-2}$	$.122 \times 10^{-1}$
RB-1	0.551	$.132 \times 10^{-1}$	$-.229 \times 10^{-3}$	$.231 \times 10^{-1}$
H-5	1.229	$.162 \times 10^{-1}$	$+.202 \times 10^{-3}$	$.224 \times 10^{-1}$
D-2	0.511	$.121 \times 10^{-1}$	$-.223 \times 10^{-3}$	$.291 \times 10^{-2}$
WA-5	0.623	$.121 \times 10^{-1}$	$-.140 \times 10^{-3}$	$.187 \times 10^{-2}$
WA-9	0.840	$.591 \times 10^{-2}$	$.360 \times 10^{-4}$	$.465 \times 10^{-2}$
S-2-47	0.598	$.281 \times 10^{-2}$	$-.136 \times 10^{-5}$	$.434 \times 10^{-2}$
		(WET JENNITE)		
A-1	0.114	$.874 \times 10^{-2}$	$-.217 \times 10^{-3}$	$.531 \times 10^{-2}$
A5-1	0.404	$.130 \times 10^{-1}$	$-.729 \times 10^{-4}$	$.710 \times 10^{-2}$
A-5	0.658	$.128 \times 10^{-1}$	$.146 \times 10^{-3}$	$.750 \times 10^{-3}$
RB-5	0.361	$.144 \times 10^{-1}$	$-.173 \times 10^{-3}$	$.193 \times 10^{-1}$
RB-1	0.575	$.121 \times 10^{-1}$	$-.298 \times 10^{-4}$	$.222 \times 10^{-1}$
H-5	1.143	$.294 \times 10^{-1}$	$.194 \times 10^{-3}$	$.162 \times 10^{-1}$
D-2	0.293	$.161 \times 10^{-1}$	$-.189 \times 10^{-3}$	$.105 \times 10^{-1}$
WA-5	0.302	$.132 \times 10^{-1}$	$-.157 \times 10^{-3}$	$.581 \times 10^{-3}$
WA-9	0.593	$.166 \times 10^{-1}$	$-.469 \times 10^{-5}$	$.504 \times 10^{-2}$
S-2-47	0.794	$.172 \times 10^{-1}$	$.133 \times 10^{-3}$	$.226 \times 10^{-2}$

APPENDIX 4

SIMPLIFIED ANALYSIS OF SKIDDING DISTANCE

In the tests conducted by NBS, the vehicle was loaded with lead so that $F_{zF} \doteq F_{zR}$ in the static condition. Due to load transfer during deceleration, $F_{zF} \neq F_{zR}$ while the vehicle is coming to a stop. However, $F_{zF} + F_{zR} \doteq \frac{mg}{2}$. Since the same tires are mounted front and rear, the coefficients in the friction expressions for the front and rear tires are equal. Thus

$$\mu_{xF} = \mu_{ox} - A_x V_s - B_x F_{zF}$$

and

$$\mu_{xR} = \mu_{ox} - A_x V_s - B_x F_{zR}$$

or combining the appropriate terms

$$\mu_{xF} F_{zF} + \mu_{xR} F_{zR} = \mu_{ox} \frac{mg}{2} - A_x \frac{V_s mg}{2} - B_x [(F_{zF})^2 + (F_{zR})^2] \tag{4-1}$$

The amount of load transfer, ΔF_z, from front to rear on one front tire is

$$\Delta F_z = \frac{m|\ddot{x}|h}{2\ell}$$

where

h is the c.g. height

ℓ is the wheelbase

For the 1968 Chevrolet making a 0.5g stop

$$\Delta F_z \doteq 250 \text{ lbs.}$$

For the front tire, where $F_s = \frac{mg}{4}$ is the static load,

$$F_{zF} = F_s + \Delta F_z \,.$$

For the rear tire

$$F_{zR} = F_s - \Delta F_z$$

and

$$(F_{zF})^2 + (F_{zR})^2 = 2(F_s)^2 + 2(\Delta F_z)^2. \qquad (4\text{-}2)$$

On combining Equations (9), (4-1), and (4-2), we obtain

$$m\ddot{x} = \mu_{ox} \frac{mg}{2} - A_x V_s \frac{mg}{2} - B_x[2(F_s)^2 + 2(\Delta F_z)^2] \qquad (4\text{-}3)$$

Since B_x is usually less than 10^{-4}, the quantity $2B_x(\Delta F_z)^2$ is less than 13 pounds and therefore can be neglected in making skidding distance calculations. Equation (4-3) reduces to Equation (10) of the body of the report.

The solution for skidding distance, i.e., (11) and (12), was differentiated to obtain the rate of change of skidding distance with respect to the friction parameters, tire load, and initial velocity. The values of skidding distance and the derivatives of skidding distance are given in Table 21 for each tire on each surface at 30 and 50 mph initial velocities.

TABLE 21

SKIDDING DISTANCE, X ,AND SENSITIVITY COEFFICIENTS FOR WET CONCRETE. VO = 30 MPH.

TIRE	X	UOX	AX	BX	DXDUOX	DXDAX	DXDBX	DXDW	DXDVO
A-1	0.138E 03	0.630E 00	0.767E-02	-0.327E-04	-0.329E 03	0.107E 05	0.412E 06	-0.269E-02	0.617E 01
A5-1	0.123E 03	0.690E 00	0.511E-02	0.386E-04	-0.257E 03	0.807E 04	0.322E 06	0.248E-02	0.655E 01
A-5	0.119E 03	0.806E 00	0.588E-02	0.982E-04	-0.240E 03	0.758E 04	0.300E 06	0.589E-02	0.643E 01
RB-5	0.111E 03	0.766E 00	0.545E-02	0.491E-04	-0.208E 03	0.654E 04	0.261E 06	0.256E-02	0.588E 01
RB-1	0.105E 03	0.732E 00	0.392E-02	0.342E-04	-0.184E 03	0.566E 04	0.231E 06	0.157E-02	0.528E 01
H-5	0.105E 03	0.841E 00	0.554E-02	0.833E-04	-0.187E 03	0.585E 04	0.234E 06	0.390E-02	0.554E 01
D-2	0.119E 03	0.727E 00	0.826E-02	-0.238E-04	-0.245E 03	0.795E 04	0.307E 06	-0.145E-02	0.694E 01
WA-5	0.118E 03	0.862E 00	0.622E-02	0.132E-03	-0.237E 03	0.754E 04	0.297E 06	0.787E-02	0.646E 01
WA-9	0.107E 03	0.850E 00	0.323E-02	0.156E-03	-0.193E 03	0.591E 04	0.242E 06	0.756E-02	0.533E 01
S-2-47	0.114E 03	0.656E 00	0.255E-02	0.446E-04	-0.219E 03	0.666E 04	0.275E 06	0.245E-02	0.560E 01

TABLE 21

SKIDDING DISTANCE, X ,AND SENSITIVITY COEFFICIENTS FOR WET ASPHALT.   VO = 30 MPH.

TIRE	X	UOX	AX	BX	DXDUOX	DXDAX	DXDBX	DXDW	DXDVO
A-1	0.197E 03	0.355E 00	0.596E-03	0.267E-04	-0.648E 03	0.192E 05	0.812E 06	0.434E-02	0.923E 01
A5-1	0.176E 03	0.496E 00	0.178E-02	0.818E-04	-0.519E 03	0.157E 05	0.650E 06	0.106E-01	0.866E 01
A-5	0.144E 03	0.480E 00	0.204E-02	0.297E-05	-0.349E 03	0.106E 05	0.437E 06	0.259E-03	0.707E 01
RB-5	0.136E 03	0.487E 00	0.213E-02	-0.133E-04	-0.310E 03	0.941E 04	0.388E 06	-0.103E-02	0.665E 01
RB-1	0.152E 03	0.507E 00	0.340E-02	0.892E-05	-0.391E 03	0.121E 05	0.490E 06	0.874E-03	0.789E 01
H-5	0.127E 03	0.624E 00	0.238E-02	0.654E-04	-0.271E 03	0.824E 04	0.339E 06	0.444E-02	0.624E 01
D-2	0.145E 03	0.475E 00	0.238E-02	-0.744E-05	-0.353E 03	0.108E 05	0.443E 06	-0.658E-03	0.720E 01
WA-5	0.159E 03	0.489E 00	0.136E-02	0.580E-04	-0.424E 03	0.127E 05	0.531E 06	0.616E-02	0.765E 01
WA-9	0.142E 03	0.557E 00	0.767E-03	0.907E-04	-0.339E 03	0.100E 05	0.425E 06	0.770E-02	0.666E 01
S-2-47	0.179E 03	0.385E 00	0.340E-03	0.327E-04	-0.536E 03	0.159E 05	0.672E 06	0.439E-02	0.828E 01

TABLE 21

SKIDDING DISTANCE, X ,AND SENSITIVITY COEFFICIENTS FOR WET JENNITE. VO = 30 MPH.

TIRE	X	UOX	AX	BX	DXDUOX	DXDAX	DXDBX	DXDW	DXDVO
A-1	0.321E 03	0.237E 00	0.332E-02	-0.416E-04	-0.177E 04	0.578E 05	0.222E 07	-0.184E-01	0.190E 02
A5-1	0.354E 03	0.399E 00	0.306E-02	0.107E-03	-0.215E 04	0.705E 05	0.270E 07	0.578E-01	0.210E 02
A-5	0.372E 03	0.312E 00	0.196E-02	0.729E-04	-0.233E 04	0.740E 05	0.292E 07	0.425E-01	0.202E 02
RB-5	0.236E 03	0.265E 00	0.247E-02	-0.505E-04	-0.938E 03	0.293E 05	0.117E 07	-0.118E-01	0.123E 02
RB-1	0.279E 03	0.309E 00	0.187E-02	0.297E-04	-0.130E 04	0.406E 05	0.163E 07	0.973E-02	0.144E 02
H-5	0.263E 03	0.302E 00	0.170E-02	0.178E-04	-0.115E 04	0.357E 05	0.145E 07	0.517E-02	0.133E 02
D-2	0.258E 03	0.286E 00	0.375E-02	-0.491E-04	-0.114E 04	0.369E 05	0.142E 07	-0.140E-01	0.149E 02
WA-5	0.295E 03	0.306E 00	0.204E-02	0.327E-04	-0.146E 04	0.458E 05	0.183E 07	0.119E-01	0.155E 02
WA-9	0.253E 03	0.397E 00	0.221E-02	0.744E-04	-0.107E 04	0.335E 05	0.134E 07	0.200E-01	0.132E 02
S-2-47	0.326E 03	0.289E 00	0.187E-02	0.386E-04	-0.178E 04	0.561E 05	0.224E 07	0.173E-01	0.172E 02

// END 24 NOV 71 15.554 HRS

TABLE 21

SKIDDING DISTANCE, X ,AND SENSITIVITY COEFFICIENTS FOR WET CONCRETE. VO = 50 MPH.

TIRE	X	UOX	AX	BX	DXDUOX	DXDAX	DXDBX	DXDW	DXDVO
A-1	0.694E 03	0.630E 00	0.767E-02	-0.327E-04	-0.352E 04	0.217E 06	0.441E 07	-0.288E-01	0.417E 02
A5-1	0.447E 03	0.690E 00	0.511E-02	0.386E-04	-0.125E 04	0.699E 05	0.157E 07	0.121E-01	0.170E 02
A-5	0.449E 03	0.806E 00	0.588E-02	0.982E-04	-0.128E 04	0.725E 05	0.160E 07	0.314E-01	0.180E 02
RB-5	0.398E 03	0.766E 00	0.545E-02	0.491E-04	-0.990E 03	0.548E 05	0.124E 07	0.121E-01	0.149E 02
RB-1	0.341E 03	0.732E 00	0.392E-02	0.342E-04	-0.708E 03	0.376E 05	0.887E 06	0.606E-02	0.113E 02
H-5	0.372E 03	0.841E 00	0.554E-02	0.833E-04	-0.864E 03	0.476E 05	0.108E 07	0.180E-01	0.137E 02
D-2	0.558E 03	0.727E 00	0.826E-02	-0.238E-04	-0.218E 04	0.132E 06	0.273E 07	-0.130E-01	0.301E 02
WA-5	0.457E 03	0.862E 00	0.622E-02	0.132E-03	-0.133E 04	0.762E 05	0.167E 07	0.442E-01	0.189E 02
WA-9	0.340E 03	0.850E 00	0.323E-02	0.156E-03	-0.701E 03	0.368E 05	0.878E 06	0.274E-01	0.109E 02
S-2-47	0.354E 03	0.656E 00	0.255E-02	0.446E-04	-0.758E 03	0.393E 05	0.949E 06	0.846E-02	0.110E 02

TABLE 21

SKIDDING DISTANCE, X ,AND SENSITIVITY COEFFICIENTS FOR WET ASPHALT. VO = 50 MPH.

TIRE	X	UOX	AX	BX	DXDUOX	DXDAX	DXDBX	DXDW	DXDVO
A-1	0.570E 03	0.355E 00	0.596E-03	0.267E-04	-0.195E 04	0.977E 05	0.244E 07	0.130E-01	0.163E 02
A5-1	0.549E 03	0.496E 00	0.178E-02	0.818E-04	-0.182E 04	0.952E 05	0.228E 07	0.373E-01	0.173E 02
A-5	0.447E 03	0.480E 00	0.204E-02	0.297E-05	-0.120E 04	0.627E 05	0.151E 07	0.899E-03	0.139E 02
RB-5	0.420E 03	0.487E 00	0.213E-02	-0.133E-04	-0.106E 04	0.554E 05	0.133E 07	-0.357E-02	0.130E 02
RB-1	0.522E 03	0.507E 00	0.340E-02	0.892E-05	-0.167E 04	0.913E 05	0.210E 07	0.374E-02	0.164E 02
H-5	0.395E 03	0.624E 00	0.238E-02	0.654E-04	-0.945E 03	0.491E 05	0.118E 07	0.154E-01	0.123E 02
D-2	0.459E 03	0.475E 00	0.238E-02	-0.744E-05	-0.128E 04	0.671E 05	0.160E 07	-0.238E-02	0.147E 02
WA-5	0.478E 03	0.489E 00	0.136E-02	0.580E-04	-0.137E 04	0.704E 05	0.172E 07	0.199E-01	0.143E 02
WA-9	0.411E 03	0.557E 00	0.767E-03	0.907E-04	-0.101E 04	0.507E 05	0.127E 07	0.230E-01	0.117E 02
S-2-47	0.509E 03	0.385E 00	0.340E-03	0.327E-04	-0.155E 04	0.769E 05	0.194E 07	0.127E-01	0.142E 02

TABLE 21

SKIDDING DISTANCE, X ,AND SENSITIVITY COEFFICIENTS FOR WET JENNITE.   VO = 50 MPH.

TIRE	X	UOX	AX	BX	DXDUOX	DXDAX	DXDBX	DXDW	DXDVO
A-1	0.162E 04	0.237E 00	0.332E-02	-0.416E-04	-0.192E 05	0.119E 07	0.241E 08	-0.200E 00	0.983E 02
A5-1	0.182E 04	0.399E 00	0.306E-02	0.107E-03	-0.247E 05	0.154E 07	0.310E 08	0.664E 00	0.114E 03
A-5	0.142E 04	0.312E 00	0.196E-02	0.729E-04	-0.129E 05	0.738E 06	0.162E 08	0.236E 00	0.586E 02
RB-5	0.833E 03	0.265E 00	0.247E-02	-0.505E-04	-0.432E 04	0.238E 06	0.541E 07	-0.546E-01	0.307E 02
RB-1	0.955E 03	0.309E 00	0.187E-02	0.297E-04	-0.563E 04	0.306E 06	0.705E 07	0.418E-01	0.33[illegible] 02
H-5	0.869E 03	0.302E 00	0.170E-02	0.178E-04	-0.461E 04	0.247E 06	0.578E 07	0.206E-01	0.294E 02
D-2	0.118E 04	0.286E 00	0.375E-02	-0.491E-04	-0.970E 04	0.585E 06	0.121E 08	-0.119E 00	0.622E 02
WA-5	0.105E 04	0.306E 00	0.204E-02	0.327E-04	-0.689E 04	0.381E 06	0.863E 07	0.564E-01	0.393E 02
WA-9	0.833E 03	0.397E 00	0.221E-02	0.744E-04	-0.483E 04	0.265E 06	0.605E 07	0.898E-01	0.320E 02
S-2-47	0.116E 04	0.289E 00	0.187E-02	0.386E-04	-0.852E 04	0.472E 06	0.106E 08	0.824E-01	0.439E 02

// END 24 NOV 71 16.248 HRS

APPENDIX 5

SIMPLIFIED ANALYSIS OF A J-TURN

By making a number of assumptions and approximations, a simplified analysis of the J-turn maneuver can be obtained. First, all four tires are assumed to have the same properties. Second, the lateral force produced by the tires is assumed to be normal to the vehicle path. (This assumption neglects the influence of vehicle sideslip angle.) Third, load transfer effects due to vehicle roll are ignored and one-fourth the total weight is assumed to approximate the average load on the 4 tires. The center of gravity is assumed to be at mid-wheelbase.

Using these assumptions,

$$mA_y = \sum_{i=1}^{4} F_{y_i} \doteq 4F_y \tag{5-1}$$

where

- m is the mass of the vehicle
- A_y is the lateral acceleration
- F_{y_i} is the force from each of the tires
- $4F_y$ is an approximation of the total tire force.

From the tire model [2]

$$F_y = \mu_y F_z \left(1 - \frac{\mu_y F_z}{4C_\alpha \tan \alpha} \right) \tag{5-2}$$

Thus, after combining (5-1) and (5-2) and using $F_z = \frac{W}{4}$

$$A_y = g\left(\mu_y - \frac{\mu_y^2 W}{16C_\alpha \tan \alpha} \right) \tag{5-3}$$

For a steady turn of radius R, the lateral acceleration is

$$A_y = \frac{V^2}{R}$$

where V is the velocity. In this simplified view of the J-turn maneuver, it is assumed that the driver finds the maximum steady turn possible and that the maximum side force from the front tires is equal to the maximum side force from the rear tires. Since the center of gravity is equally distant from the front and rear wheels for the loaded SSL '68 Chevrolet, the yaw moment on the vehicle is nearly zero when the tire side forces are maximum. (It is assumed that at speeds above the limit velocity, V_L, the vehicle will develop a diverging or oscillatory yaw rate.) By equating the lateral acceleration for a limit velocity steady turn with (5-3), one obtains

$$\frac{V_L^2}{R} = g\left(\mu_y - \frac{\mu_y^2 W}{16C_\alpha \tan \alpha_p}\right) \tag{5-4}$$

where α_p is the slip angle for maximum tire force.

For example, on assuming that the test vehicle is executing a J-turn on wet concrete using the S-2-47 tire, the solution to (5-4) for V_L is 74.9 ft/sec (51.0 mph). This computation shows that the approximate model predicts limit velocities that are higher than the driver was able to achieve (i.e., 46.0 mph). This result is to be expected since the idealized model assumed that the driver-vehicle combination will operate in a manner that achieves maximum lateral tire force output from all 4 tires and further neglects the influence of lateral load transfer.

Table 22 gives the J-turn limit velocity obtained from (5-4) for each tire on each surface. In addition, Table 22 gives the rate of change of limit velocity with respect to μ_{oy}, A_y, B_y, C_α, and W (vehicle weight).

TABLE 22

J-TURN SENSITIVITY COEFFICIENTS FOR WET CONCRETE @ (8° SLIP ANGLE, 1250 LBS.)

TIRE	VL	DVLDUOY	−DVLDAY	−DVLDBY	DVLDCA	DVLDW
A-1	0.711E 02	0.432E 02	0.430E 03	0.541E 05	0.361E-03	0.210E-01
A5-1	0.738E 02	0.423E 02	0.437E 03	0.529E 05	0.442E-03	0.135E-01
A-5	0.738E 02	0.410E 02	0.424E 03	0.514E 05	0.622E-03	0.805E-02
RB-5	0.756E 02	0.395E 02	0.418E 03	0.494E 05	0.582E-03	0.106E-01
RB-1	0.795E 02	0.385E 02	0.430E 03	0.483E 05	0.584E-03	0.601E-02
H-5	0.792E 02	0.359E 02	0.398E 03	0.449E 05	0.657E-03	0.107E-01
D-2	0.749E 02	0.386E 02	0.405E 03	0.484E 05	0.423E-03	0.217E-01
WA-5	0.744E 02	0.438E 02	0.456E 03	0.548E 05	0.454E-03	0.719E-02
WA-9	0.751E 02	0.410E 02	0.431E 03	0.514E 05	0.602E-03	0.631E-02
S-2-47	0.749E 02	0.454E 02	0.476E 03	0.569E 05	0.420E-03	0.293E-02

TABLE 22

J-TURN SENSITIVITY COEFFICIENTS FOR WET ASPHALT.

TIRE	VL	DVLDUOY	-DVLDAY	-DVLDBY	DVLDCA	DVLDW
A-1	0.650E 02	0.543E 02	0.495E 03	0.680E 05	0.285E-03	0.974E-02
A5-1	0.713E 02	0.473E 02	0.473E 03	0.592E 05	0.411E-03	0.599E-02
A-5	0.758E 02	0.386E 02	0.410E 03	0.483E 05	0.688E-03	0.804E-02
RB-5	0.735E 02	0.442E 02	0.455E 03	0.553E 05	0.549E-03	0.283E-02
RB-1	0.749E 02	0.412E 02	0.432E 03	0.516E 05	0.442E-03	0.144E-01
H-5	0.774E 02	0.388E 02	0.420E 03	0.486E 05	0.614E-03	0.798E-02
D-2	0.713E 02	0.467E 02	0.467E 03	0.585E 05	0.391E-03	0.903E-02
WA-5	0.730E 02	0.439E 02	0.448E 03	0.549E 05	0.409E-03	0.127E-01
WA-9	0.758E 02	0.407E 02	0.432E 03	0.510E 05	0.634E-03	0.430E-02
S-2-47	0.674E 02	0.557E 02	0.526E 03	0.698E 05	0.298E-03	-0.265E-02

TABLE 22

J-TURN SENSITIVITY COEFFICIENTS FOR WET JENNITE.

TIRE	VL	DVLDUDY	-DVLDAY	-DVLDBY	DVLDCA	DVLDW
A-1	0.594E 02	0.545E 02	0.454E 03	0.683E 05	0.184E-03	0.318E-01
A5-1	0.602E 02	0.549E 02	0.463E 03	0.687E 05	0.201E-03	0.274E-01
A-5	0.567E 02	0.593E 02	0.471E 03	0.743E 05	0.223E-03	0.243E-01
RB-5	0.622E 02	0.517E 02	0.450E 03	0.647E 05	0.265E-03	0.251E-01
RB-1	0.648E 02	0.520E 02	0.472E 03	0.651E 05	0.261E-03	0.185E-01
H-5	0.692E 02	0.429E 02	0.416E 03	0.538E 05	0.363E-03	0.247E-01
D-2	0.605E 02	0.532E 02	0.451E 03	0.666E 05	0.194E-03	0.314E-01
WA-5	0.617E 02	0.521E 02	0.450E 03	0.653E 05	0.205E-03	0.301E-01
WA-9	0.623E 02	0.513E 02	0.448E 03	0.643E 05	0.274E-03	0.251E-01
S-2-47	0.638E 02	0.522E 02	0.466E 03	0.654E 05	0.212E-03	0.245E-01

// END 06 DEC 71 17.115 HRS

APPENDIX 6

J-TURN SIMULATION

Since the tire-vehicle system testing was done using a specially equipped 1968 Chevrolet Belair sedan, it was decided early in this program to simulate this vehicle and to compare the vehicle test results with the simulation results as a means of obtaining a better understanding of the internal details of the J-turn and locked-wheel diagonal-braking maneuvers. The decision to simulate the '68 Chevrolet meant that vehicle parameters had to be obtained. Accordingly, various test devices were set up to measure an extensive set of parameters for the '68 Chevrolet as it was delivered to HSRI by the sponsor. These measurements, the parameter data furnished by the sponsor, and published specifications were used to deduce a set of vehicle parameters suitable for the simulation. (See References [7] or [8] for a description of the simulation.) The necessary parameter data are tabulated in Table 23.

To address the question of what constitutes breakaway, a preliminary simulation of a series of J-turns was conducted on an analog computer. Figure 16 shows a typical result. In this example, the steering wheel is displaced by 70° and the vehicle attains a steady turn in a relatively short period of time. When the steering input is increased to 80°, a leveling off of the lateral acceleration, A_y, is observed and then a further increase in A_y takes place. In the field tests made by NBS the recorded lateral acceleration signal was used to identify breakaway. (The driver's "feel" of the situation was also used to help interpret whether or not breakaway took place.) However, by examination of Figure 16, it can be seen that the yaw rate, r, becomes divergent for the 80° steer angle case. Thus, it appears that for some driver-vehicle-tire-surface combinations a divergent yaw rate

TABLE 23. PARAMETERS FOR SIMULATION OF TIRE TEST CAR (1968 BELAIR CHEVROLET)

Symbol	Name	Value
m	Mass	158.5 slugs
t_f	Front wheel half tread	2.65 ft
t_r	Rear wheel half tread	2.65 ft
a	Distance, C.G. to front axle	4.96 ft
b	Distance, C.G. to rear axle	4.96 ft
h	C.G. height	1.767 ft
A_D	Cross-sectional (frontal) area	25 ft^2
I_z	Yaw moment of inertia	4025 slug ft^2
I_{xs}	Roll moment of inertia	325 slug ft^2
I_{ys}	Pitch moment of inertia	3210 slug ft^2
$\omega_{n\phi}$	Roll natural frequency	12.2 rad/sec
ζ_ϕ	Roll damping	0.18
$\omega_{n\theta}$	Pitch natural frequency	7.14 rad/sec
ζ_θ	Pitch damping	0.152
C_D	Aerodynamic drag coefficient	0.45
$K_{f\phi}$	Front roll stiffness	36,200 ft lb/rad
$K_{r\phi}$	Rear roll stiffness	12,250 ft lb/rad
K_θ	Pitch stiffness	165,300 ft lb/rad
K_{ss}	Steering system stiffness	9,600 ft lb/rad
τ_{ss}	Steering system lag	variable
k	Kingpin offset	0.2 ft
I_{wy}	Wheel inertia about axle	1.417 slug ft^2
C_r	Rear Roll steer coefficient	-0.047

TABLE 23. (Continued)

Symbol	Name	Value
K_f	Front spring rate	1280 lbs/ft
C_α	Tire lateral stiffness	variable
C_s	Tire longitudinal stiffness	variable
C_γ	Tire camber stiffness	$C\alpha/6$ lb/rad
μ_o	Nominal (zero speed) friction coefficient	variable
A_s	Friction reduction factor	variable (A_x or A_y)
x_p	Pneumatic trail	0.1 ft
R	Nominal tire radius	1.167 ft
C_z	Tire vertical deflection rate	15,000 lbs/ft
C_x	Tire vertical force offset rate	24,000 lbs/ft
x_r	Tire rolling resistance factor	.02

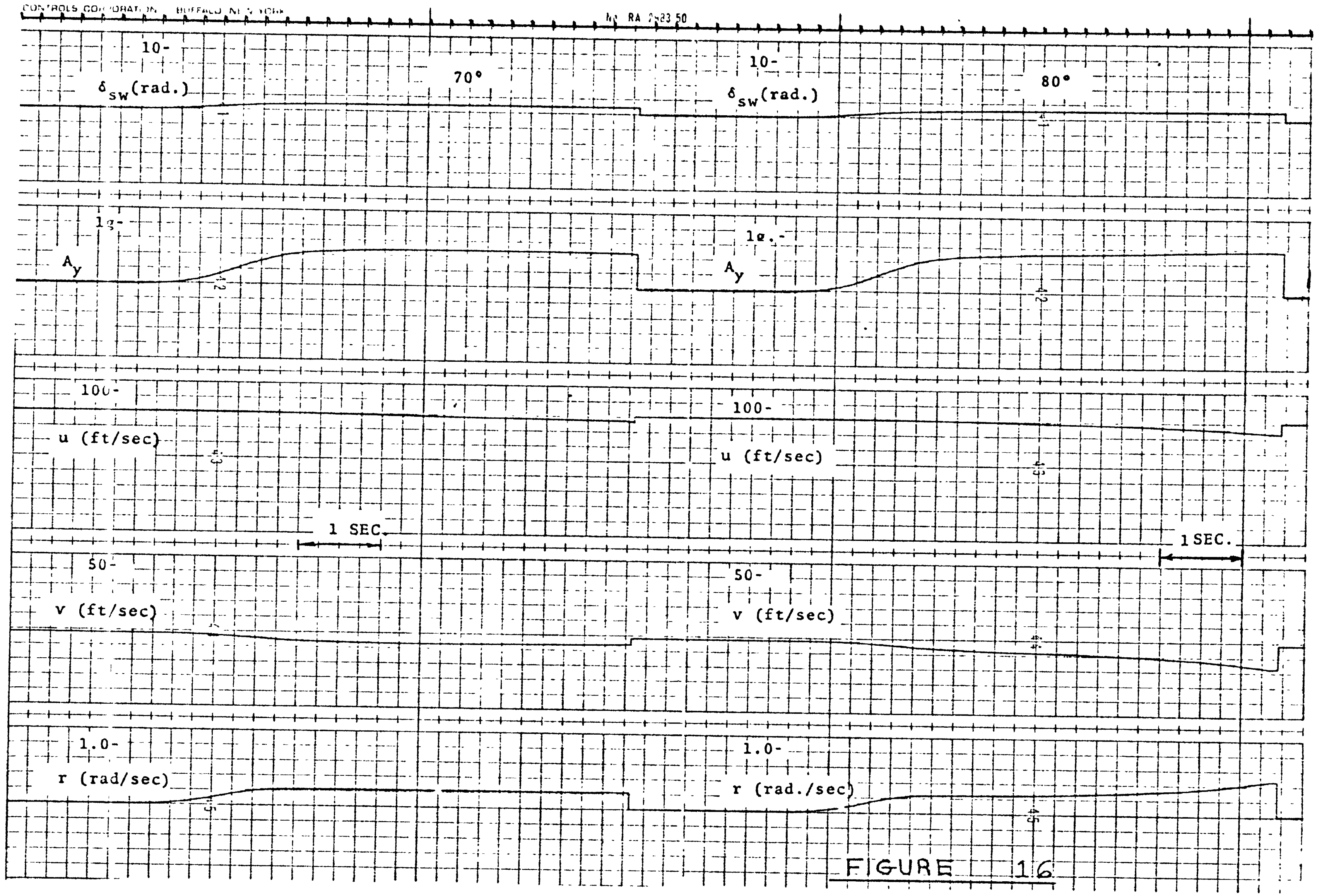

FIGURE 16. PRELIMINARY SIMULATION RESULT FOR A J-TURN.

signal is a much clearer way to determine breakaway than a small fluctuation in lateral acceleration.

Since the A-1 and RB-1 tires differ widely in their friction properties, additional studies using the hybrid computer have been based on these two tires. Figure 17 shows the time histories and trajectories computed for a closed-throttle J-turn performed with A-1 tires at an initial velocity of 70 ft/sec, with a steering wheel input of 100° and a radius of approximately 288'. These results were obtained by an interactive iterative process in which the trajectory was observed and steer angle and speed were adjusted in a series of computer runs to obtain a curved trajectory of the desired radius. At an initial velocity of 70 ft/sec the yaw rate signal remains fairly constant as the vehicle slows down. At an initial velocity of 72 ft/sec the yaw rate signal diverges (see Figure 2). Further, the speed of the vehicle at the point where the yaw rate has diverged by 0.05 rad/sec from the steady value is about 55 ft/sec.

Figure 18 shows the response of the vehicle equipped with RB-1 tires and operated at the same conditions which caused a divergent yaw rate signal when the vehicle had A-1 tires. With the RB-1 tire the lateral acceleration achieved is higher than with the A-1 tire and the yaw rate does not diverge as it did for the A-1 tire. The trajectory produced by the same steer displacement has a radius of curvature less than 288'. Clearly, a 288' radius J-turn can be negotiated at a higher velocity with the RB-1 tire than with the A-1 tire.

In order to obtain a larger radius turn, the velocity and steer angle were increased through a range of values up to 90 ft/sec at 150° steer angle. The yaw rate signal did not diverge for any of these cases; rather it developed an oscillatory behavior. The lateral acceleration signal decreased in magnitude and then increased again. (This is the criteria used by NBS to help

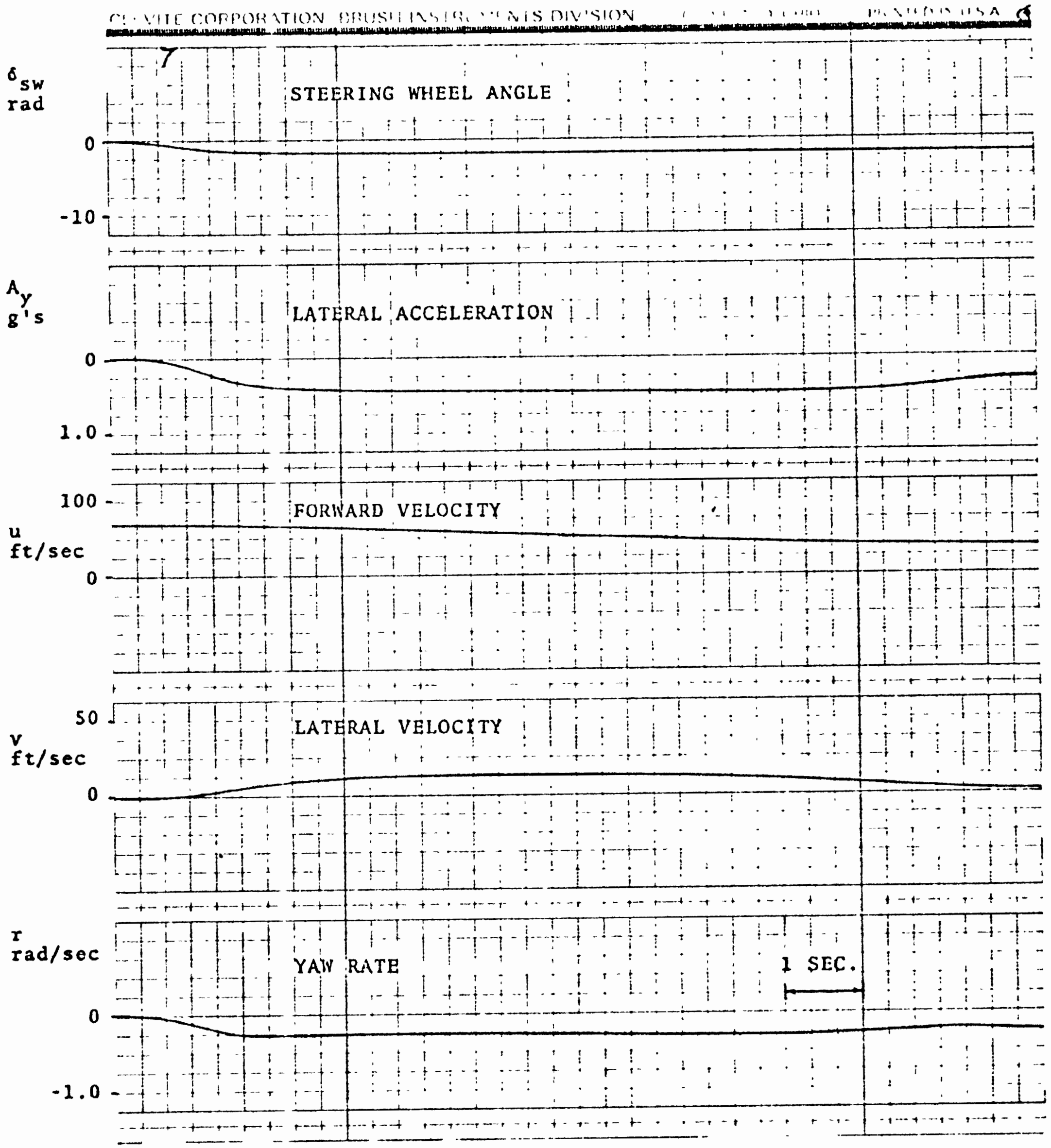

Figure 17a. u(0) = 70 ft/sec δ_{sw} = 100° Wet Concrete

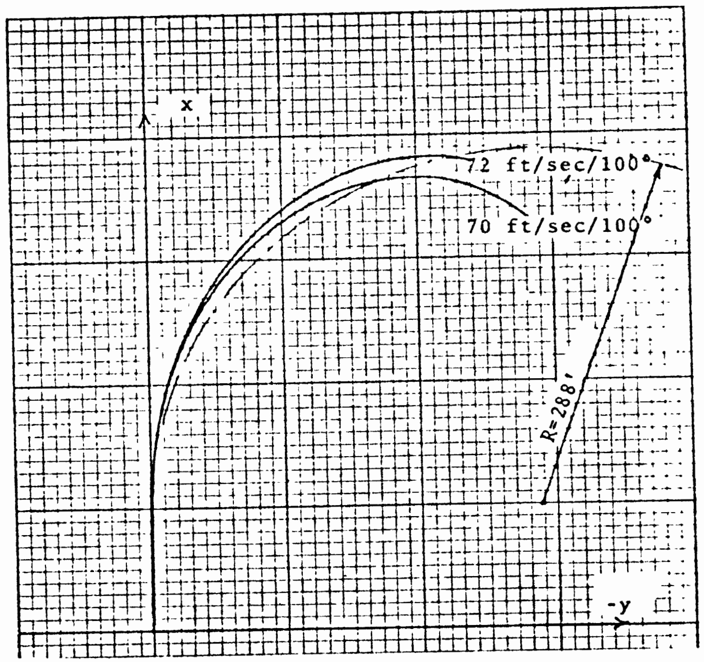

Scale: 1" ≡ 100'

Figure 17b.

FIGURE 17. J-TURN TIME HISTORIES AND TRAJECTORIES FOR AN A-1 TIRE.

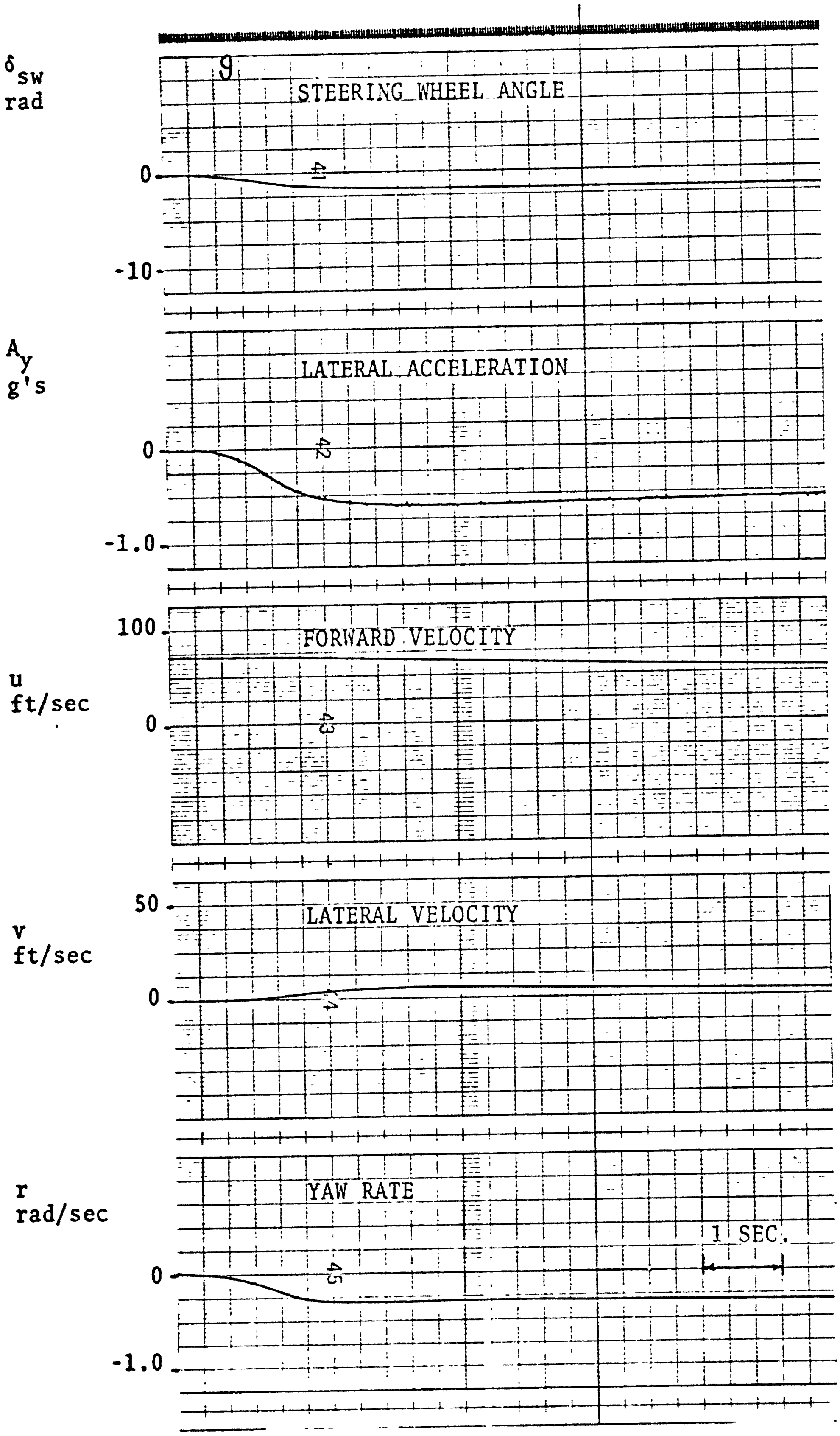

$u(0)$ = 72 ft/sec δ_{sw} = 100° Wet Concrete

FIGURE 18. J-TURN RESPONSE FOR RB-1 TIRE AT LIMIT RESPONSE CONDITION FOR A-1 TIRE.

identify breakaway.) The "dip" in lateral acceleration became noticeable at an initial velocity of about 85 ft/sec and 120° of steer angle. Motion time histories are shown in Figure 3 (in the body of this report) for an initial velocity of 90 ft/sec and a steer angle of 150°. The velocity of the vehicle, existing during the time the dip in lateral acceleration occurred, varies from 70 to 65 ft/sec.

In Figure 19 the influences of 4 different vehicle parameter changes on the response of the vehicle equipped with A-1 tires are illustrated. In the first case, Figure 19a, the center of gravity of the vehicle is displaced rearward from mid-wheelbase by 5% of the wheelbase. The character of the vehicle response is changed from a divergent yaw rate response to an oscillatory type of response.

In the second case the center of gravity was moved forward by 5% of the wheelbase. The same divergent yaw rate response, which was observed for the c.g. at mid-wheelbase, appears again.

In the third case the total roll stiffness of the vehicle was held constant but the rear roll stiffness was made equal to the front roll stiffness. (Originially the front roll stiffness was 3 times the rear roll stiffness. To achieve the assumed change in roll stiffness distribution, the front anti-roll bar could presumably be removed and stiffer rear springs could be installed.) This design condition makes the load transfer due to lateral acceleration (side force) equal on the front and rear tires. The resulting influence on the response of the vehicle is shown in Figure 19c. Note that lateral velocity, v, (and consequently the vehicle sideslip angle β) becomes very large. The yaw rate response is still divergent.

In the fourth case the total roll damping was doubled corresponding to installing more effective shock absorbers. The influence of this change was negligible as is shown in Figure 19d.

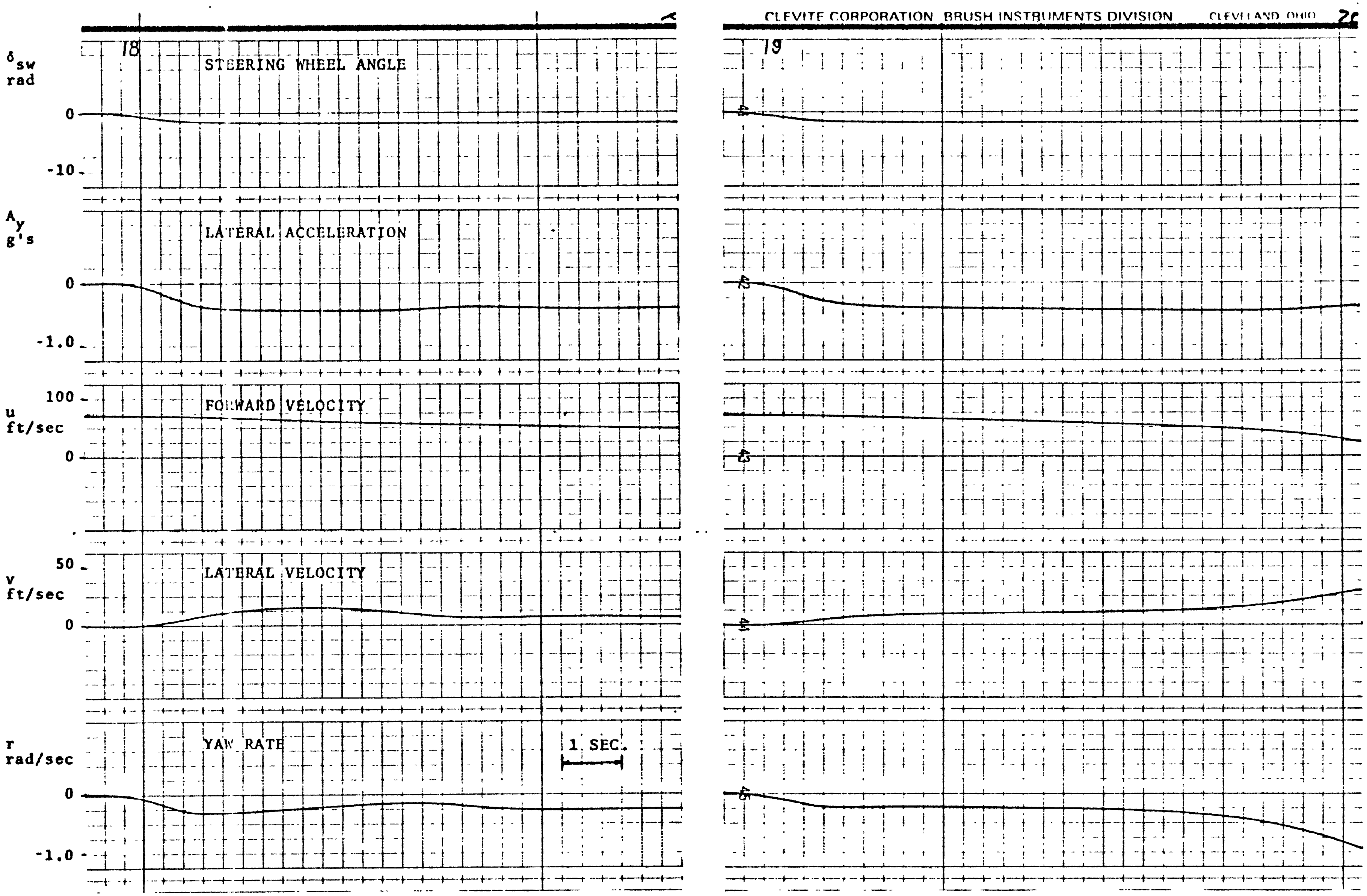

Figure 19a. u(0) = 72 ft/sec δ_{sw} = 100° Wet Concrete
a = 5.456 ft. b = 4.464 ft.

Figure 19b. a = 4.464 ft. b = 5.456 ft.

FIGURE 19. INFLUENCES OF VEHICLE PARAMETERS ON RESPONSE WITH RB-1 TIRES.

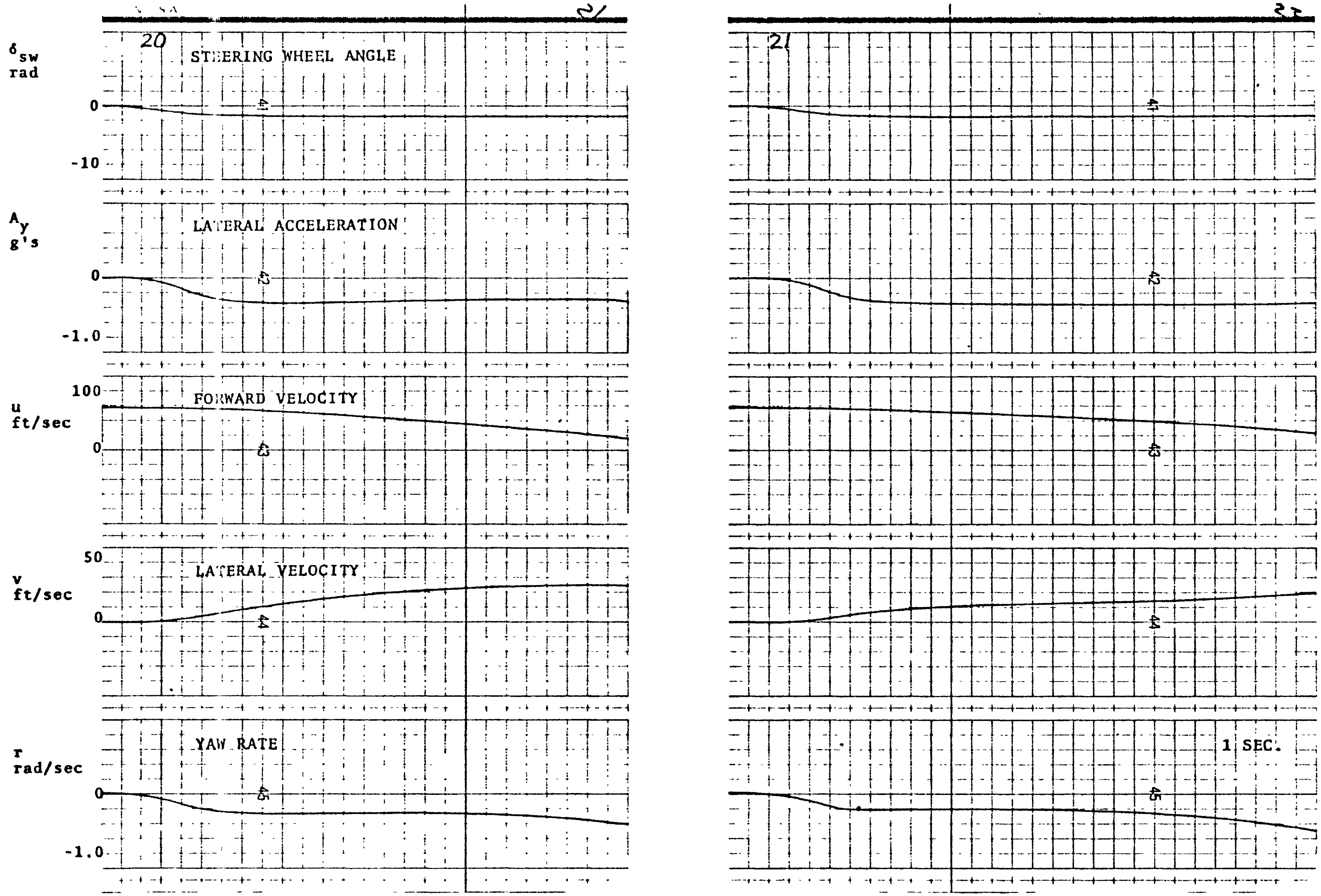

Figure 19c. $u(0) = 72$ ft/sec $\delta_{SW} = 100°$ Wet Concrete
$K_{f\phi} = K_{r\phi} = 24{,}225$ ft lbs/rad

Figure 19d. $\zeta_\phi = 0.36$

FIGURE 19. INFLUENCES OF VEHICLE PARAMETERS ON RESPONSE WITH A-1 TIRES.

In Figure 20, time histories of vehicle response for different c.g. locations, roll stiffness distribution and roll damping are presented for the test car equipped with RB-1 tires. These runs were made at the level of steering angle and velocity which produced a small but noticeable dip in lateral acceleration for the basic vehicle. While the lateral velocity and yaw rate traces change somewhat in character from one condition to another, the lateral acceleration continues to exhibit a dip for each of these cases.

In the vehicle tests, the test driver held the throttle constant at the setting required to maintain velocity on a straight path. For the test vehicle running in a straight line, about 80 lbs of drive thrust is required from each rear wheel at 45 mph. A very small amount of longitudinal slip is required to generate this force. The influence of this amount of longitudinal slip is probably negligible. The main influence of driver thrust is to increase the radius of the turn and to reduce the tendency of the path of the vehicle to spiral in more as time goes on. These effects are shown in Figure 21 for the RB-1 tire. To maintain the same radius path, a larger steer angle is required with driving torque than without driving torque. Since this amount of driving torque appears to make little difference, the vehicle tests could be run either with or without driving torque. Maintaining throttle has an advantage in that the path curvature increases less rapidly as time proceeds.

Simulation results for the A-1 tire and the RB-1 tire on the asphalt surface are shown in Figures 22a and 22b, respectively. On this surface the vehicle equipped with the A-1 tire has an oscillatory yaw rate response when initiating a J-turn at 70 ft/sec. The vehicle equipped with the RB-1 tire has a divergent yaw rate response when initiating a J-turn at 80 ft/sec. Results for the jennite surface are shown in Figure 23. In this case, the A-1 tire has a divergent yaw rate response at 50 ft/sec and the RB-1 tire has an oscillatory yaw rate response at 70 ft/sec.

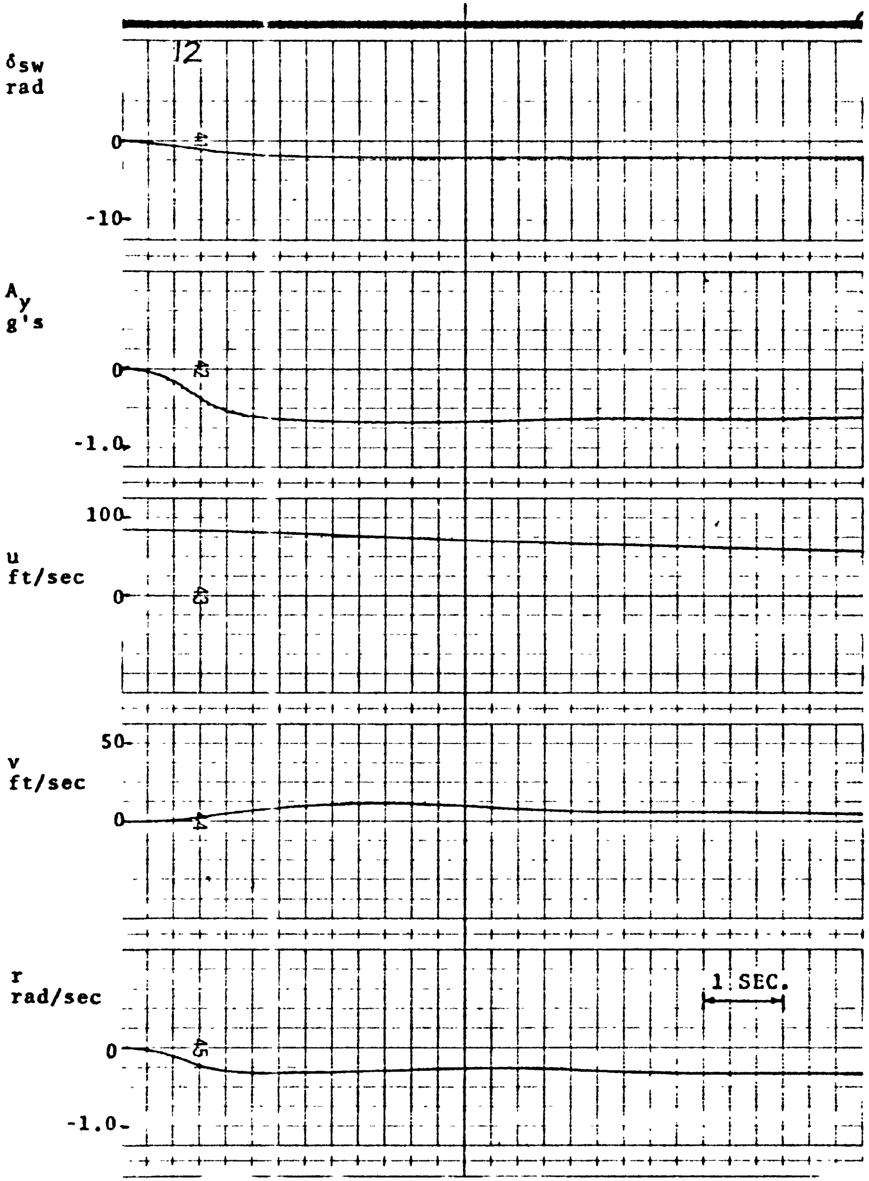

Figure 20a. a = b
u(0) = 85 ft/sec

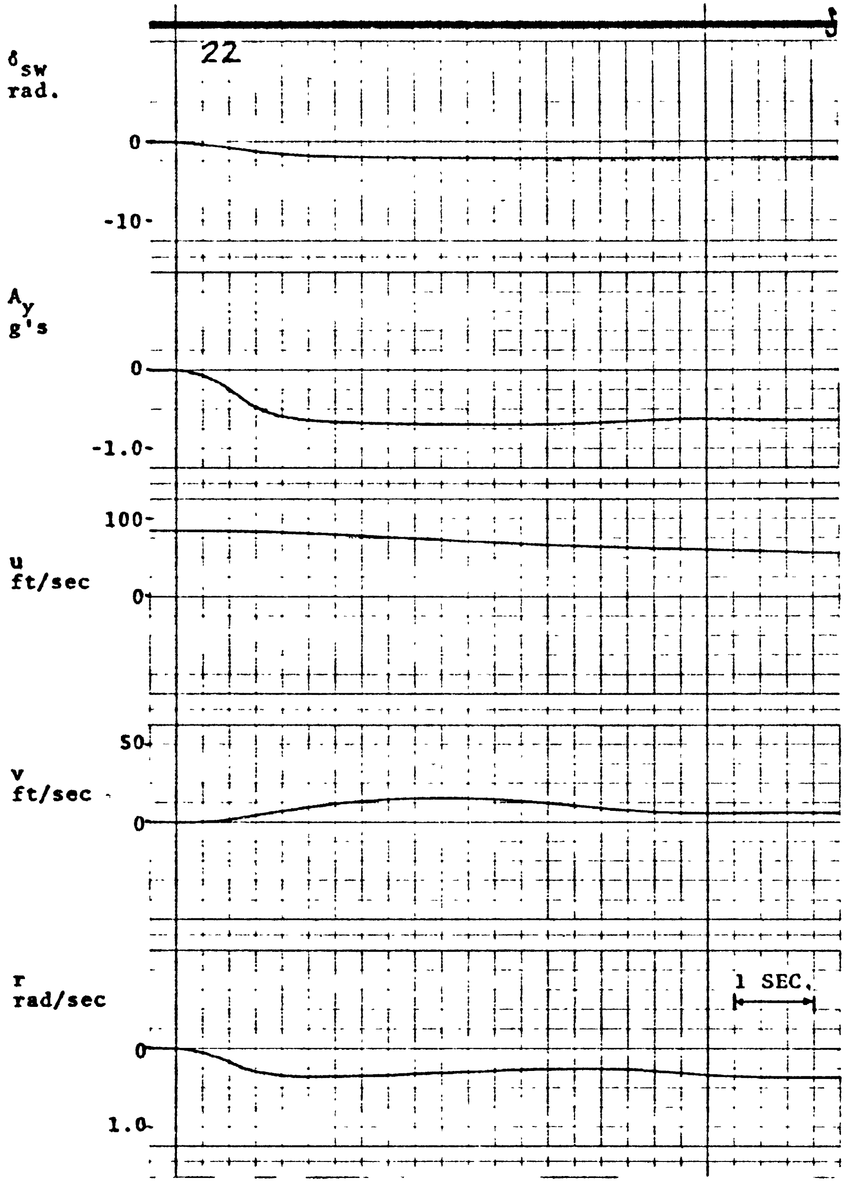

Figure 20b. a = 4.464 ft. b = 5.456 ft.
Wet Concrete

$\delta_{sw} = 120°$

FIGURE 20. INFLUENCES OF VEHICLE PARAMETERS ON RESPONSE WITH RB-1 TIRES.

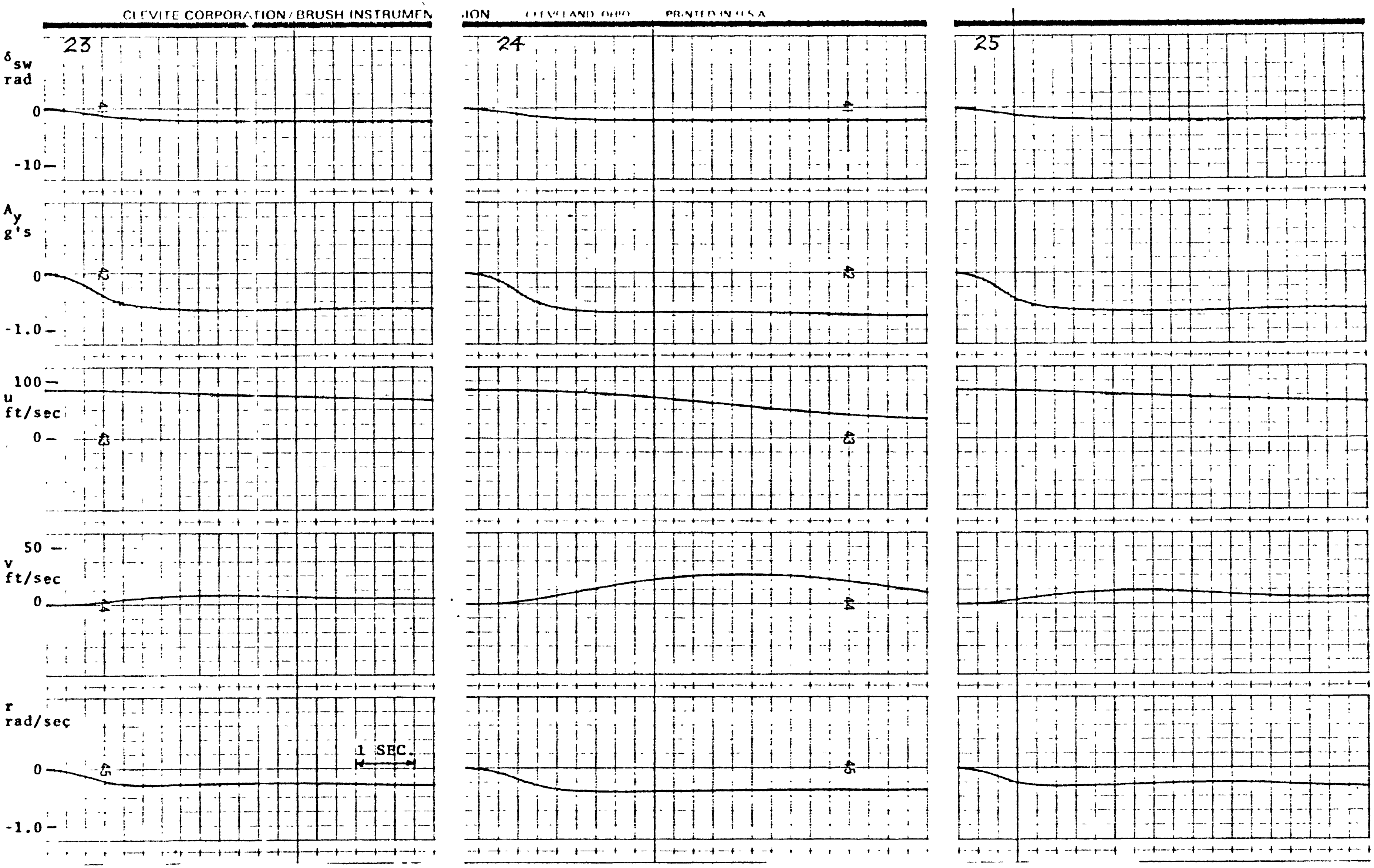

Figure 20c. $u(0) = 85$ ft/sec $\delta_{sw} = 120°$
$a = 5.456$ ft. $b = 4.464$ ft. Wet Concrete

Figure 20d. $K_{r\phi} = K_{f\phi} = 24{,}225$ ft lb/rad

Figure 20e. $\zeta_{\phi} = 0.36$

FIGURE 20. INFLUENCES OF VEHICLE PARAMETERS ON RESPONSE WITH RB-1 TIRES.

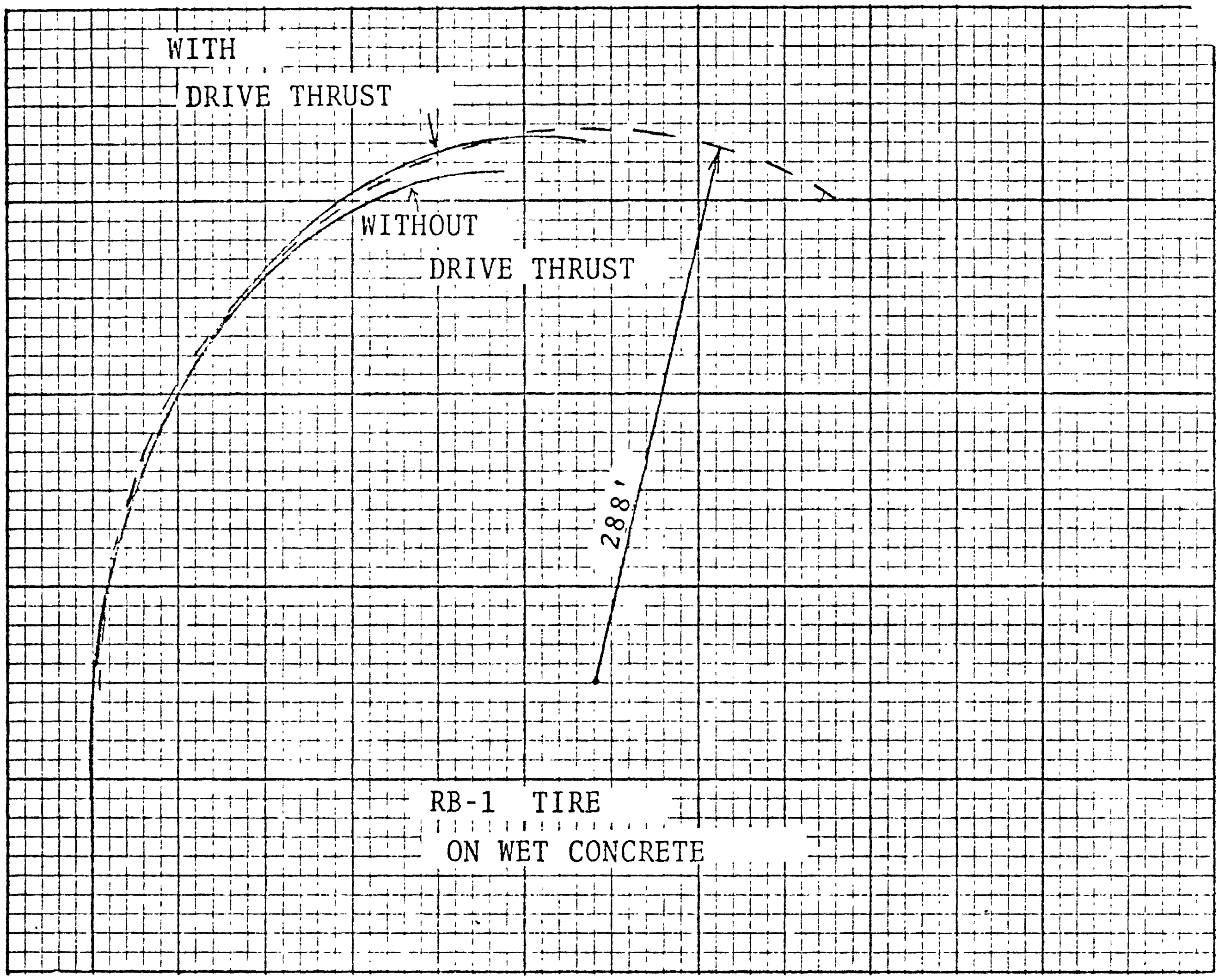

FIGURE 21. INFLUENCE OF DRIVE THRUST.

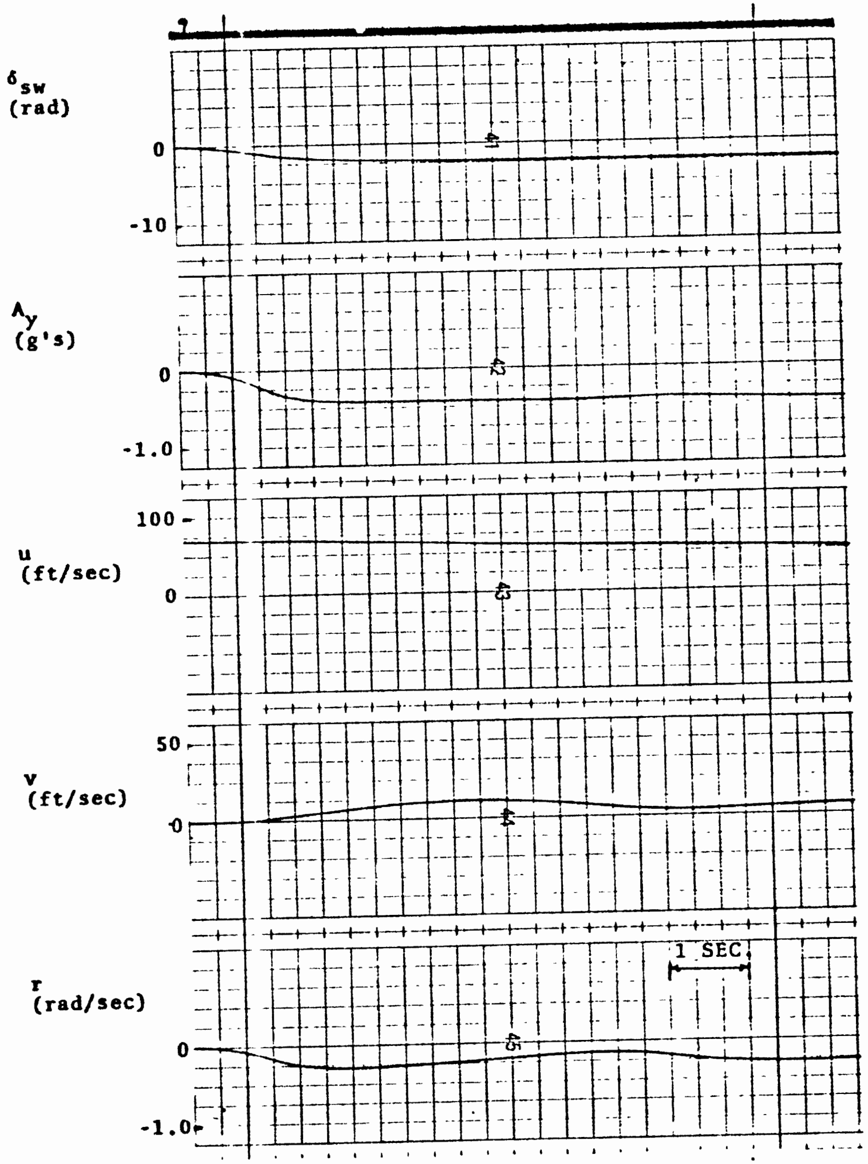

FIGURE 22a. A-1 TIRE RESULTS FOR ASPHALT

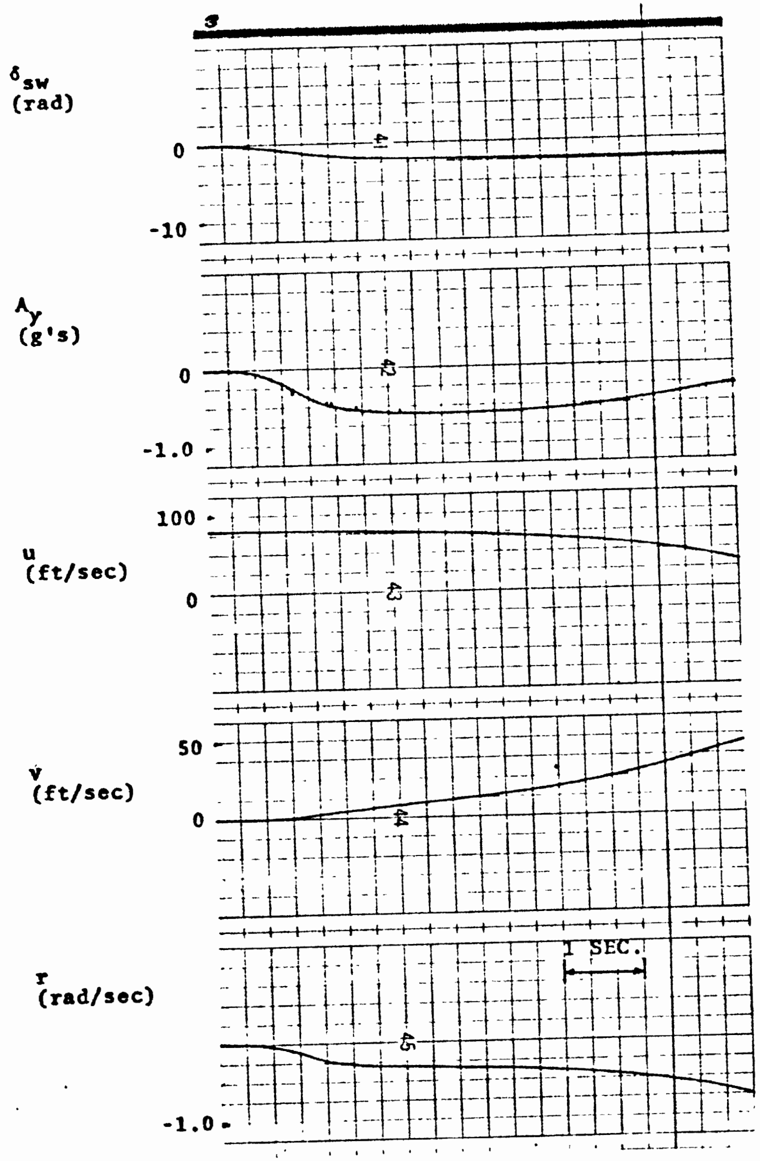

FIGURE 22b. RB-1 TIRE RESULTS FOR ASPHALT

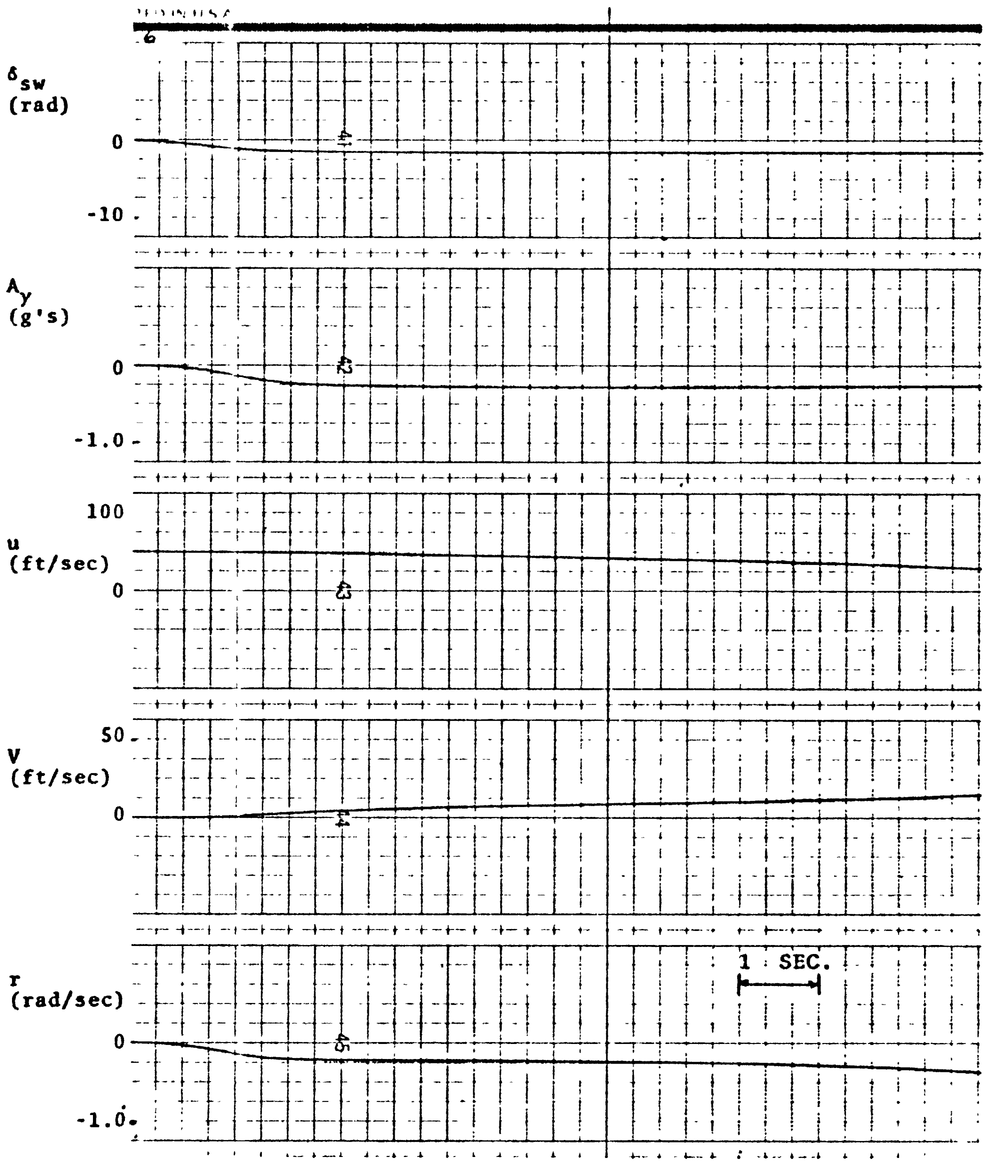

FIGURE 23a. A-1 TIRE RESULTS FOR JENNITE.

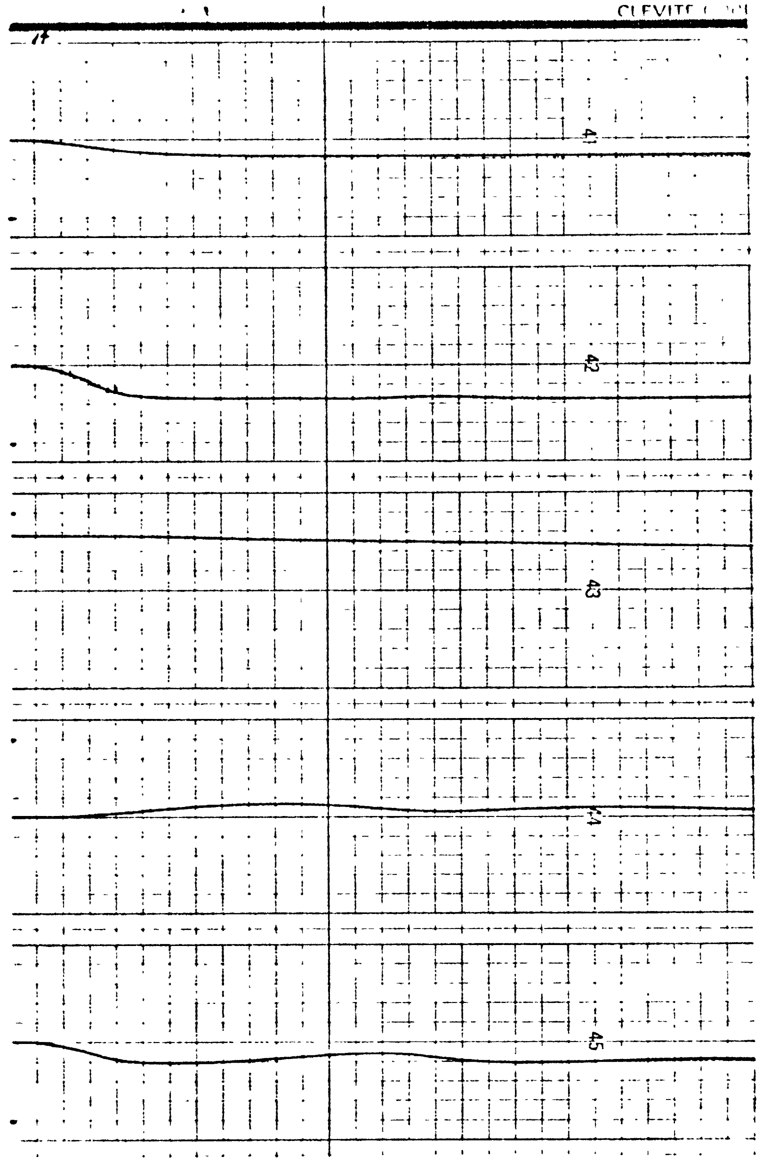

FIGURE 23b. RB-1 TIRE RESULTS FOR JENNITE.

REFERENCES

1. Dugoff, H. and Brown, B.J., "Measurement of Tire Shear Forces." SAE Paper No. 700092, January, 1970.

2. Dugoff, H., Fancher, P.S., and Segel, L., "Tire Performance Characteristics Affecting Vehicle Response to Steering and Braking Control Inputs." Final Report, NBS Contract CST-460, Highway Safety Research Institute, University of Michigan, Ann Arbor, August, 1969.

3. Cooper, B.E., Statistics for Experimentalists. Pergamon Press.

4. Clark, S.K. (Ed.), Mechanics of Pneumatic Tires. NBS Monograph 122, November, 1971.

5. Fancher, P.S., et al., "Experimental Studies of Tire Shear Force Mechanics - A Summary Report." Final Report, NBS Contract CST-928-5, Highway Safety Research Institute, University of Michigan, Ann Arbor, July, 1970.

6. Neill, A.H., Private Communication.

7. Fancher, P.S. and Grote, P., "Development of a Hybrid Simulation for Extreme Automobile Maneuvers." Summer Computer Simulation Conference Proceedings, Boston, Massachusetts, July, 1971.

8. Dugoff, H., Segel, L., and Ervin, R., "Measurement of Vehicle Response in Severe Braking and Steering Maneuvers," SAE Paper No. 710080, January, 1971.